ENTRAPMENT CHARACTERISTICS IN A RECIRCULATING EDDY

By

IOANNIS D. ANESTIS

A thesis submitted to the Faculty of Graduate Studies and Research in partial fulfillment of the requirements for the degree of Master of Engineering

McGill University

November 1979

To my beloved

family and to the

persons in Montreal

who helped my dreams

come true

ABSTRACT

This thesis is concerned with the study of pollutant effluents discharged from a side channel into rivers or coastal cross currents. Experiments were carried out to study the reattachment of the jet effluent and the entrapment of pollutant in the recirculating eddy immediately downstream of the discharge channel.

The flow was simulated in the laboratory by discharging dyed water from a side channel perpendicularly into an open channel crossflow. Geometric characteristics of the reattachment eddy were obtained from flow visualization. The transient variation of dye concentration in the eddy was determined from a series of light absorption probes, which were developed specifically for this investigation.

Attempts were made to characterize the entrapment process by overall parameters such as retention time and average steady-state concentration. The results were correlated through a convenient set of dimensionless variables which were derived from approximating the jet effluent as a point source of momentum flux.

RÉSUMÉ

Le sujet de cette thèse est l'étude de la décharge des effluents polluants d'un canal secondaire débouchant dans une riviére ou encore émergeant dans des courrants côtiers. Des expériences ont été faites pour étudier comment le jet d'effluents est capté par le courrant principal et comment les polluants sont retenus par le tourbillon de recirculation immediatement en aval du canal de décharge.

L'écoulement a été simulé au laboratoire en envoyant de l'eau teintée depuis un canal secondaire débouchant perpendiculairement dans un canal principal en circulation ouverte. Les charactéristiques géometriques du tourbillon de recirculation sont obtenues par visualization. La variation en régime non établi de la concentration en colorants a été mesurée dans le tourbillon à l'aide de sondes spécialement mises au point pour cette étude.

On a cherché à charactériser le processus de rétention des effluents polluants par des paramètres globaux tels que un temps de rétention et une concentration moyenne stationnaire. Les résultats se corrèlent convenablement lorsqu'ils sont présentés à l'aide de grandeurs adimmensionnelles obtenus en supposant que le jet d'effluents est une source ponctuelle de flux de quantité de movement.

TABLE OF CONTENTS

ACKNOWLEDGEMENTS

I would first like to express my gratitude to my advisor, Professor V.H. Chu, for his guidance throughout the entire course of this study.

The apparatus was constructed by Mr. T. Rigby. Mr S. Attia helped in putting together the final version of the light absorption probes. Special acknowledgement goes to Mr. Lenny Lesser for his assistance in computer programming and in performing most of the experiments.

Finally, I would like to thank Ms. J. Kaufmann for her personal support, editorial guidance, and thorough typing.

LIST OF FIGURES

LIST OF TABLES

LIST OF SYMBOLS

B	= main channel width
b	= side channel width
$\bar{c}$	= average concentration
c_f	= friction factor
$c_{m,\ e,\ r}$	= concentration at different regions
c_o	= initial concentration at the exit of the side channel
c_s	= steady-state concentration; average of $c_{1,\ 2,\ 3,\ 4,\ 5}$
$c_{1,\ 2,\ 3,\ 4,\ 5}$	= concentration in the eddy at x = L/4, L/2, 3L/4, L/3, and 2L/3 respectively
d	= depth of flow
H	= height of eddy, based on dividing stream line
H_i	= height of the eddy, based on inner jet boundary
H_o	= height of the eddy, based on outer jet boundary
$h_{1,\ 2,\ 3,\ 4,\ 5}$	= local heights of the eddy at x = L/4, L/2, 3L/4, L/3, and 2L/3 respectively, based on inner jet boundary
L	= length of the eddy
l_s	= length scale = M_o/U^2
M_o	= momentum flux (per unit depth) = V^2b
$Q_{e,\ r,\ m}$	= volume flux (per unit depth) at different regions
Q_o	= volume flux (per unit depth) at the exit = Vb
Q_s	= volume flux scale = $M_o/U = V^2b/U$
τ	= average retention time

$\tau_{1\ 2\ 3\ 4\ 5}$ = retention time in the eddy at x = L/4, L/2, 3L/4, L/3, and 2L/3 respectively

t = time

t_s = time scale = $l_s/U = M_o/U^3 = V^2b/U^3$

U = crossflow velocity in the main channel

V = exit velocity of side channel

$\forall$ = volume of the eddy

x = coordinate along the channel

y = coordinate in the traverse direction of the channel

z = vertical coordinate

Subscripts

e = external flow

i = conditions at location P_i

m = mixed fluid at the reattachment region

o = exit conditions

r = return flow

CHAPTER I

INTRODUCTION

A common method of waste disposal into river and coastal environment, for reason of simplicity and construction economy, is through a side channel into the full depth of the receiving water. The effluent, in the form of a turbulent jet deflected by the cross current, is often observed to reattach onto the shoreline and form a low flow recirculation region immediately downstream of the discharge channel. Fluid particles that are entrapped in the recirculation region generally tend to stay for longer periods of time; the velocity and turbulent level is lower, and there is a tendency for particulate and flocculant matters to settle here. In the case of cooling water discharge, heat dissipation in such a region may be significant. Although the highest concentration and temperature occur along the jet center line, knowledge of the transport process in the recirculation region is important in many environmental design considerations. The degree of pollution contamination further downstream along the shoreline is also critically dependent on the process within the recirculation region.

The recirculation flow is simulated in the laboratory by discharging water from a side channel into an open channel crossflow, as shown in Figures 1 and 2. The discharging jet can be seen to be deflected by the crossflow; at the same time, it forces the crossflow to contract and bend toward the far bank.

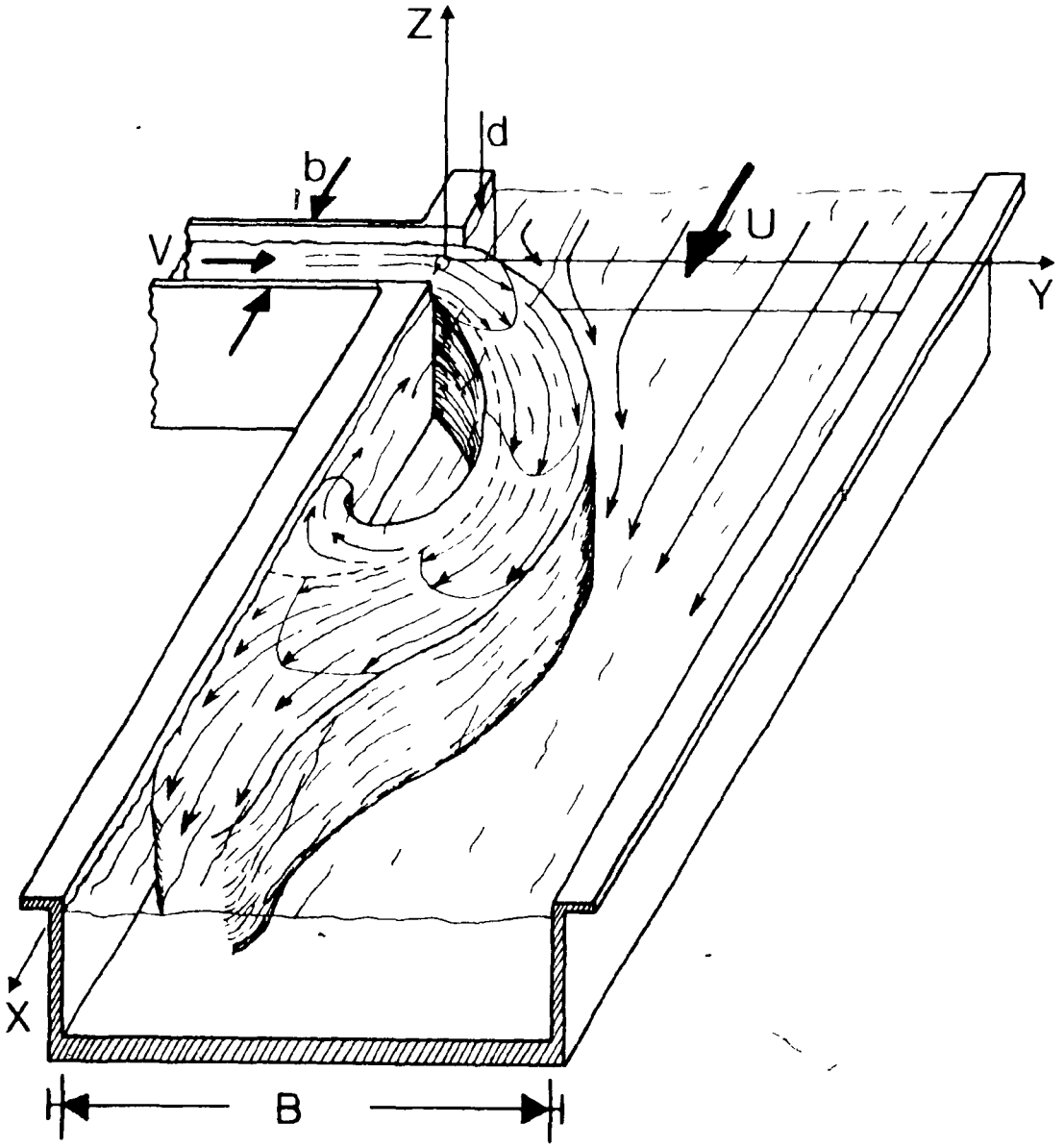

FIGURE 1. JET REATTACHMENT IN A CROSSFLOW

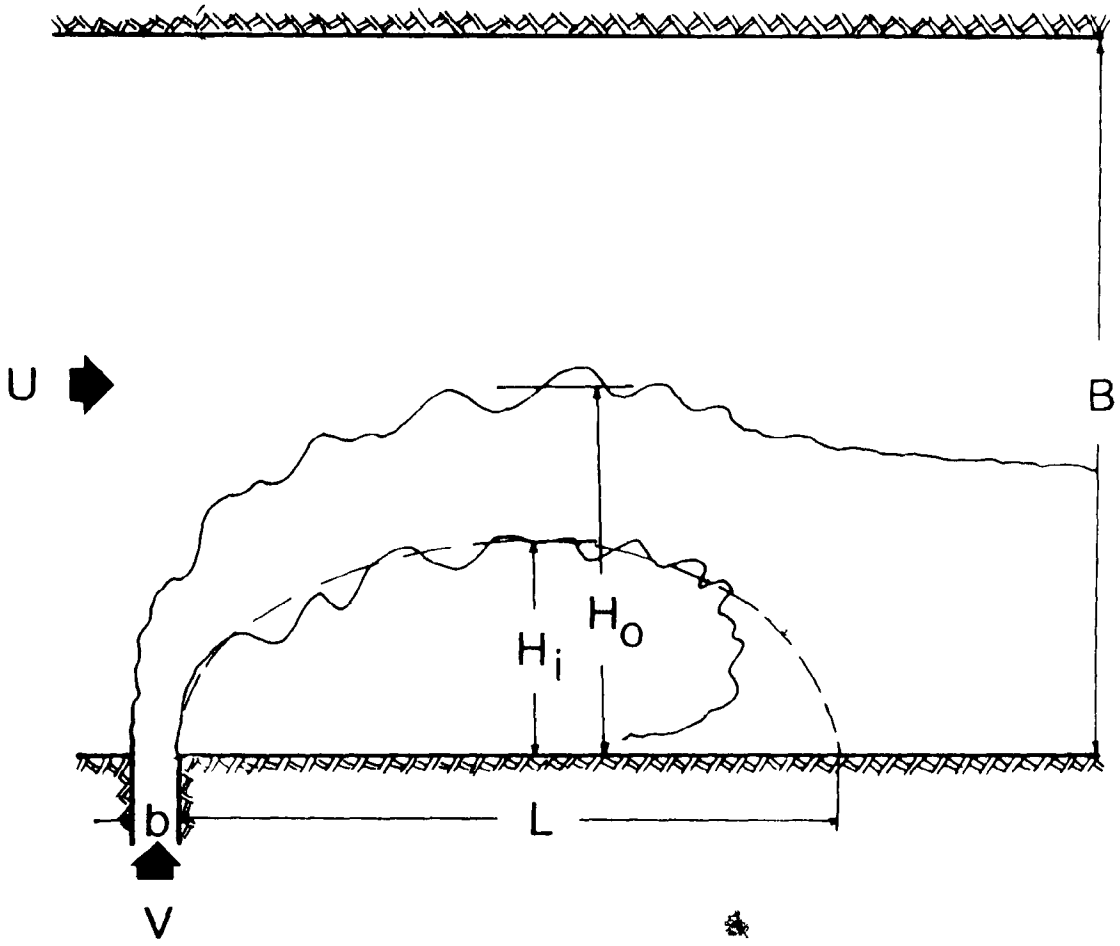

FIGURE 2. DEFINITION SKETCH

As the jet reaches the maximum penetration point, the directions of the crossflow and the jet become parallel, but the jet velocity is still somewhat higher. Further downstream, the jet continues its curved trajectory, due to the centrifugal pull induced by the low pressure region behind the jet. It eventually impinges on the bank. Entrainment is restricted by the presence of the solid boundary and this causes the formation of the recirculation region.

During the experiment, the dye is turned on for a period of time until the concentration in the recirculation region reaches steady state. The geometry of the recirculating eddy is determined from flow visualization. The steady-state concentration distribution is determined from a series of light absorption probes. The dye at the discharge channel is subsequently turned off, and the transient decay of dye concentration within the recirculation region is again determined from the light absorption probes. The sequence of events during the experiment is demonstrated in a series of photographs in Figure 3. The photographs show clearly the existence of a recirculation region with a relatively uniform concentration distribution.

The existence of a region of uniform concentration has suggested that a simplified description of the problem may be possible. In this simplified model, the flow is divided into regions, namely, a curved shear layer and a recirculation region. It is assumed that complete mixing is achieved instantly in the shear layer.

In the recirculation region, the spatial concentration distribution is assumed uniform. The temporal variation is characterized by a "retention time". For a steady discharge of substance from the side channel,

FIGURE 3. THE SEQUENCE OF EVENTS SHOWING THE ENTRAPMENT PROCESS IN THE RECIRCULATION ZONE

(a) dye injection is on; (b) maximum jet penetration; (c) reattachment; (d) dye injection is off; (e), (f), (g), (h) transient decay of concentration in the recirculation region

(a)

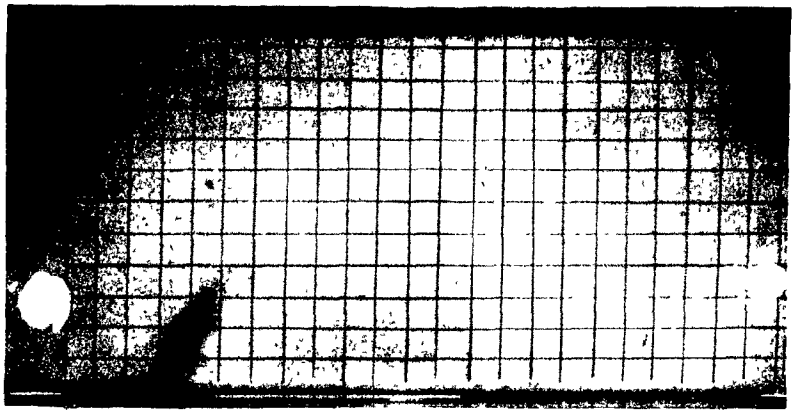

(b)

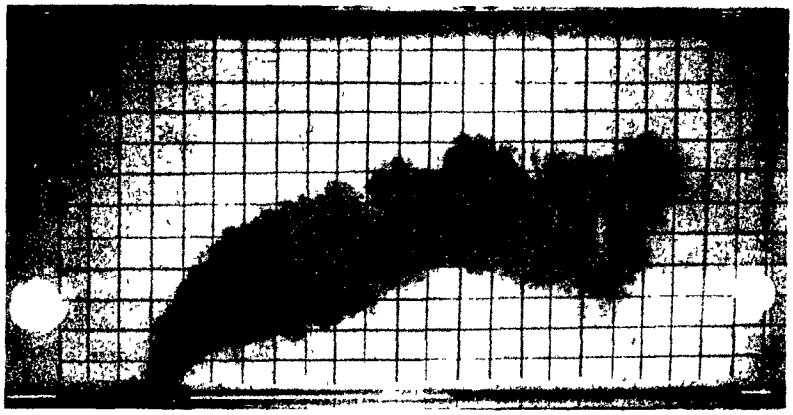

(c)

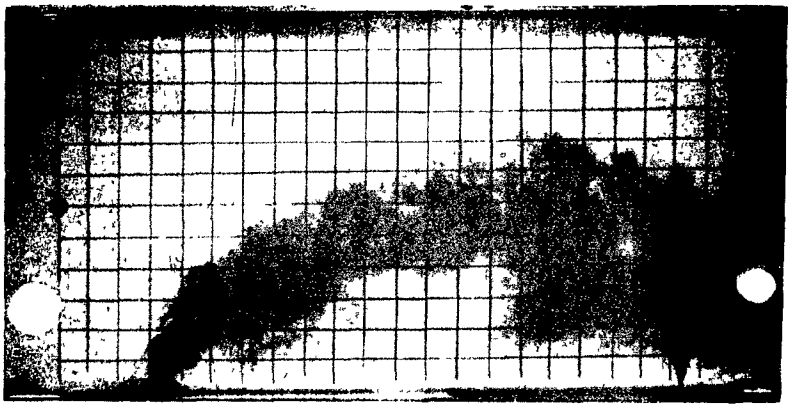

(d)

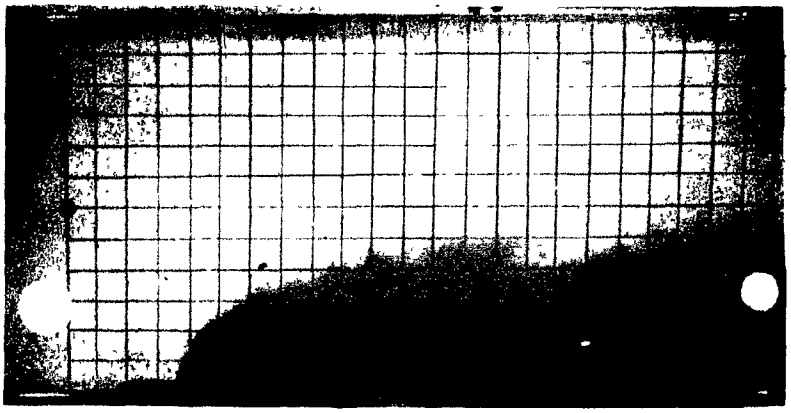

(e)

(f)

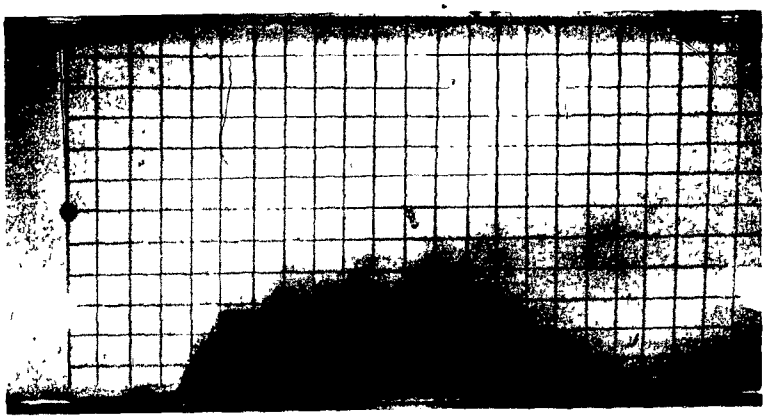

(g)

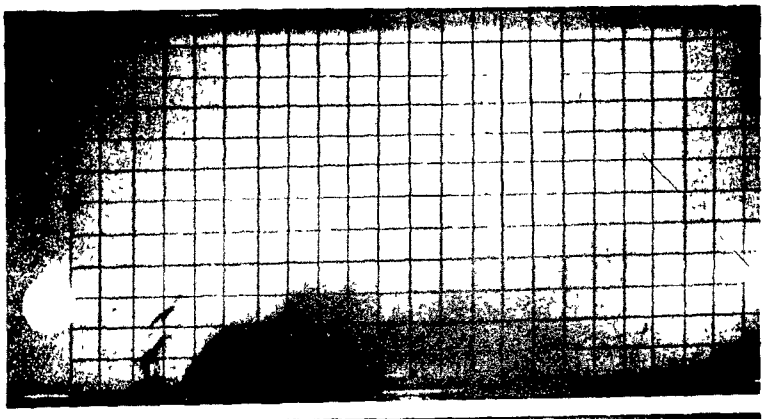

(h)

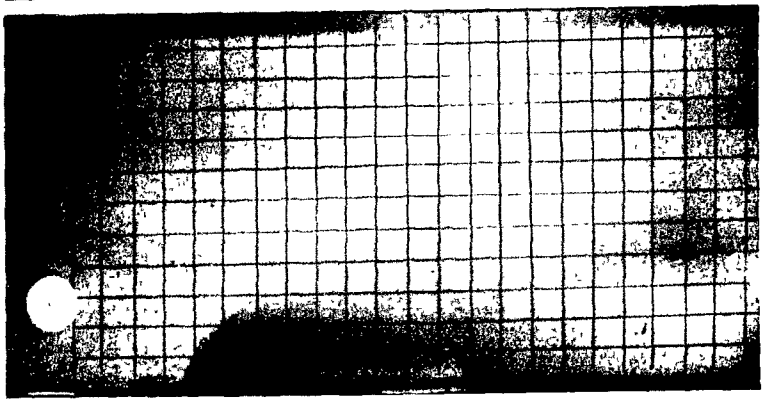

the concentration in the recirculation region will eventually reach a certain "steady-state concentration". The major effort of this thesis will be to determine these two parameters, the retention time τ and the steady-state concentration c_s, and to show how they are related to the overall transport process in the recirculation flow.

1.1 Review of Previous Investigations

One of the earliest experimental investigations was on the reattachment of plane jets in crossflows, done by Rouse (1957). Rouse performed experiments in what he considered an unconfined wind tunnel crossflow, and proposed the following expression for the length of the recirculation eddy:

$$\frac{L}{b} \simeq 20 \left(\frac{V}{U}\right)^{\frac{3}{2}}$$

Mikhail et al. (1975) measured the width and length of the recirculating eddy in a confined open channel crossflow. The experimental results were correlated by a set of dimensionless variables derived from a point source model. The jet was approximated as a point source of momentum. For a range of exit and crossflow conditions, they concluded that the shapes of the eddy were nearly similar, and that the relative size of the eddy, H/B, depends mainly on the momentum flux ratio, (V^2b/U^2B).

The first experimental study concerned with measurements of concentration distribution in the eddy was done by Carter (1969). He measured temperature fields induced by a warm water discharge into a flume. Temperature contours were provided for a number of exit-to-crossflow velocity ratios. It is not known whether the effect of buoyancy is important in

his experiments.

Strazisar and Prahl (1973) have examined the effect of bottom friction. The jet trajectory was determined from dye photographs in their experiments.

An extensive numerical calculation for the side channel discharge problem has been carried out by McGuirk and Rodi (1978). Their results were found to be in close agreement with experiments by Mikhail et al. (1975) and Carter (1969).

1.2 Objective of Present Investigation

From the above review of previous studies, it is clear that experimental information related to the concentration distribution is rather insufficient. The only measurement in the concentration field is that of Carter (1969). Carter obtained steady-state temperature distributions for three different flow situations, but there was no systematic correlation with the exit conditions. The measurement was carried out in a hot jet in cold crossflow; it is not certain whether some of Carter's results might not have been affected by buoyancy.

Instead of obtaining detailed spatial concentration distributions, the attention of the present study is focusing on a number of parameters that govern the overall transport process. The overall parameters under consideration are the length, L; the height, H_1, of the eddy; the steady-state concentration, c_s; and the retention time, τ. The objective is to simplify the description of the process to a finite number of parameters so that the results can be systematically correlated with the exit conditions. In many engineering applications, it is often the overall

parameters that are required. It is hoped that the correlation provided in this thesis would be readily applicable in many preliminary design considerations.

The thesis will begin with a discussion of the physical meanings of the two overall parameters: the steady-state concentration, c_s, and the retention time, τ. This will be followed by a description of the experiments. Finally, the result will be correlated by a set of dimensionless variables that are derived from a point source approximation.

CHAPTER II

THEORETICAL CONSIDERATIONS

A brief description of the entrapment process in the recirculating eddy is presented in this chapter. A simplified model is introduced in order to relate the physical process with two overall parameters, namely, the "retention time" and the "steady-state concentration". Finally, plausible forms of dimensionless relations are introduced. They will provide a basis for correlation and analysis of experimental data to be presented in subsequent chapters.

2.1 The Two Parameters Description

A simplified description of transport processes in recirculating flows was proposed by Chu (1978; personal communication). In this simplified model, the flow is assumed to consist of a thin curved shear layer and a slow recirculating eddy, as sketched in Figure 4. It is assumed that mixing is achieved instantly in the shear layer.

The fluxes of concentration that enter and leave the shear layer are equal, i.e.

$$c_o Q_o + c_r Q_r + c_e Q_e = c_m (Q_r + Q_o + Q_e) \qquad (1)$$

where c is the concentration and Q the volume flux; subscript "o" refers to the condition at the discharge channel, "e" to the external flow,

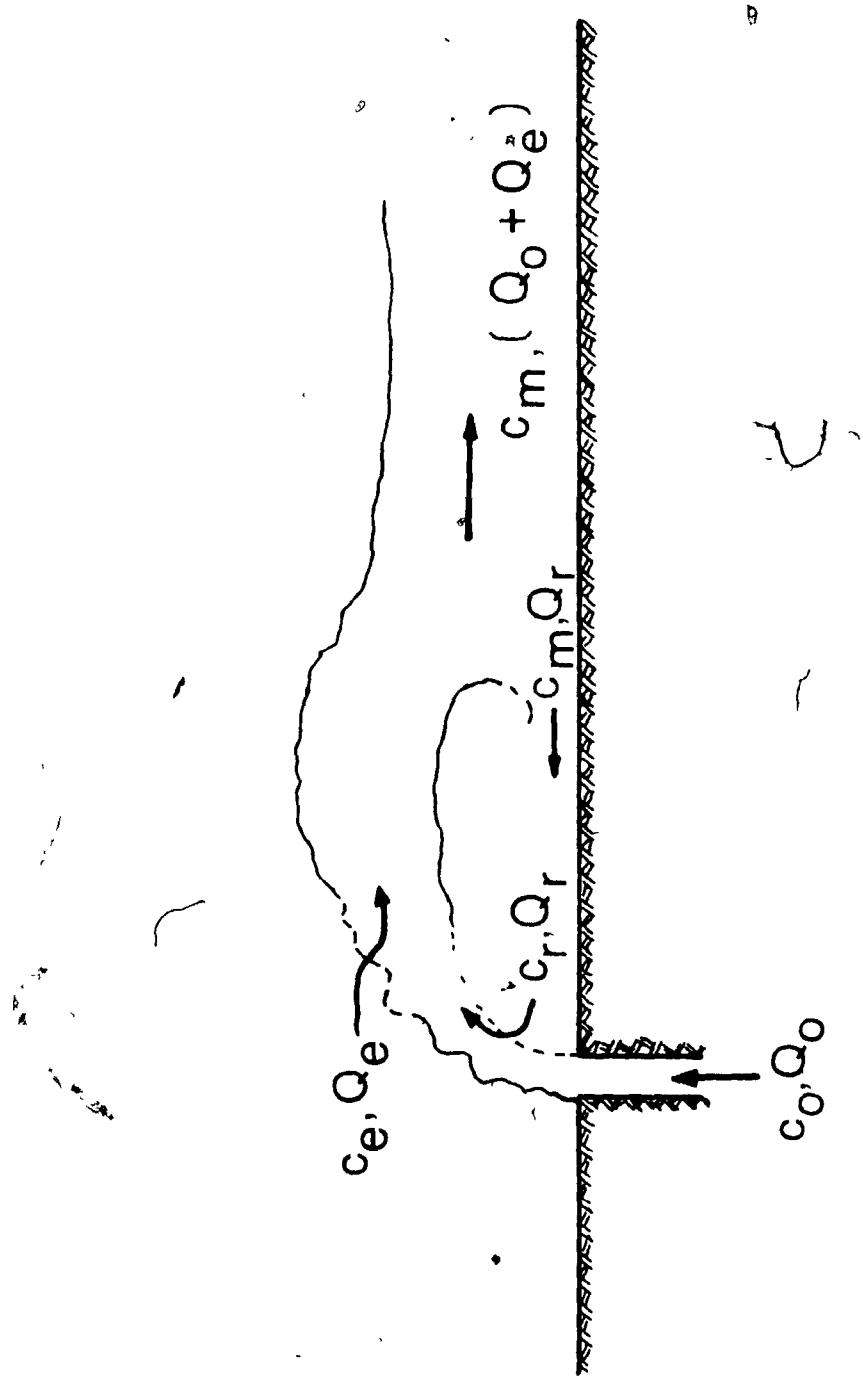

FIGURE 4. DEFINITION SKETCH FOR THEORETICAL CONSIDERATION

"r" to the return flow from the eddy, and "m" to the mixed fluid at the reattachment point.

The mass balance in the eddy is

$$\frac{d(\bar{c}\forall)}{dt} = (c_m - c_r)Q_r \tag{2}$$

where $\forall$ is the volume of the eddy and $\bar{c}$ is the mean concentration within the eddy. Eliminating c_m from Equations 1 and 2,

$$\frac{d(\bar{c}\forall)}{dt} = -\frac{c_r(Q_o + Q_e)Q_r}{(Q_o + Q_e + Q_r)} + \frac{(c_oQ_o + c_eQ_e)Q_r}{(Q_o + Q_e + Q_r)} \tag{3}$$

The second term on the right side of Equation 3 is the source term.

To study the transport process, let us consider the following two problems.

(i) First, consider the transient decay of substance in the eddy as the source term is turned off. Let c_o and $c_e = o$, and, as a first approximation, let $\bar{c} = c_r$. The transient decay is given by the solution of Equation 3, i.e.,

$$\frac{\bar{c}}{c_s} = \exp\left\{-\frac{t}{\tau}\right\} \tag{4}$$

where c_s is the eddy concentration at $t = 0$.

where

$$\tau = \frac{(Q_o + Q_e + Q_r)\forall}{(Q_o + Q_e)Q_r} = \left[\frac{1}{Q_r} + \frac{1}{Q_o + Q_e}\right]\forall \qquad (5)$$

which will be referred to as the "retention time" of the recirculating eddy.

(ii) The second problem of significance is the steady-state concentration distribution in the eddy. Consider a steady injection of concentration c_o from the side channel, and let $c_e = o$. As the concentration reaches steady-state, both sides of Equation 2 become zero. Under this condition, $c_r = c_m$, and both approach the steady-state concentration in the eddy, c_s.

From Equation 1,

$$c_s = \frac{c_o Q_o}{(Q_o + Q_e)} \qquad (6)$$

We see now that the two parameters, τ and c_s, are uniquely related to the volume fluxes $(Q_o + Q_e)$ and Q_r. The transport process in the eddy is governed by the magnitudes of $(Q_o + Q_e)$, Q_r, or, alternatively, by the two parameters (τ, c_s). In the experimental program to be described in the subsequent chapters, we chose to measure τ and c_s. Once these two parameters are known, the overall transport phenomenon in the eddy will be determined from Equations 1 and 2, with Q_e and Q_r being determined by Equations 5 and 6.

2.2 Concentration Variation in the Experiment

During the experiment, the dye from the side channel was turned on for a period of time until the steady-state concentration was reached in the recirculating eddy. The dye was then turned off to observe the transient decay. The rise of concentration in the eddy is given by

$$\frac{\bar{c}}{c_s} = 1 - \exp\{-\frac{t-t_1}{\tau}\} \tag{7}$$

The decay of concentration is

$$\frac{\bar{c}}{c_s} = \exp\{-\frac{t-t_2}{\tau}\} \tag{8}$$

Equations 7 and 8 are both solutions of Equation 3, but with different initial conditions. A schematic representation of the concentration variation is shown in Figure 5.

2.3 Dimensional Considerations

The experimental results will be correlated in a manner suggested by Mikhail et al. (1975). The side channel discharge will be approximated by a point source of momentum flux. The important independent variables of the problem are:

M_0 = jet momentum flux (per unit depth and per unit density)

U = crossflow velocity

B = width of the crossflow

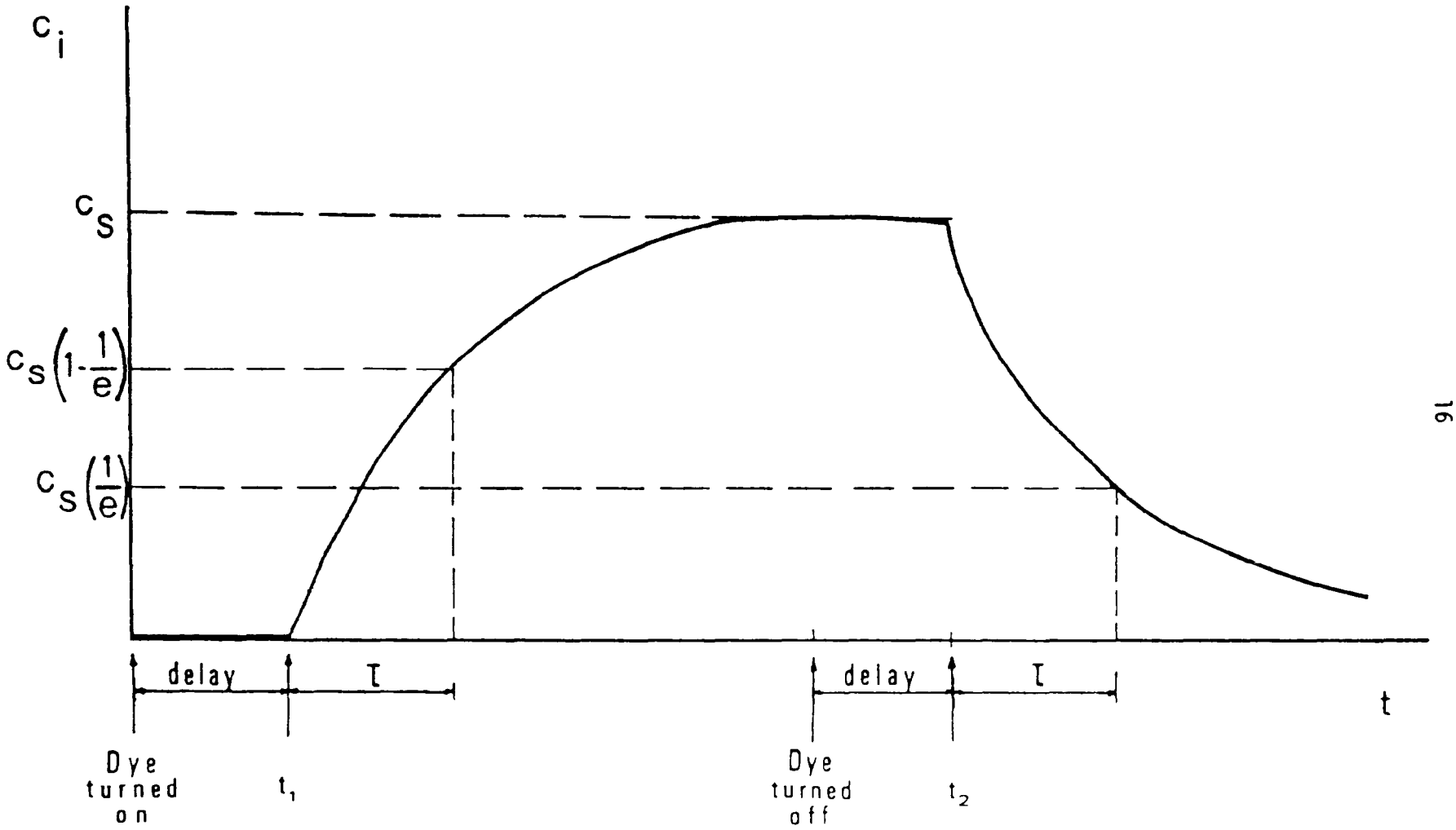

FIGURE 5. TEMPORAL CONCENTRATION VARIATION IN THE EDDY

where V and b are the velocity and width of the side channel discharge.

Four dependent variables are determined in the experiment. These are:

H_i = height of the eddy

L = length of the eddy

c_s = average steady-state concentration within the eddy

τ = retention time

The dimensionless relationships derived from the above characteristics are:

$$\frac{H_i}{l_s} = \text{fn.}\ (\frac{l_s}{B})$$

$$\frac{L}{l_s} = \text{fn.}\ (\frac{l_s}{B}) \qquad (9)$$

$$\frac{c_s U l_s}{c_o Q_o} = \text{fn.}\ (\frac{l_s}{B})$$

$$\frac{\tau U}{l_s} = \text{fn.}\ (\frac{l_s}{B})$$

where c_o and Q_o are the concentration and volume flux at the exit, and l_s is a length scale defined as

$$l_s = \frac{M_o}{U^2} \qquad (10)$$

Since

$$Q_o = Vb \quad \text{and} \quad M_o = V^2 b \tag{11}$$

the relationships in Equation 9 can be rewritten in more explicit forms:

$$\begin{aligned}
\frac{H_i U^2}{bV^2} &= \text{fn.}\ \left(\frac{bV^2}{BU^2}\right) \\
\frac{LU^2}{bV^2} &= \text{fn.}\ \left(\frac{bV^2}{BU^2}\right) \\
\frac{c_s V}{c_o U} &= \text{fn.}\ \left(\frac{bV^2}{BU^2}\right) \\
\frac{\tau U^3}{bV^2} &= \text{fn.}\ \left(\frac{bV^2}{BU^2}\right)
\end{aligned} \tag{12}$$

Two limiting cases may be considered. In the case of unbounded crossflow, i.e., $\frac{l_s}{B} = \frac{bV^2}{BU^2} \to 0$, we have

$$\begin{aligned}
\pi_1 &= \frac{H_i}{l_s} = \frac{H_i U^2}{bV^2} = \text{constant} \\
\pi_2 &= \frac{L}{l_s} = \frac{LU^2}{bV^2} = \text{constant} \\
\pi_3 &= \frac{c_s U l_s}{c_o Q_o} = \frac{c_s V}{c_o U} = \text{constant}
\end{aligned} \tag{13}$$

$$\pi_4 = \frac{\tau U}{l_s} = \frac{\tau U^3}{bV^2} = \text{constant}$$

On the other hand, when the width of the main channel crossflow is small compared to the length scale M_0/U^2, i.e., when $\frac{l_s}{B} = \frac{bV^2}{BU^2} \to \infty$ M_0 is no longer significant, and may be dropped. The results are

$$\pi_5 = \frac{H_f}{B} = \text{constant}$$

$$\pi_6 = \frac{L}{B} = \text{constant} \qquad (14)$$

$$\pi_7 = \frac{c_s BU}{c_0 bV} = \text{constant}$$

$$\pi_8 = \frac{\tau U}{B} = \text{constant}$$

Equation 14 can be rewritten in the form of Equation 12, as follows:

$$\frac{H_f U^2}{bV^2} = \pi_5 \left(\frac{bV^2}{BU^2}\right)^{-1}$$

$$\frac{LU^2}{bV^2} = \pi_6 \left(\frac{bV^2}{BU^2}\right)^{-1} \qquad (15)$$

$$\frac{c_s V}{c_0 U} = \pi_7 \left(\frac{bV^2}{BU^2}\right)^{+1}$$

$$\frac{\tau U^3}{bV^2} = \pi_8 \left(\frac{bV^2}{BU^2}\right)^{-1}$$

The constants $\pi_1, \pi_2, \pi_3, \pi_4, \pi_5, \pi_6, \pi_7, \pi_8$ that appear in the asymptotic relationships in Equations 13 and 14 will be determined from experimental observation.

2.4 Assumptions

Two basic approximations have been employed in the derivation presented in the previous sections. They are the "point source approximation" and the assumption of a "two-dimensional flow". The limitation of these assumptions is discussed in the following sections.

2.4.1 The Point Source Approximation

In general, the conditions of the jet effluent can be characterized by its velocity V and width b at the exit. Alternatively, the dependency on b and V can be expressed in terms of the two fluxes defined as follows:

Q_o = exit volume flux = bV

M_o = exit momentum flux = bV^2

The investigation of Mikhail et al. (1975) has pointed out the importance of these flux variables. In fact, the dependency on the exit-volume flux Q_o has been shown to be of minor importance. This is due to the fact that the volume flux Q at some distance from the exit is significantly larger than Q_o, and that there is a tendency for turbulent flow to "forget" or

lose track of quantities that are not conserved.

The size of the source can be expressed in terms of Q_o and M_o as follows:

$$b = \frac{Q_o^2}{M_o}$$

For a fixed M_o, $b \to 0$ as $Q_o \to 0$. The approximation which makes use of the tendency of the jet to forget about exit volume flux Q_o or the source size b will be referred to in this study as a "point source" approximation. This approximation would be useful only when the size of the eddy is large compared with the exit channel width. Breakdown of the approximation may occur when the discharge velocity, V, is small compared with the crossflow velocity, U.

2.4.2 "Two-Dimensional Flow" Assumption

Throughout the presentation in this thesis, the flow is regarded as two-dimensional. The velocity and concentration variation over the depth of the water is ignored. The frictional force exerted on the channel bottom is assumed to be negligible. To estimate the effect of bottom friction, the following dimensionless parameter is defined:

$$\frac{\text{bottom frictional force}}{\text{exit-momentum flux}} = \frac{c_f V^2 bH}{V^2 bd} = c_f \frac{H}{d} \qquad (16)$$

where c_f is the bottom friction co-efficient, H the height of the eddy, and d the depth of water. In the present experiment, $c_f \approx 0.003$, $H/d \approx 0.5 \sim 3$. Thus, the effect of bottom frictional force is likely to

be negligible. In practical discharge problems, H/d can be very large, and bottom friction is not always negligible.

Further discussion of the two-dimensional flow approximation will be given in later chapters.

CHAPTER III

EXPERIMENTAL SET-UP AND PROCEDURES

3.1 General Set-Up

The experiments were conducted in a rectangular open channel 800 cm long, 60.96 cm wide, and 15 cm deep (Figure 6). The main channel was equipped with a diffuser, a gravel screen, and a series of flow straighteners, to reduce the swirling and secondary currents as well as turbulence in the crossflow. A plexiglass window 40 cm long was installed on one side of the main channel, immediately downstream of the exit of the side channel, to permit flow visualization in the recirculation zone.

Typical velocity profiles of the main channel flow are given in Figures 8 and 9. The thicknesses for the horizontal boundary layer and vertical profiles are approximately 6 cm and 0.5 cm respectively. The crossflow velocity, U, is obtained by timing floating pieces of paper over a known distance. The surface velocity obtained in this manner is not significantly different from the mean velocity, as can be seen from Figure 9.

The side channel was constructed from plexiglass, and was 60.6 cm long, 2.50 cm wide, and 15 cm deep. It was connected flush with the main channel, and at a distance of 141 cm from the upstream end of the main channel. A screen of pebbles was inserted to prevent dirt and rust from passing into the side channel. The result is more accurate concentration readings and low turbulence level at the exit (Figure 7).

FIGURE 6. MAIN CHANNEL AS VIEWED FROM THE DOWNSTREAM END

FIGURE 7. SIDE CHANNEL, DYE RESERVOIR, AND DIFFUSER

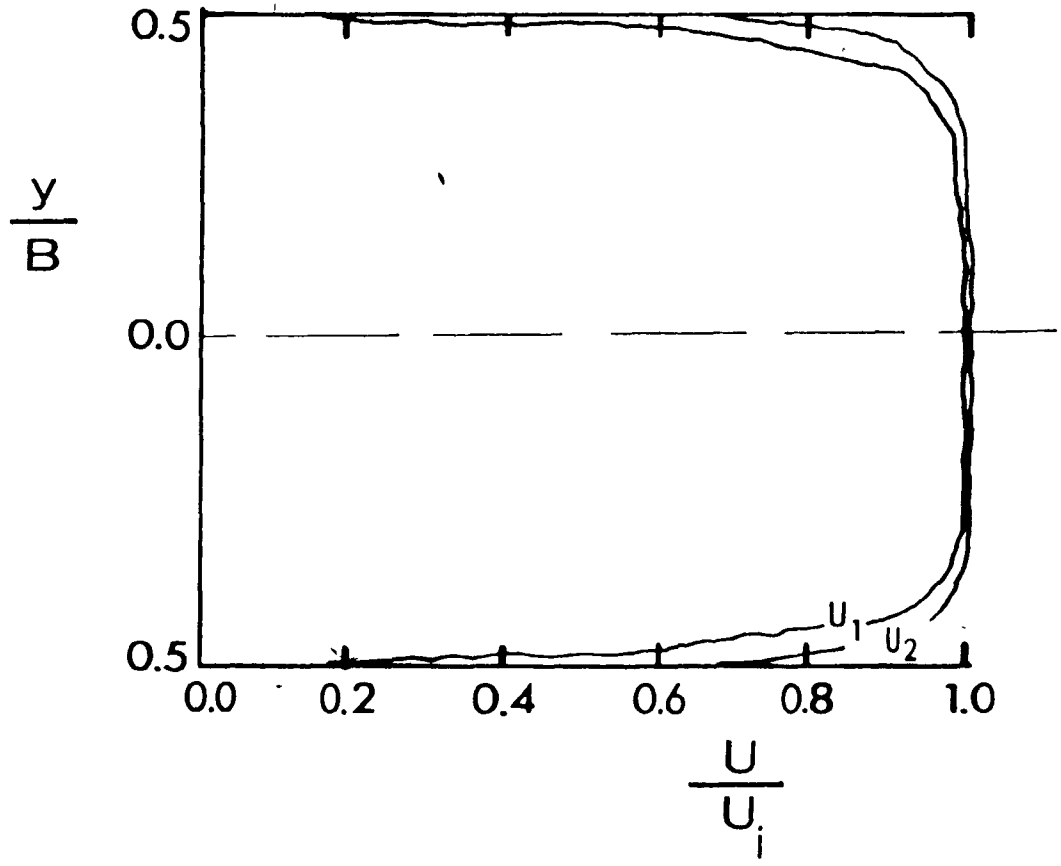

FIGURE 8. HORIZONTAL VELOCITY PROFILE OF THE CROSSFLOW

U_1 = 6 cm/sec, U_2 = 12 cm/sec, d = 10.4 cm

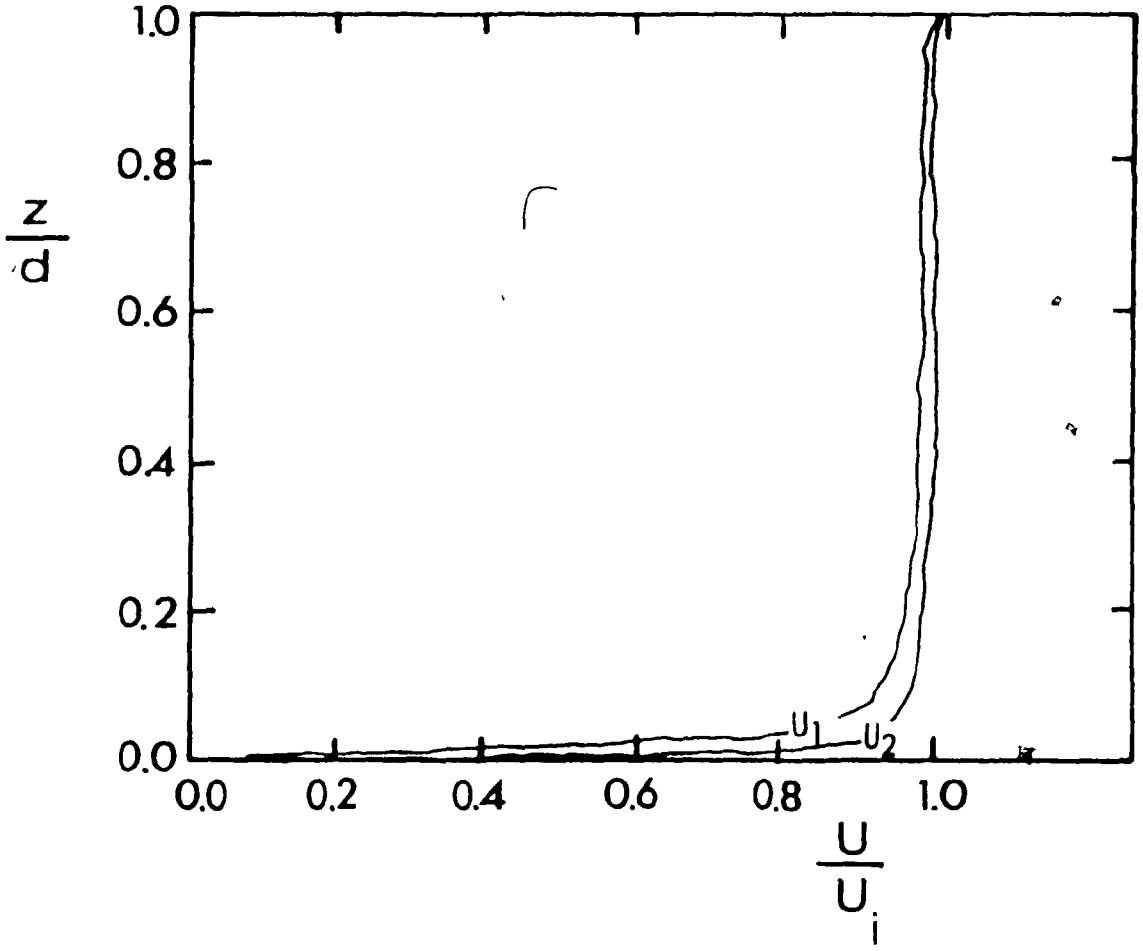

FIGURE 9. VERTICAL VELOCITY PROFILE OF THE CROSSFLOW

U_1 = 6 cm/sec, U_2 = 12 cm/sec, d = 10.4 cm

Both channels were fed with tap water of the same temperature, ranging between 22°C and 24°C, for the course of the experiments.

The discharge from the side channel was determined by a rotameter which had a range of 2-22 U.S. gpm (BROOKS TYPE 1110-10-B-0000). Side channel velocity, V, listed in Table 1, was determined by dividing the discharge by the cross-sectional area.

During the experiment, india ink solutions were used as the dye tracer. The solution was supplied from a constant head tank and was introduced through a diffuser located at the upstream end of the side channel. A stirrer was installed immediately downstream of the diffuser to promote further mixing (see Figures 7 and 15).

Dye concentration at the exit and in the eddy was determined by a light absorption probe, which is described in the next section.

3.2 Light Absorption Probes

Concentration of the india ink solution was determined by a light absorption probe. The principal elements of the probe consist of a Light Emitting Diode (L.E.D.) (TIL 23), and a phototransistor (TIL 78), as shown in Figure 10. During the measurements, india ink solution would pass through a 2 cm gap between the L.E.D. and the phototransistor. Changes in ink concentration would result in changes in light transmission, and this would in turn change the current passing through the phototransistor circuitry. The probe circuit diagram is sketched in Figure 11. The voltage across the phototransistor was maintained at 6.8V using a Zener Diode (IN 5342). The voltage signal of the phototransistor was transmitted to the DATAC computer facility at McGill University.

(a) Light Absorption Probe

(b) Tip of the Probe with Photo-transistor Mounted on the Top Cell, and L.E.D. on the Bottom

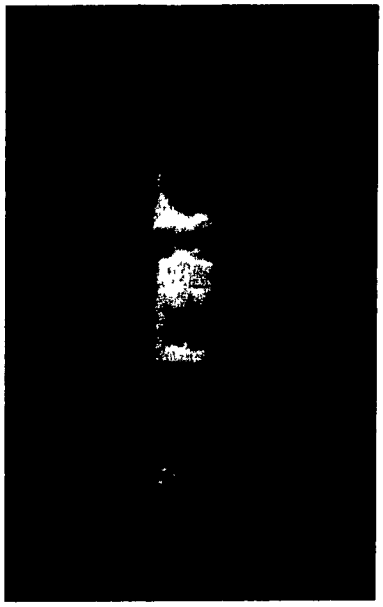

FIGURE 10. LIGHT ABSORPTION PROBE

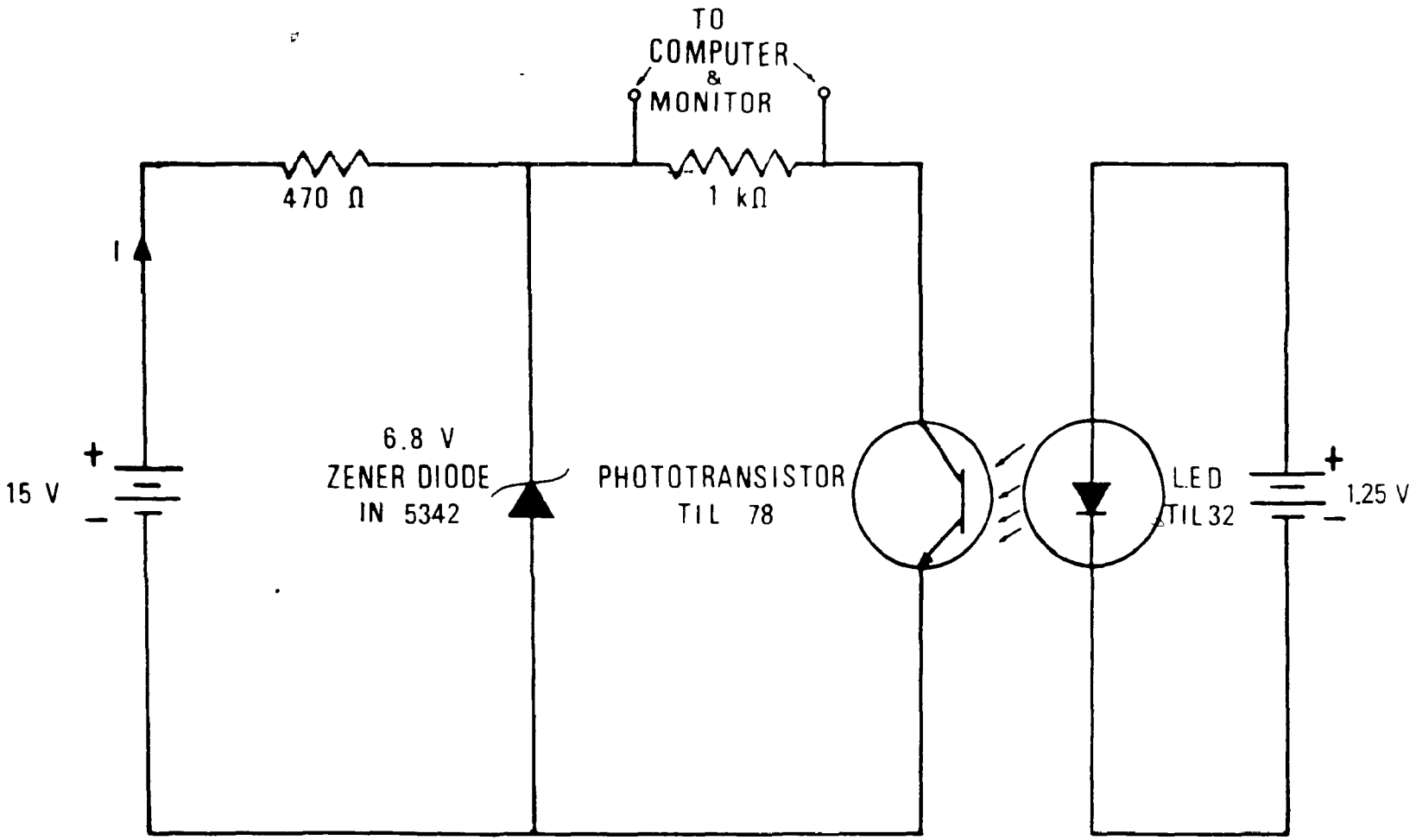

FIGURE 11. PROBE CIRCUIT

Many different dye tracers were tried, and india ink solutions were chosen. The reason is that most dye tended to decay rapidly with time. India ink was preferred for its stability and opacity.

3.3 Calibration of Light Absorption Probes

Calibration was carried out by submerging the probes in standard solutions. Samples were prepared immediately before the calibration. Starting with a high concentration of 5.128 mℓ of india ink per liter of solution. The sample was diluted by doubling its volume each time with clear water. The minimum concentration of standard solutions was 0.016 mℓ/ℓ (16 ppm).

Calibration data for the three probes used in the experiment is shown in Figures 12, 13, and 14. The equations for the calibration curves were obtained through a least square fitting. The sensitive part of the calibration is seen only in the range between 0.1 ~ 1 mℓ/ℓ. Attempts were made during the experiment to maintain the concentration in the eddy within this sensitive range.

Note that several calibration curves were carried out for each probe. The clear water reading tends to vary somewhat from test to test. However, the slope of the curves is not significantly different. The calibration curves used were obtained by fitting them on one set of data points. Small variations of clear water readings were corrected during the experiments by adjusting the power supply of the L.E.D.

3.4 Experimental Procedures

The experimental information gathered in this report consists of

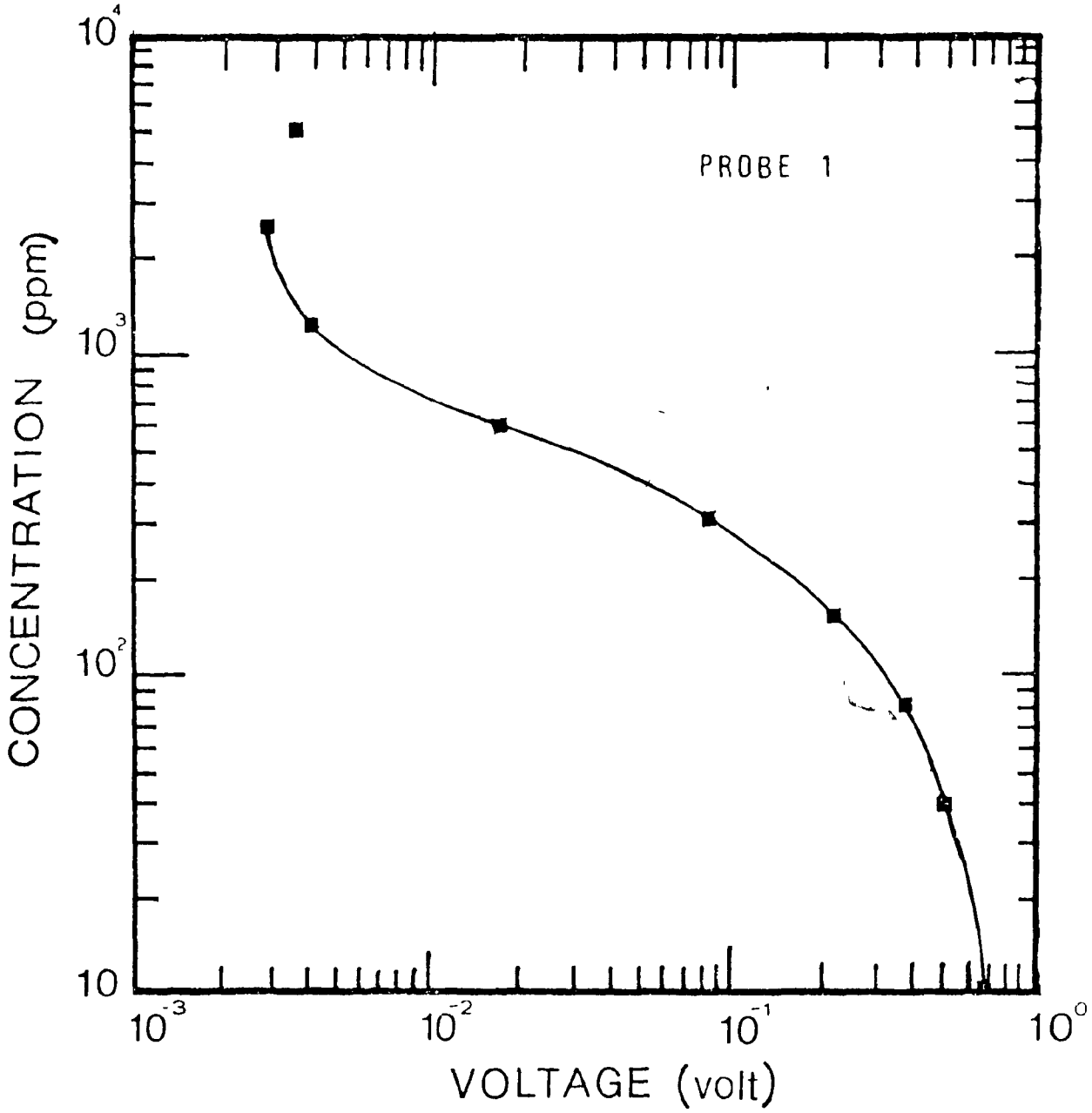

FIGURE 12. CALIBRATION CURVE, PROBE 1

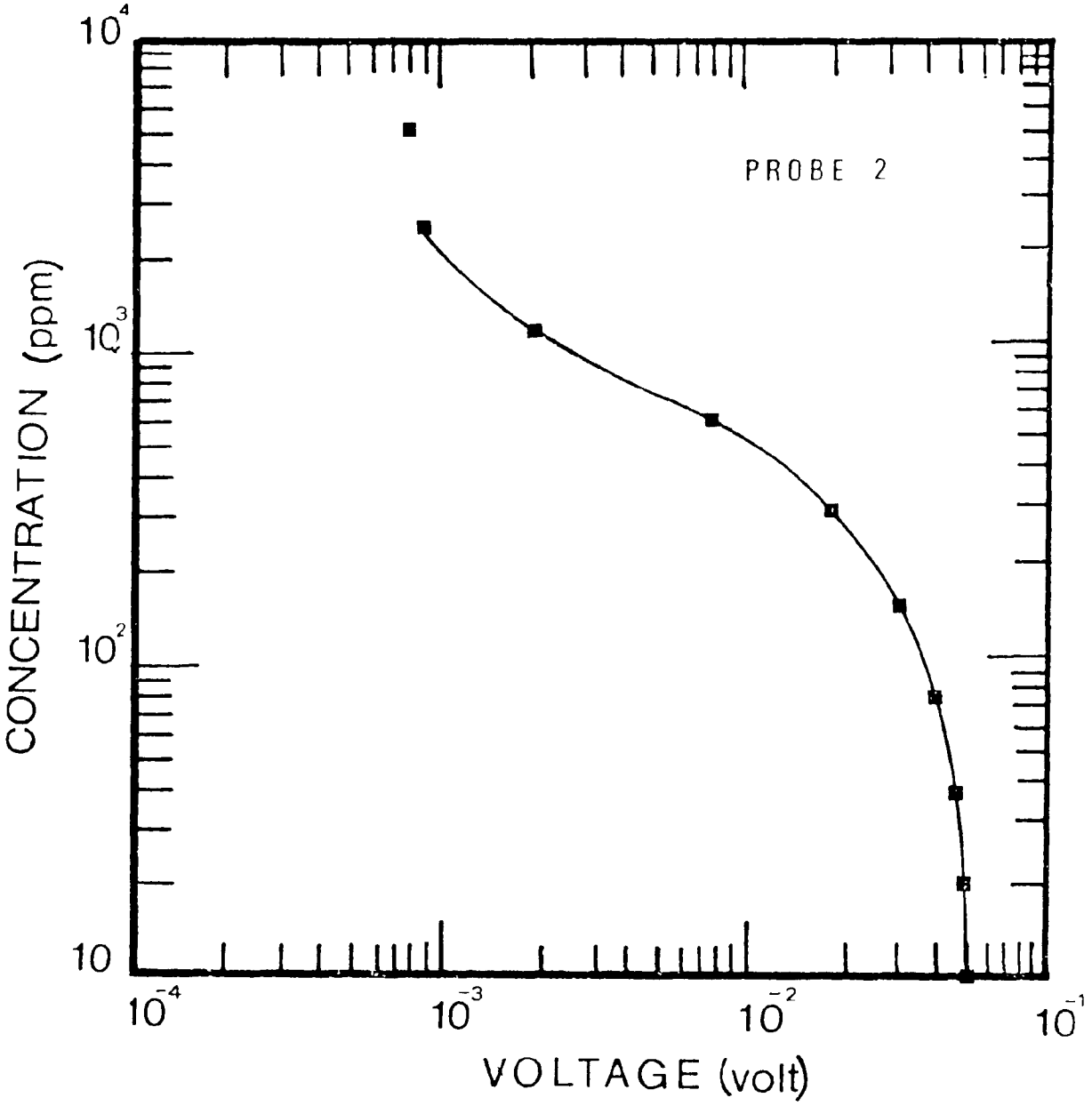

FIGURE 13. CALIBRATION CURVE, PROBE 2

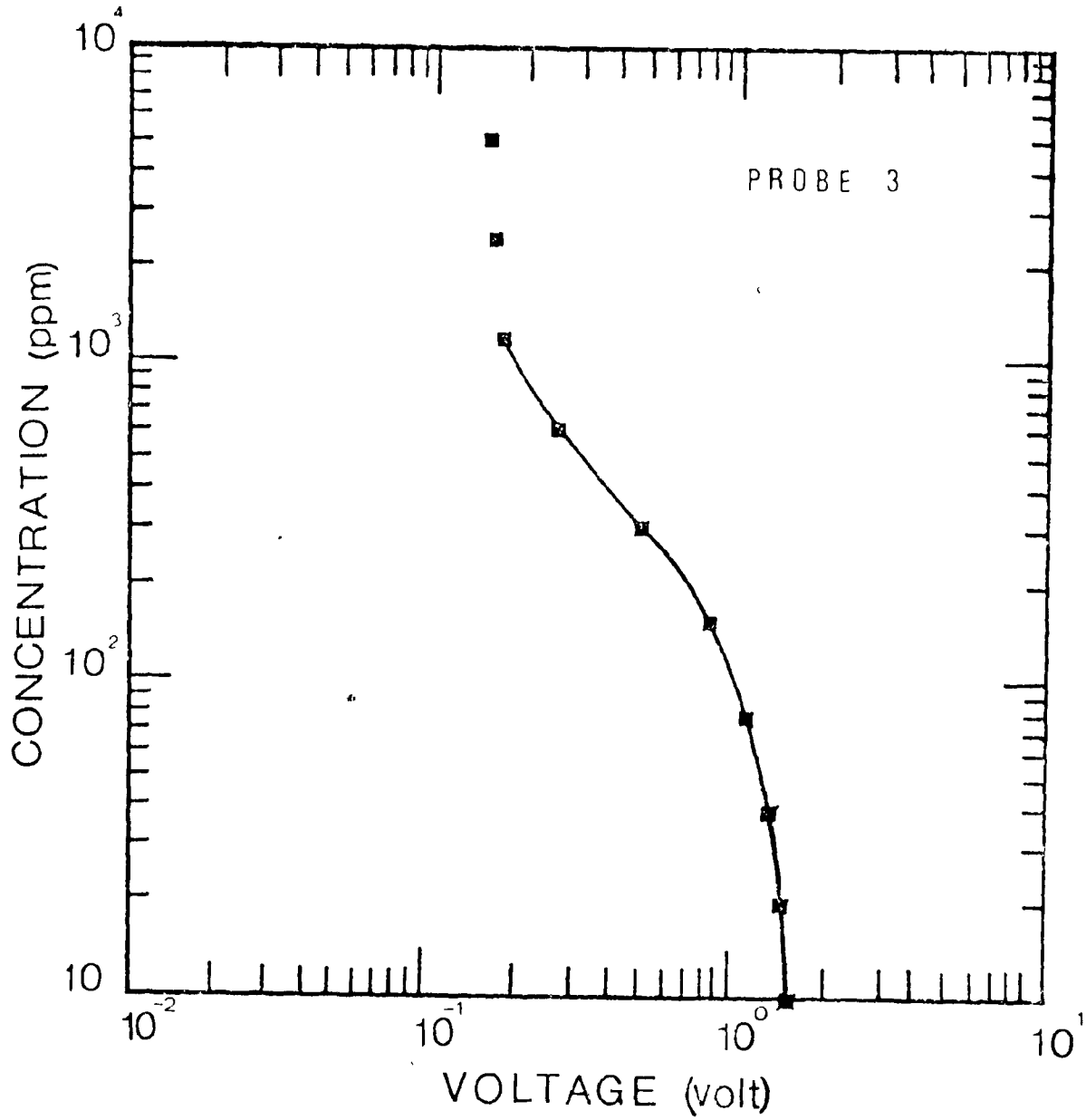

FIGURE 14. CALIBRATION CURVE, PROBE 3

eddy geometry and concentration variation in the eddy. Parameters related to the eddy geometry, such as eddy height, H_i, eddy length, L, and jet width, $H_o - H_i$, are determined from flow visualization. Concentration within the eddy was determined from measurements using the optical probes. From the transient variation of concentration within the eddy, two parameters were obtained, these being retention time, τ, and steady-state concentration, c_s

A series of twenty-two tests were carried out The test conditions are summarized in Table 1. During the experiments, dye was released from the upstream end of the side channel through a diffuser. The diffuser was constructed from rigid plastic tube with a pattern of holes drilled diametrically on it. Some of the holes were blocked temporarily to obtain uniformity of dye concentration throughout the depth.

Further mixing was achieved by using a stirrer immediately downstream of the diffuser, as shown in Figure 15.

3.4.1 Determination of Eddy Geometry

The eddy geometry was determined from flow visualization. The typical sequence of events as dye was released from the side channel is shown in Figure 3 (a - h). The dyed jet can be seen in the series of photos to be bent by the crossflow. It then impinges on the side wall. The point of impingement can be approximately determined by the flow situation, as shown in Figure 3 (c) (see the position of the arrow). For the present study, this point of impingement is taken to be the stagnation point. Due to very high levels of oscillations in the impinging region of the jet, the determination of this stagnation point is difficult and subjective. More accurate determination of the stagnation point

TABLE 1. TEST CONDITIONS

TEST NO.	U (cm/sec)	V (cm/sec)	d (cm)	V^2b/U^2B	c_o (ppm)
1-1-B	10.56	5.37	11.27	0.0106	660
1-1-T	10.56	5.37	11.27	0.0106	665
2-1-B	10.54	10.74	11.27	0.0426	700
2-2-B	10.80	10.74	11.27	0.0406	470
2-1-T	11.11	10.74	11.27	0.0383	555
2-2-T	10.56	10.74	11.27	0.0424	500
3-1-B	10.52	21.04	11.27	0.1640	1180
3-2-B	10.51	21.04	11.27	0.1670	1300
3-3-T	10.91	21.04	11.27	0.1530	870
3-4-T	10.72	21.49	11.27	0.1650	530
4-1-B	10.65	42.54	11.27	0.6540	1000
4-2-B	10.92	40.30	11.27	0.5590	820
4-1-T	10.92	42.54	11.27	0.6220	760
4-2-T	10.17	42.54	11.27	0.6680	1000

b = 2.50 cm

B = 60.96 cm

TABLE 1 (continued)

TEST NO.	U	V	d	V^2b/U^2B	C_o
5-1-B	5.91	5.64	11.19	0.0370	720
5-1-T	6.00	5.64	11.19	0.0360	730
6-1-B	5.96	11.27	11.19	0.1470	1150
6-1-T	5.91	11.27	11.19	0.1490	770
7-1-B	6.09	22.39	11.27	0.5540	900
7-1-T	5.96	22.39	11.27	0.5790	910
8-1-B	6.21	44.78	11.27	2.1300	900
8-1-T	6.09	44.78	11.27	2.2200	500

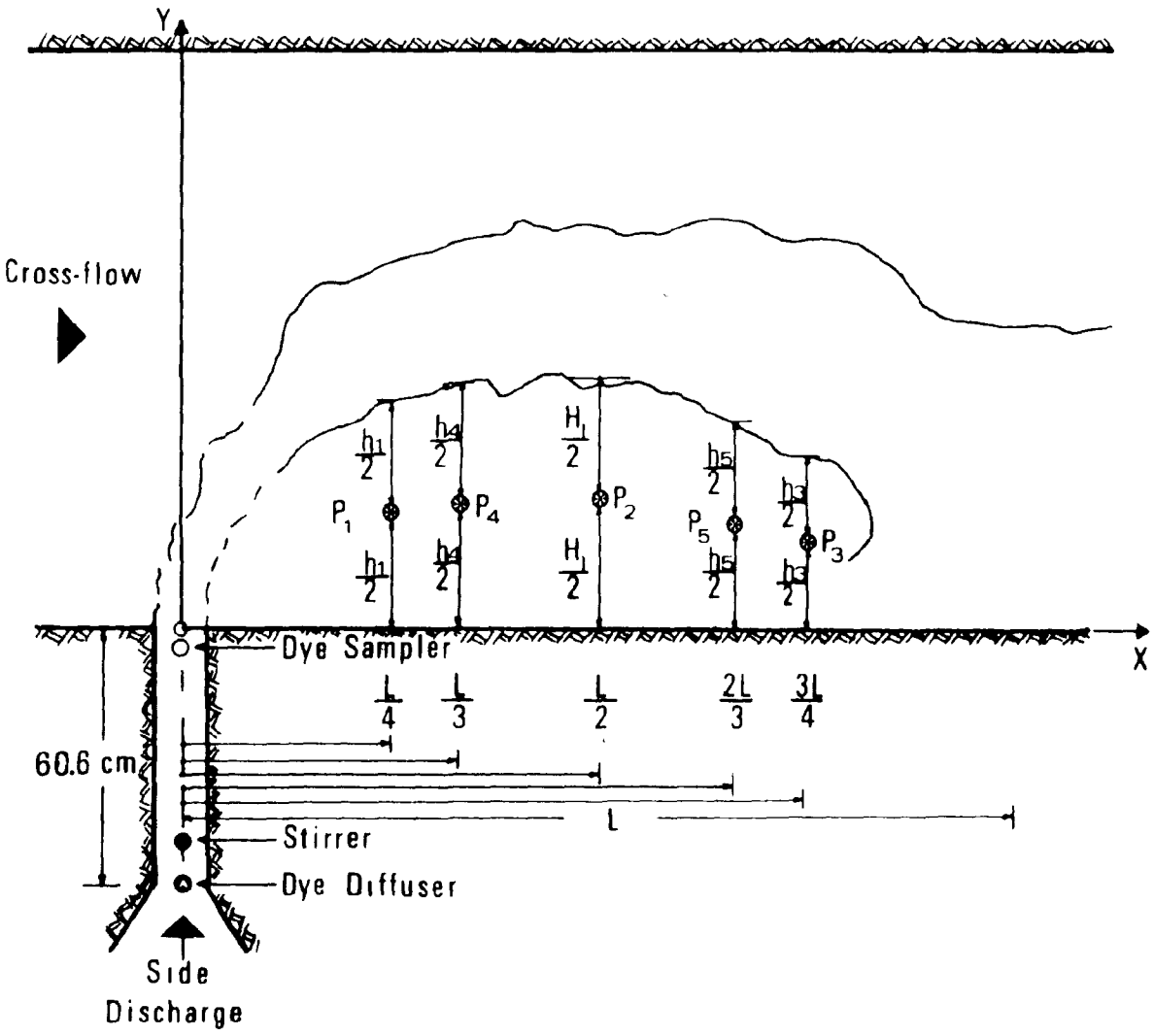

FIGURE 15. EXPERIMENTAL SET-UP

was obtained by observing the movement of paper chips floating on the free surface of the impinging region. The length of the eddy is defined as the distance from the exit to the stagnation point.

The height of the eddy is characterized by two length scales, H_1 and H_0, as defined in Figure 2. H_0 is defined as the height of the average outer boundary of the dyed jet, as in Figure 3 (c). The height of the inner boundary, H_i, was determined by turning the dye off and observing the average boundary of the eddy in situation, as shown in Figure 3 (d). Jet width at the crest of the eddy can be estimated by taking the difference between H_0 and H_i.

3.4.2 Determination of Dye Concentration

The concentration distribution within the eddy is determined by means of the optical probes located within the recirculating zone, as can be seen from Figure 15. Three probes were used. The x and y coordinates of the probe positions were:

$$P_1 \left(\frac{L}{4}, \frac{h_1}{2}\right)$$

$$P_2 \left(\frac{3L}{2}, \frac{H_1}{2}\right)$$

$$P_3 \left(\frac{3L}{4}, \frac{h_3}{2}\right)$$

or

$$P_4 \left(\frac{L}{3}, \frac{h_4}{2}\right)$$

$$P_5 \left(\frac{2L}{3}, \frac{h_5}{2}\right)$$

where h_1, H_1, h_3, h_4, and h_5 are the total heights of the eddy. The probes were positioned on the proper coordinates by means of a supporting frame. Concentration measurements were carried out with the probes located at two different elevations. Test numbers in Table 1, designated as "B" and "T", correspond to the elevations z = d/4 and 3d/4 from the bottom, respectively.

Small drift was sometimes observed in the output of the optical probes. Clear water voltage readings different from the values obtained during the calibration of the probes could be corrected by small adjustments of the voltage supply to the L.E.D.

Analog signals form the optical probes were digitized by a VIDAR voltmeter at a rate of five samples per second, and were subsequently stored on the DATAC computer facility for further analysis.

Concentration at the exit was determined from dye samplers located at six different elevations. A typical concentration profile is shown in Figure 16. The exit concentration, c_0, was obtained from the average of the six samples.

To study the transient concentration variations in the eddy, dye was released from the side channel for a period of time, until a steady-state concentration, c_s, is reached.

Once the output of the optical probe reached a reasonable quasi-steady-state for approximately twenty seconds, the dye injection was ceased (while the same discharge conditions from the side channel were maintained) in order to observe the transient decay of concentration within the eddy. The retention time was then obtained from the resulting concentration variations in the eddy, as described schematically in Figure 5.

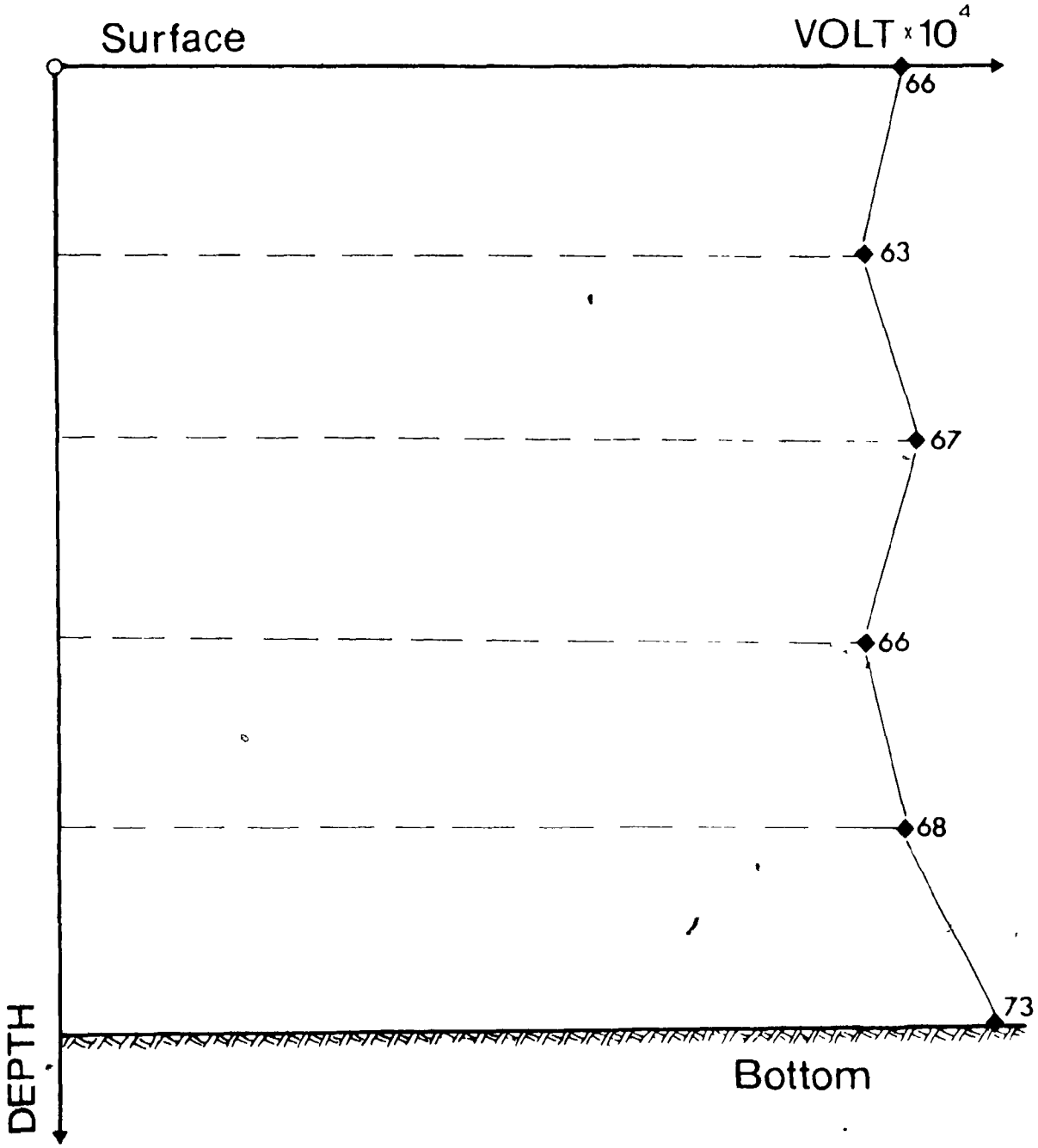

FIGURE 16. REPRESENTATIVE VOLTAGE READINGS FOR CONCENTRATION DISTRIBUTION AT THE EXIT OF THE SIDE CHANNEL; TEST NO. 7-1-B

CHAPTER IV

EXPERIMENTAL RESULTS AND DISCUSSION

The experimental results were organized based on the parameters needed to describe the overall process of the entrapment phenomenon in the recirculating eddy. The parameters describing the eddy geometry are the heights, H_o and H_i, and the length, L, which were obtained from flow visualization.

The concentration variations within the eddy, as determined by the light absorption probes, were used to determine the two other overall parameters, namely, the steady-state concentration, c_s, and the retention time, τ.

The results were correlated in terms of dimensionless variables that were derived from a point source model, as described in Chapter II. The experimental results of the present and previous investigations are tabulated in Appendix I.

4.1 Eddy Geometry

The results for the length, L, and height, H_i, of the eddy are presented in Figures 17, 18, 19, and 20. Despite the scatter of the experimental data, the results can be seen to be consistent with the data of previous investigations by Rouse (1957), Strazisar and Prahl (1973), and Mikhail et al. (1975).

Slightly different definitions for the length and height of the

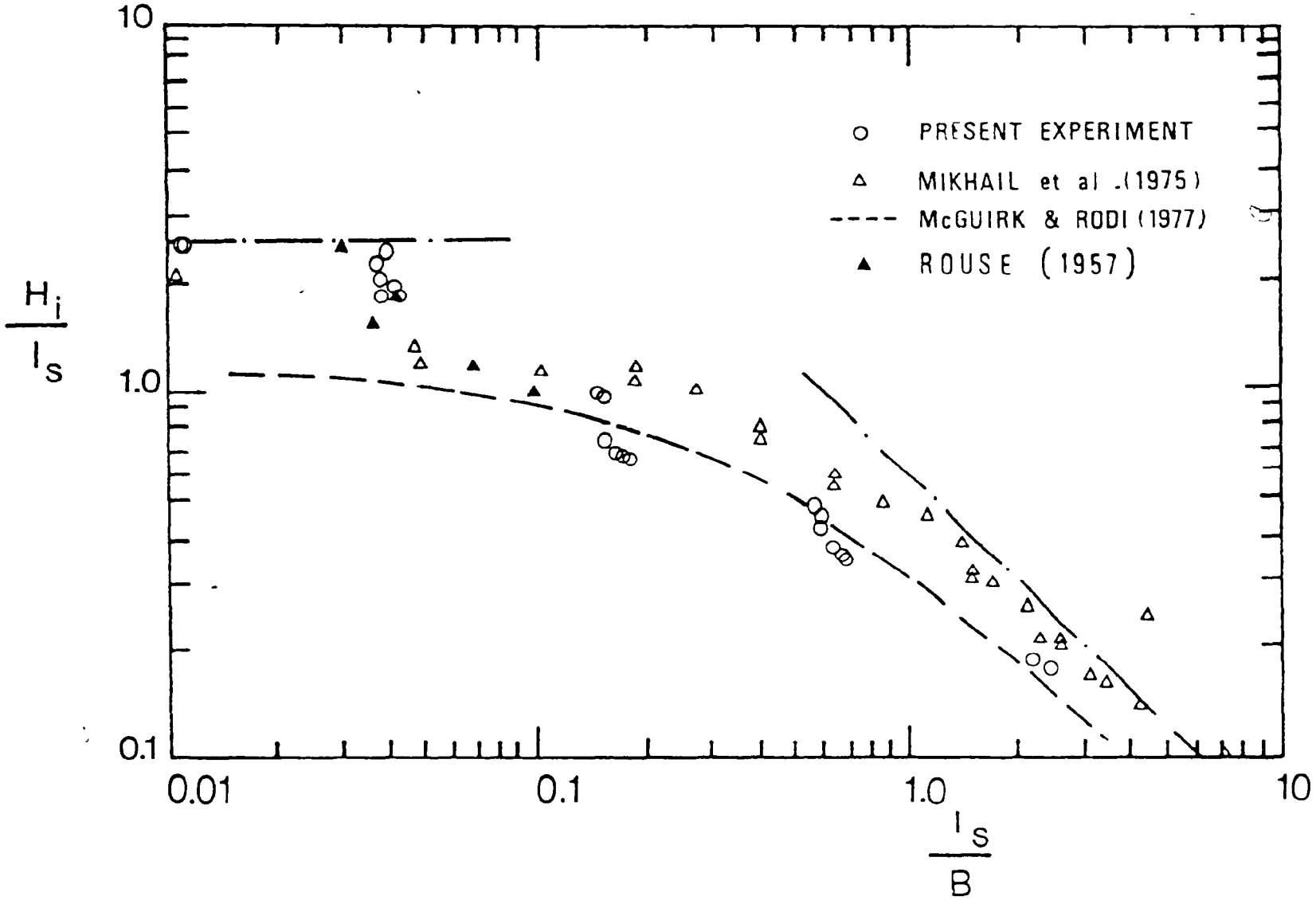

FIGURE 17. HEIGHT OF THE EDDY

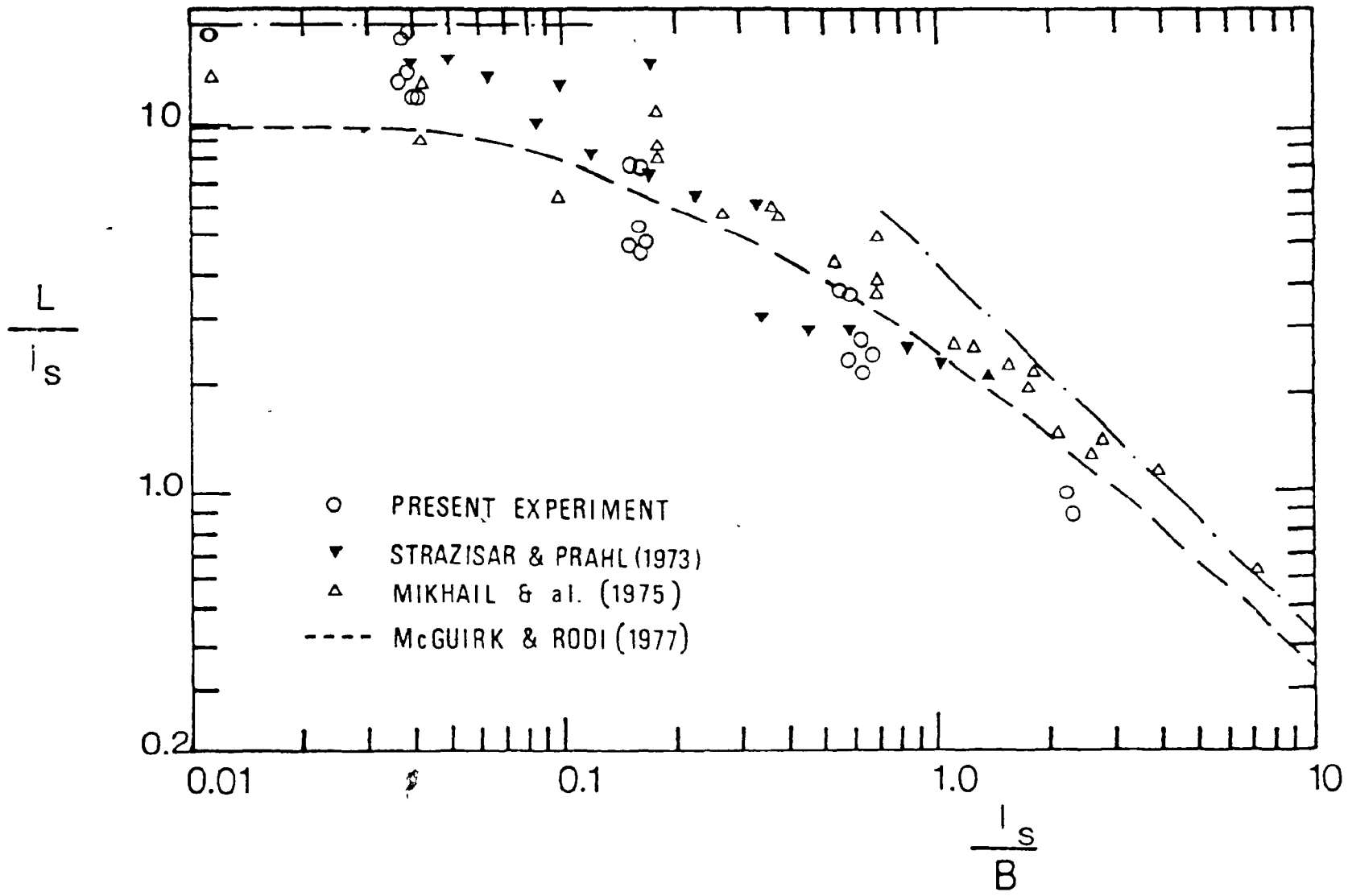

FIGURE 18. LENGTH OF THE EDDY

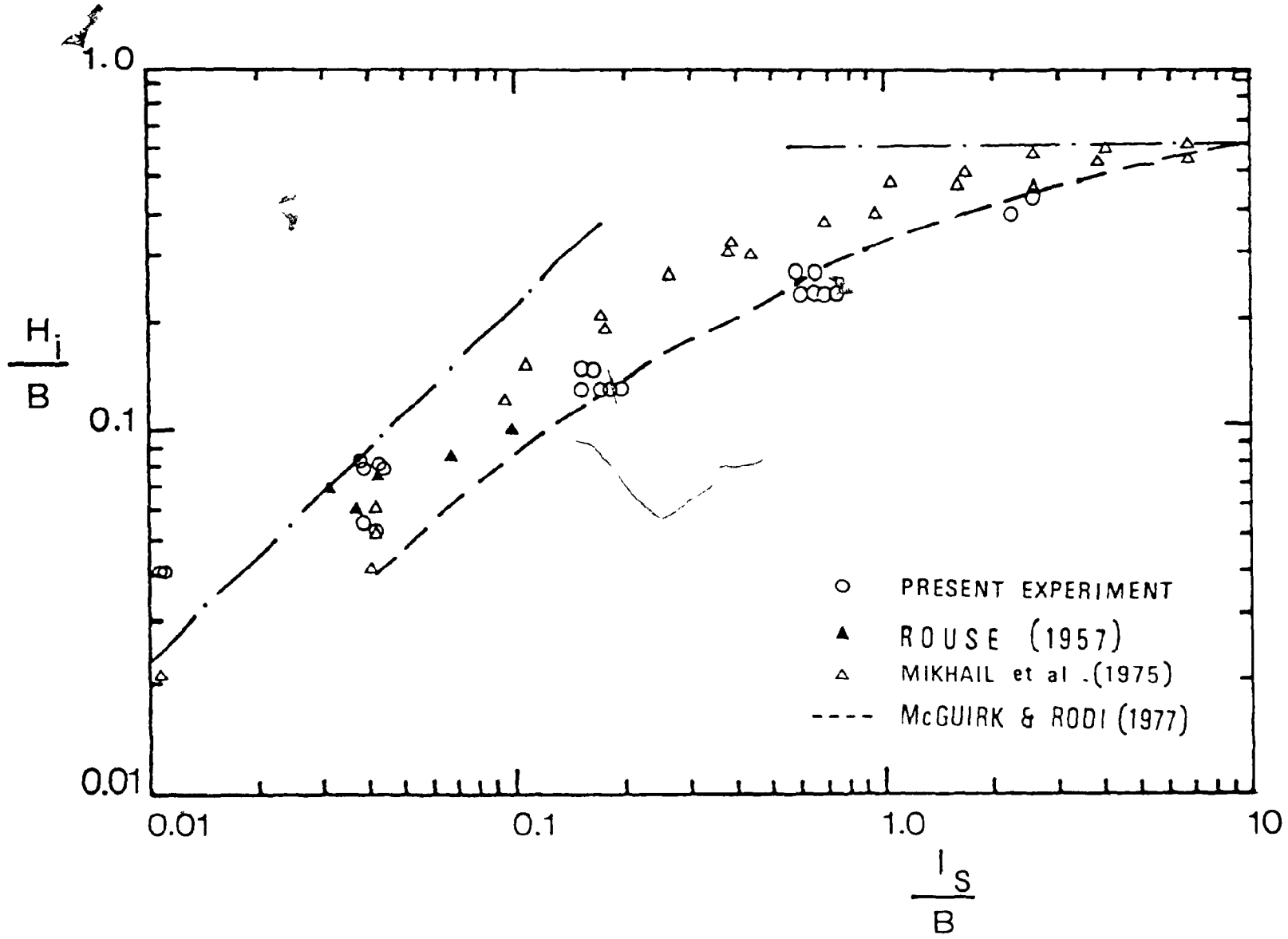

FIGURE 19. HEIGHT OF THE EDDY

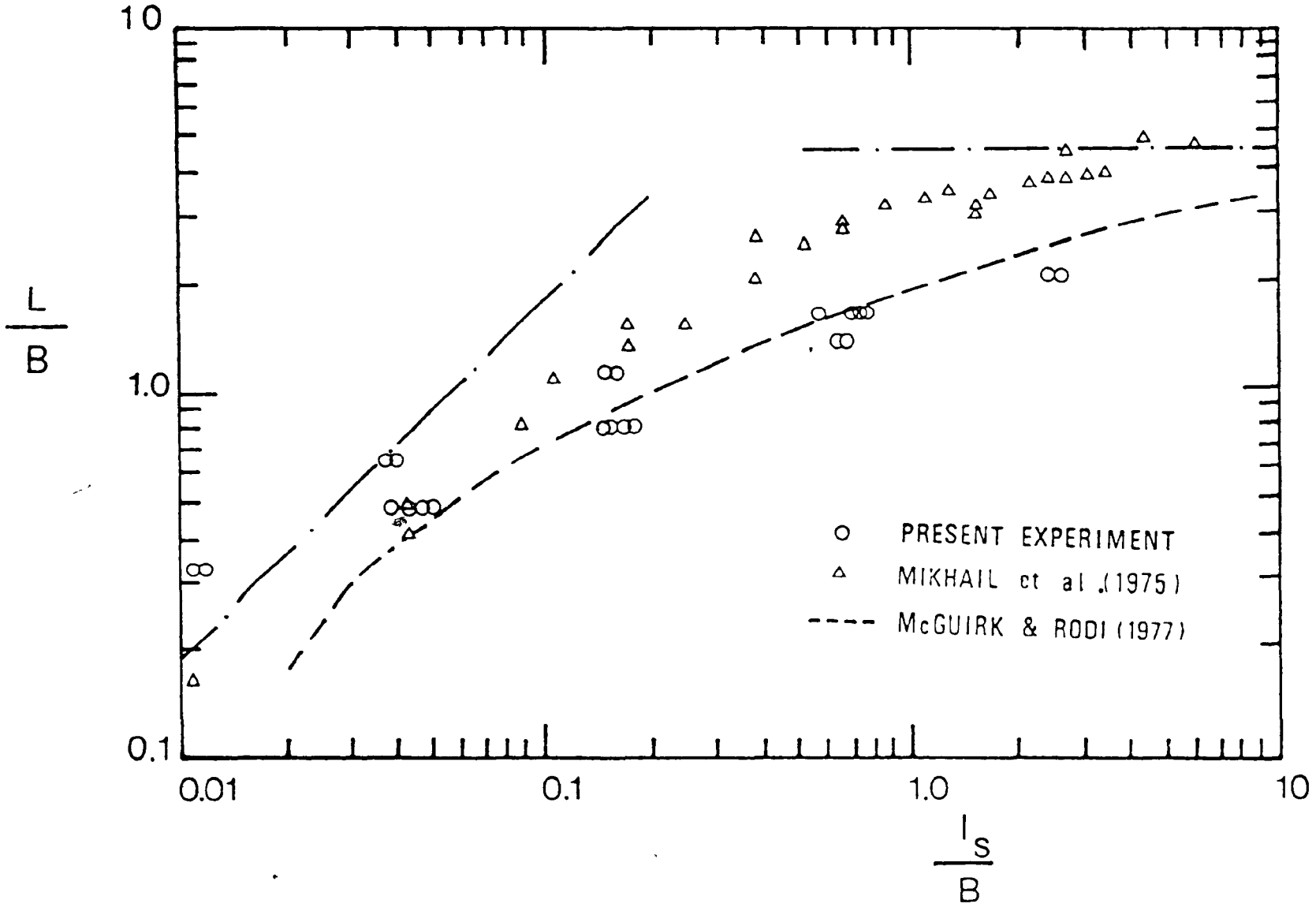

FIGURE 20. LENGTH OF THE EDDY

eddy have been used by the different investigators. Rouse (1957) defined the height and length of the eddy based on the dividing stream line, which was determined by velocity measurements. Strazisar and Prahl (1973) and Mikhail et al. (1975) used flow visualization procedures similar to those used in the present investigation.

However, the data of Mikhail et al. (1975) represent the average results of three crossflow velocities. The numerical computations for similar flow situations have been carried out by McGuirk & Rodi (1977). Their results are seen to follow the general trend of the experimental data.

The data can be seen to have an asymptotic trend, as suggested by the dimensional analysis in Chapter II. When the width of the crossflow is very large compared with the size of the eddy, i.e., $l_s/B \to 0$, the scale of the eddy is linearly proportional to the length scale l_s. On the other hand, when the eddy size is comparable to the width of the crossflow, i.e., when $l_s/B \to \infty$, the scale of the eddy is proportional to the width of the crossflow. Fitting the experimental data by asymptotic lines, as shown in Figures 17-20, the following limiting formulae are obtained:

For unconfined crossflow, i.e., $\frac{l_s}{B} = \frac{V^2 b}{U^2 B} \to 0$

$$\frac{H_i}{l_s} = 2.4 \qquad \text{and} \qquad \frac{L}{l_s} = 18 \tag{17a, b}$$

or equivalently,

$$\frac{H_i U^2}{bV^2} = 2.4 \qquad \text{and} \qquad \frac{LU^2}{bV^2} = 18 \qquad (17c, d)$$

On the other hand, for narrow crossflow, i.e., $\frac{l_s}{B} = \frac{V^2 b}{U^2 B} \to 0$

$$\frac{H_i}{l_s} = 0.6 \frac{B}{l_s} \qquad \text{and} \qquad \frac{L}{l_s} = 4.4 \frac{B}{l_s} \qquad (18a, b)$$

or,
$$\frac{H_i}{B} = 0.6 \qquad \text{and} \qquad \frac{L}{B} = 4.4 \qquad (18c, d)$$

The constants appearing in the formulae are tentative, due to the large scatter of data. The eddy sizes in two of the tests, 1-1-B and 1-1-T, with low l_s/B are very small, and they are likely affected by the boundary layer of the crossflow.

The height to length ratio, H_i/L, is presented in Figure 21. The eddy can be seen to maintain a similar shape for a wide range of values of l_s/B. On the average,

$$\frac{H_i}{L} = 0.135 \qquad (19)$$

The constants in the asymptotic formulae, Equations 17 and 18, were chosen to be consistent with Equation 19.

The width of the jet can be represented by the difference in height, $H_o - H_i$ (for a definition of the parameters, see Figure 2). Figure 22

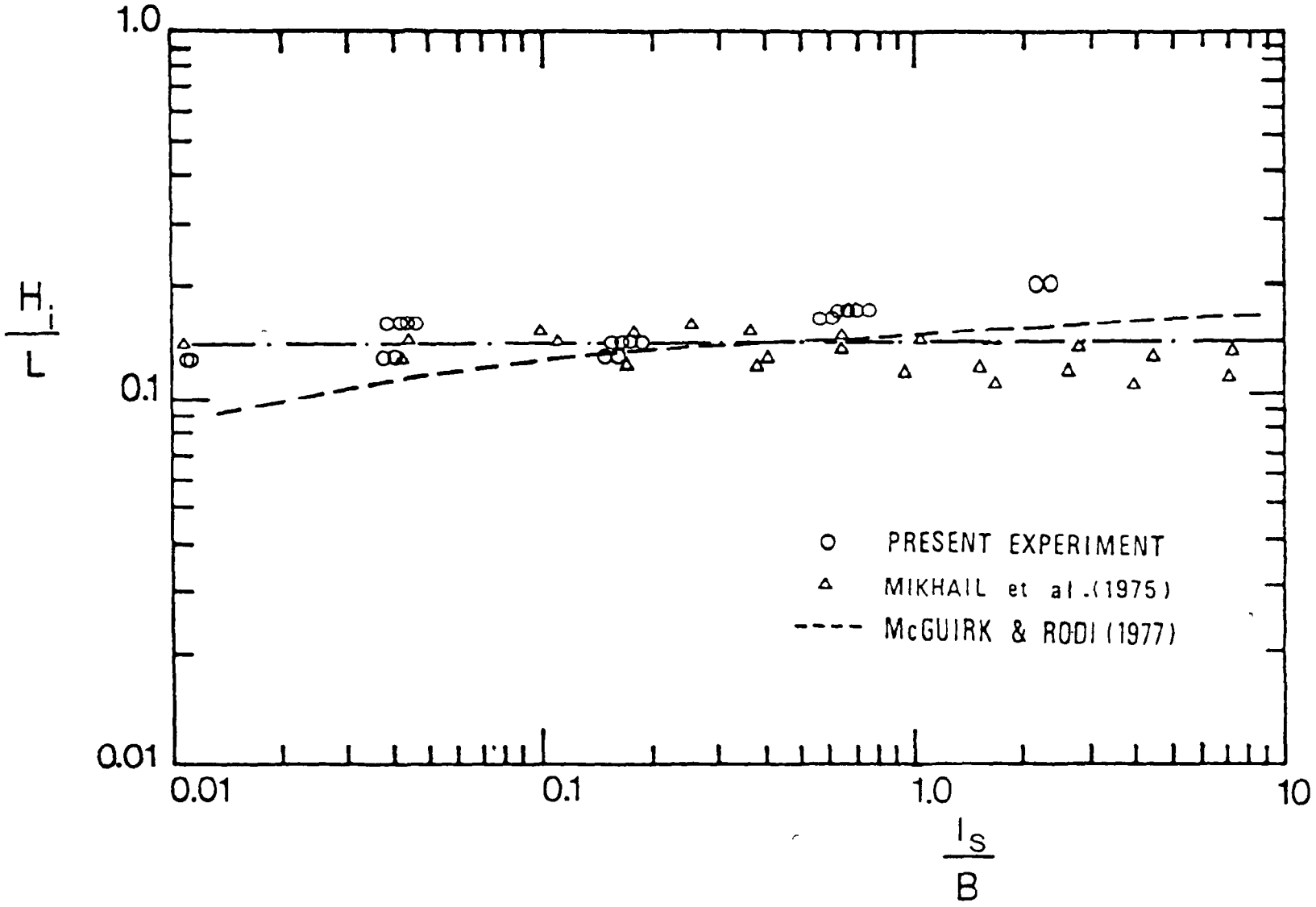

FIGURE 21. SHAPE OF THE EDDY

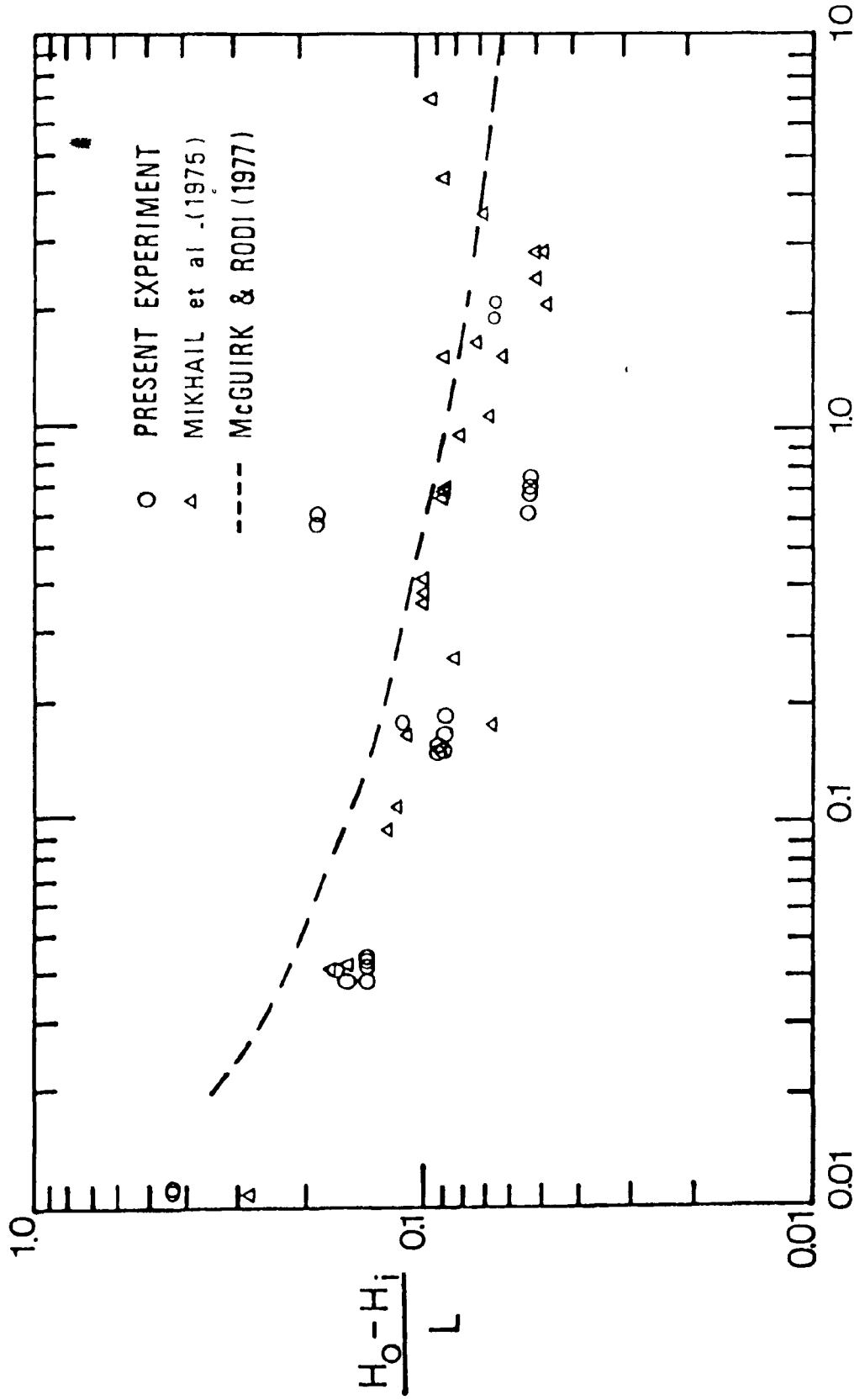

FIGURE 22. WIDTH OF THE JET

gives the spreading rate of the curved jet $\frac{H_o - H_i}{L}$. The spreading rate for a free jet is about 0.17 (based on width defined at 50% Intermittancy level). The data points in Figure 22 can be seen, in general, to lie below the free jet value; a few tests with very small eddy sizes ($l_s/B \approx 0.01$) are believed to have been affected by the crossflow boundary layer.

The reduction of the spreading rate in a narrow crossflow (large l_s/B) is apparently the result of the confinement by the width of the crossflow.

4.2 Concentration Variation

During the experiments, dye was released from the side channel for a period of time sufficient for the steady-state concentration to build up in the eddy. Typical concentration graphs for three probe locations, P_1, P_2, P_3, as obtained through a CALCOMP Plotter, are shown in Figure 23. (Other concentration graphs are summarized in Appendix II.) The concentration can be seen to rise to a quasi-steady-state for a period of time, and then decay after the dye is turned off at the side channel.

Based on these graphs, an average steady-state concentration, c_i, can be determined for each probe location P_i ($i = 1, 2, 3$). In general, the spatial concentration variations, as obtained at various locations within the eddy, are shown in Figure 24. Since the concentrations at different locations are not significantly different from each other, an average steady-state concentration, c_s, is introduced as the average of the c_i's, as follows:

$$c_s = \frac{1}{n} \sum_{i=1}^{n} c_i \qquad (20)$$

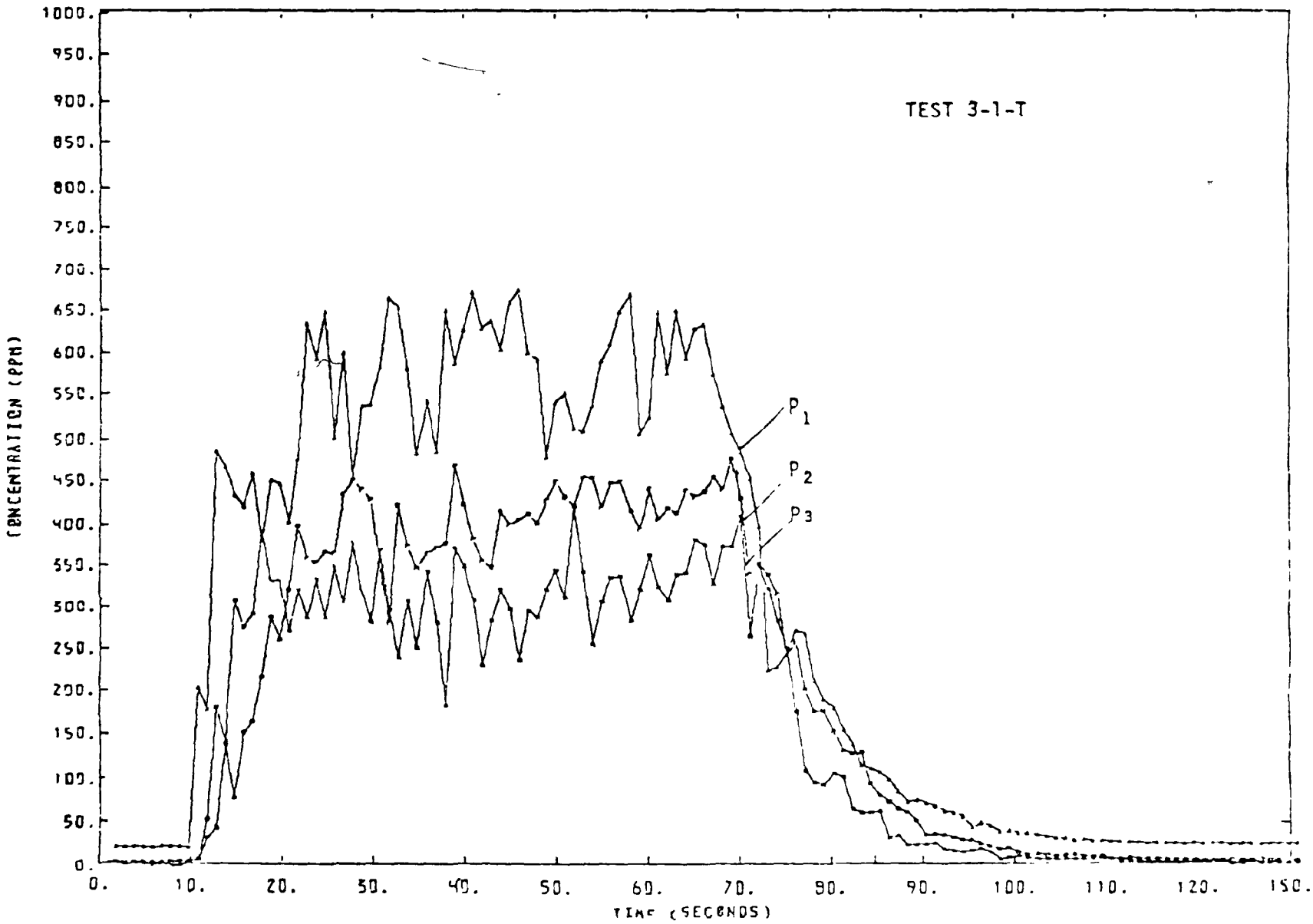

FIGURE 23. TEMPORAL CONCENTRATION VARIATION AT THREE LOCATIONS WITHIN THE EDDY

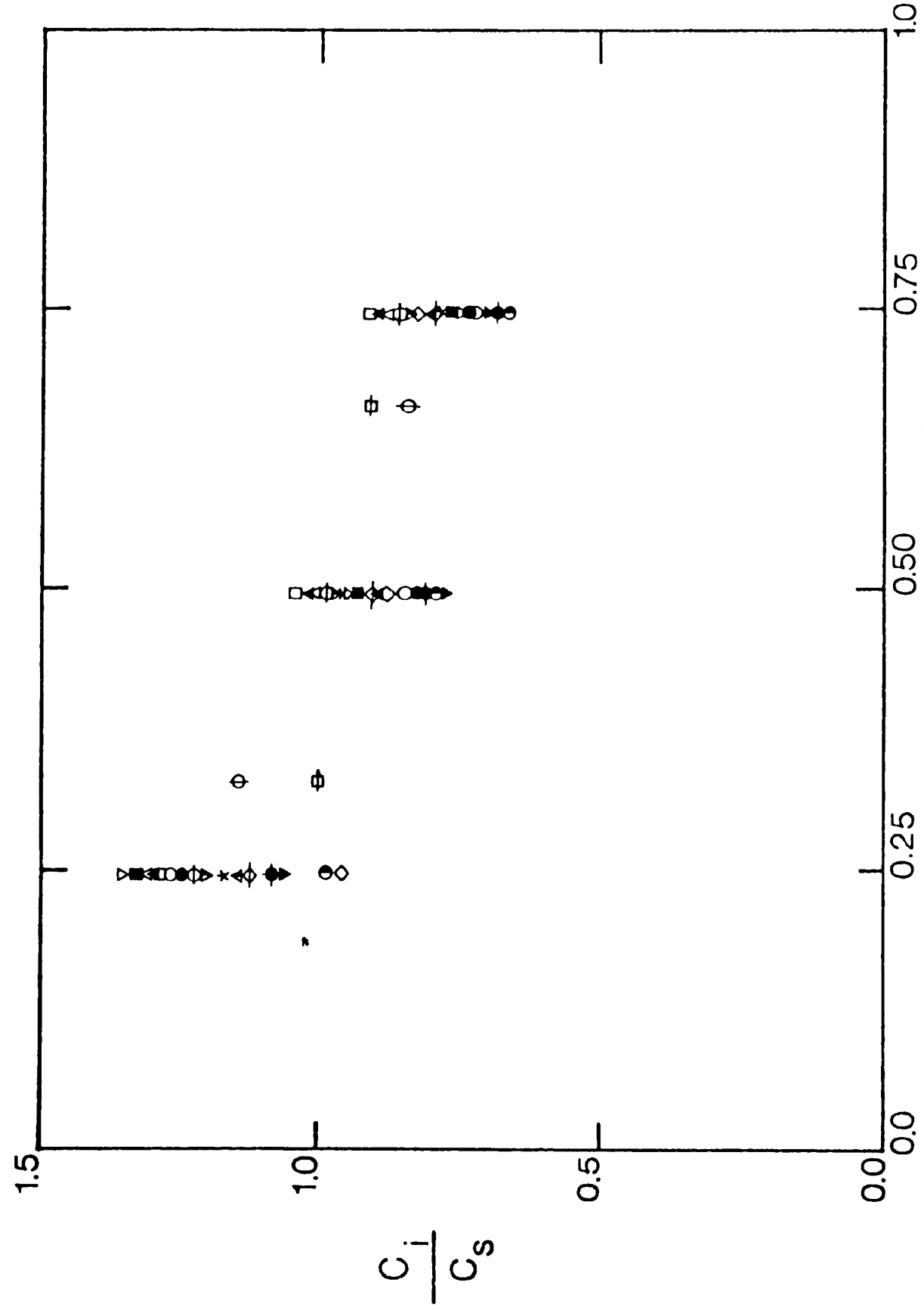

FIGURE 24. SPATIAL CONCENTRATION DISTRIBUTION WITHIN THE EDDY

where n is the number of the probes in the eddy. This concentration c_s will be considered as one of the overall parameters describing the entrapment process of the eddy. The correlation of this parameter with various exit and crossflow conditions will be discussed in the next sections.

Another important overall parameter is the retention time, τ. The existence of the retention time can be established from studying the decay, as shown in the graphs, of the concentration as the dye is turned off in the side channel. A smooth curve was fitted onto the decaying limb of the graph. Selected points were then plotted on semi-log paper. The resulting graphs generally indicated a straight line behavior (see Figure 25), which is in agreement with Equation 8. For each probe location P_i, there is a retention time τ_i. The spatial variation of the retention time, τ_i, within the eddy is presented in Figure 26. Again, the spatial variation is not large. A simple average retention time, τ, can be introduced to characterize the overall decaying process; i.e.,

$$\tau = \frac{1}{n} \sum_{i=1}^{n} \tau_i \qquad (21)$$

where n is again the number of the probes in the eddy.

Hereafter, the detailed spatial and temporal concentration variation will be ignored. The entrapment process in the recirculating eddy will be described by the two overall parameters, the steady-state concentration c_s and the retention time τ. The existence of these two overall parameters has significantly simplified the problem, and it is now possible

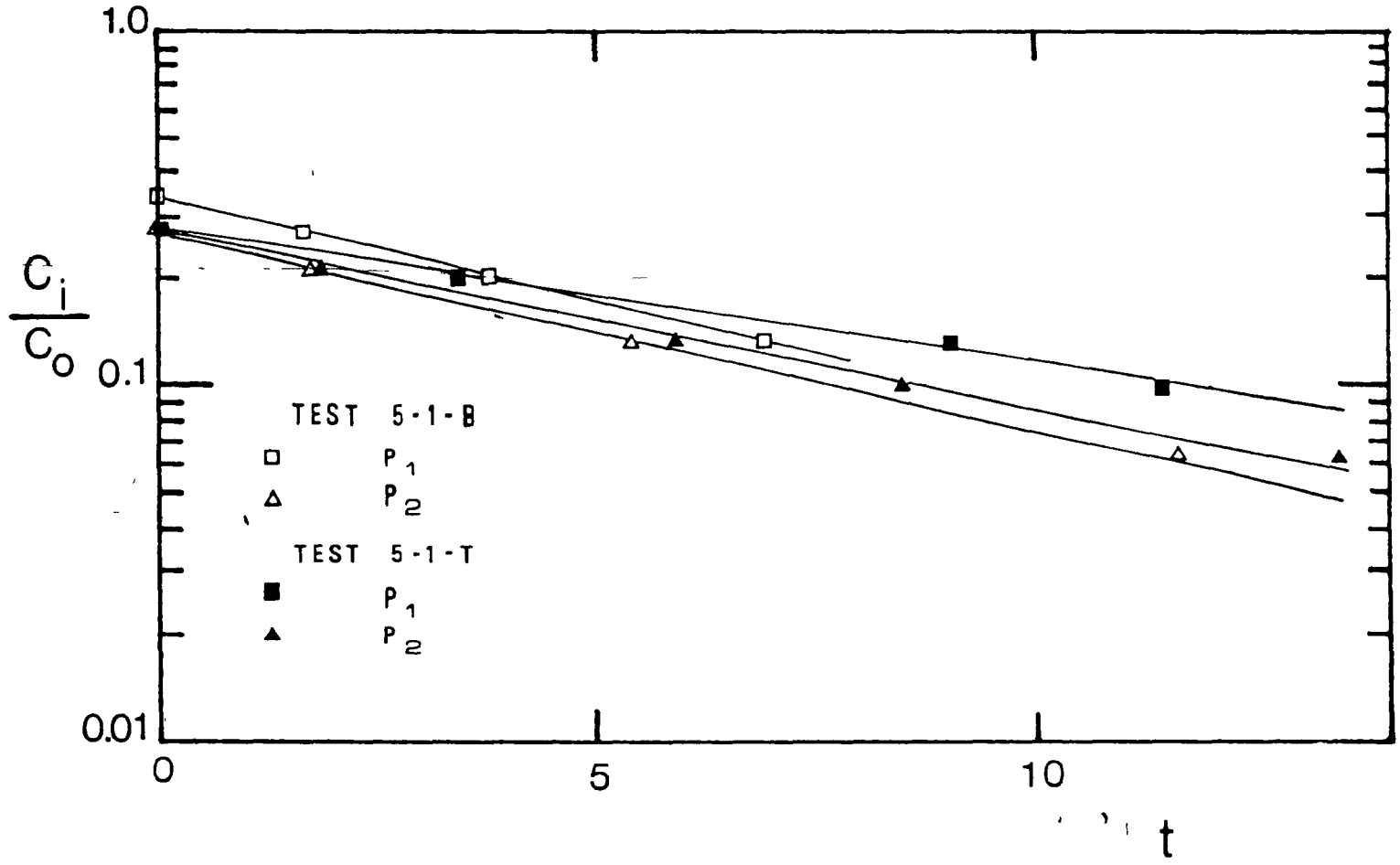

FIGURE 25. EXPONENTIAL DECAY OF CONCENTRATION WITH TIME

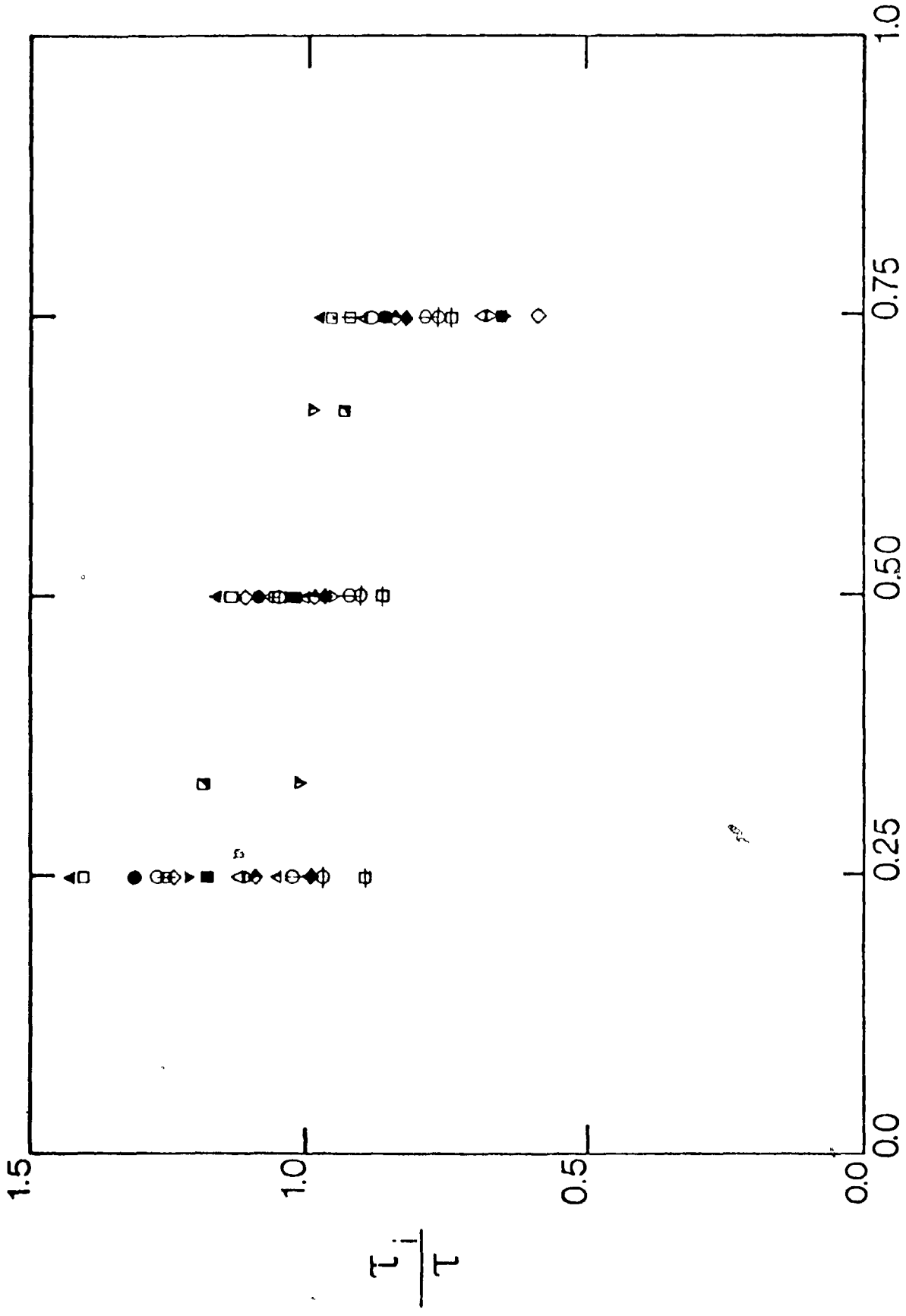

FIGURE 26. SPATIAL RETENTION-TIME DISTRIBUTION WITHIN THE EDDY

to correlate the experimental results over a very wide range of exit and crossflow conditions.

4.3 Retention Time and Steady-State Concentration

The experimental results for the steady-state concentration, c_s, and retention time, τ, are presented in Figures 27 and 28. They are correlated in terms of dimensionless variables derived from a point source model. Concentration measurements within the eddy were carried out in a previous investigation by Carter (1969). Carter discharged hot water through the side channel and obtained temperature contours for three different cases. The height and length of his eddies can be estimated by inspection of the temperature contours. The concentration data of Carter's presented in Figure 27 were obtained by averaging the concentration at three locations (P_1, P_2, P_3, as in Figure 15). Carter's results may have been affected by buoyancy effects and by our subjective estimation of length and height of the eddies. Nevertheless, his data are in general agreement with the results of the present experiment. A similar procedure was used to obtain L, H_i, and c_s from McGuirk and Rodi's (1977) temperature contours, which were based on numerical calculations. Their results are also presented in Figure 27.

Despite the large scatter of the data for both c_s and τ, it is possible to propose the following asymptotic formulae:

For unconfined crossflow, i.e., $\frac{l_s}{B} = \frac{V^2 b}{U^2 B} \to 0$

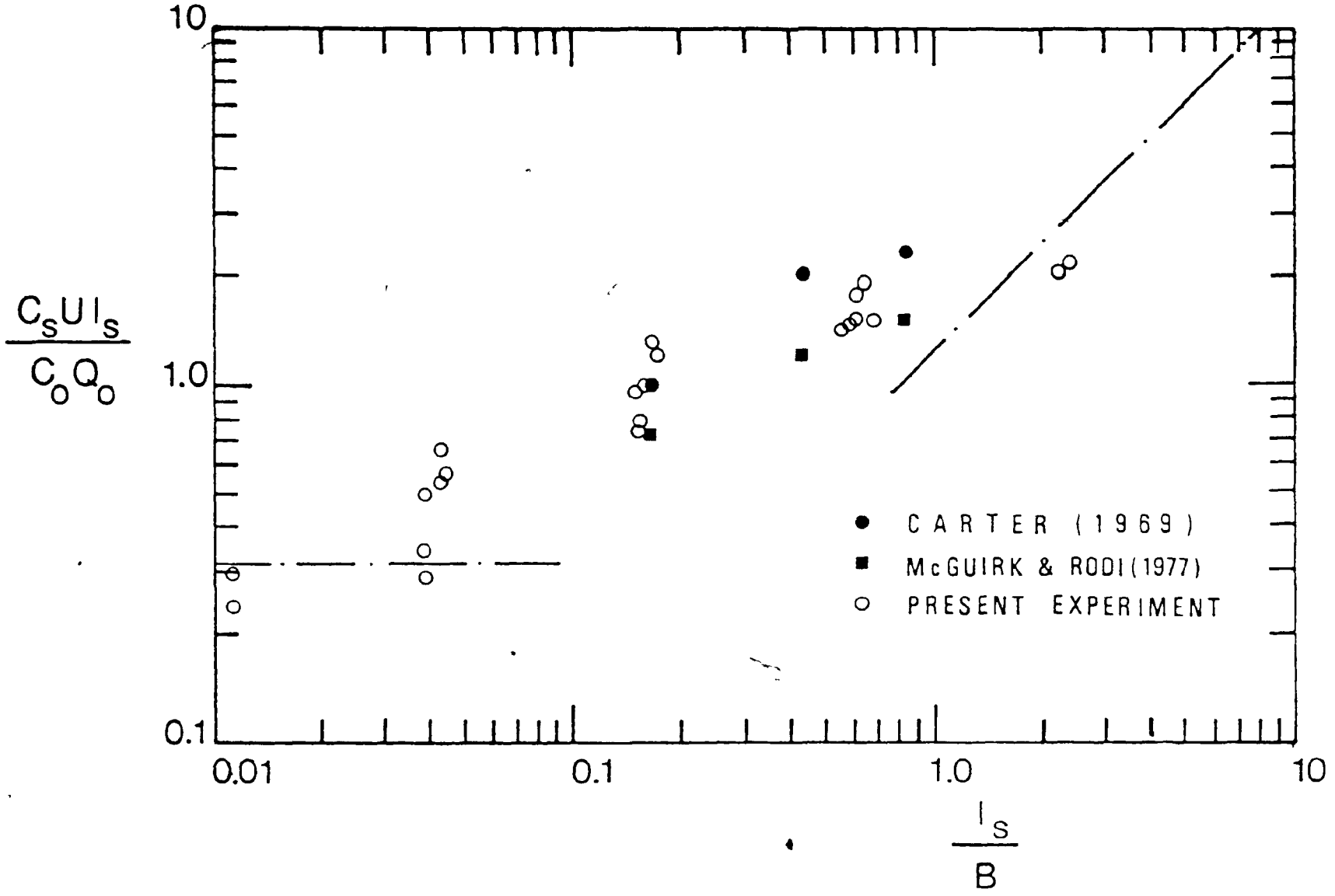

FIGURE 27. AVERAGE STEADY-STATE CONCENTRATION

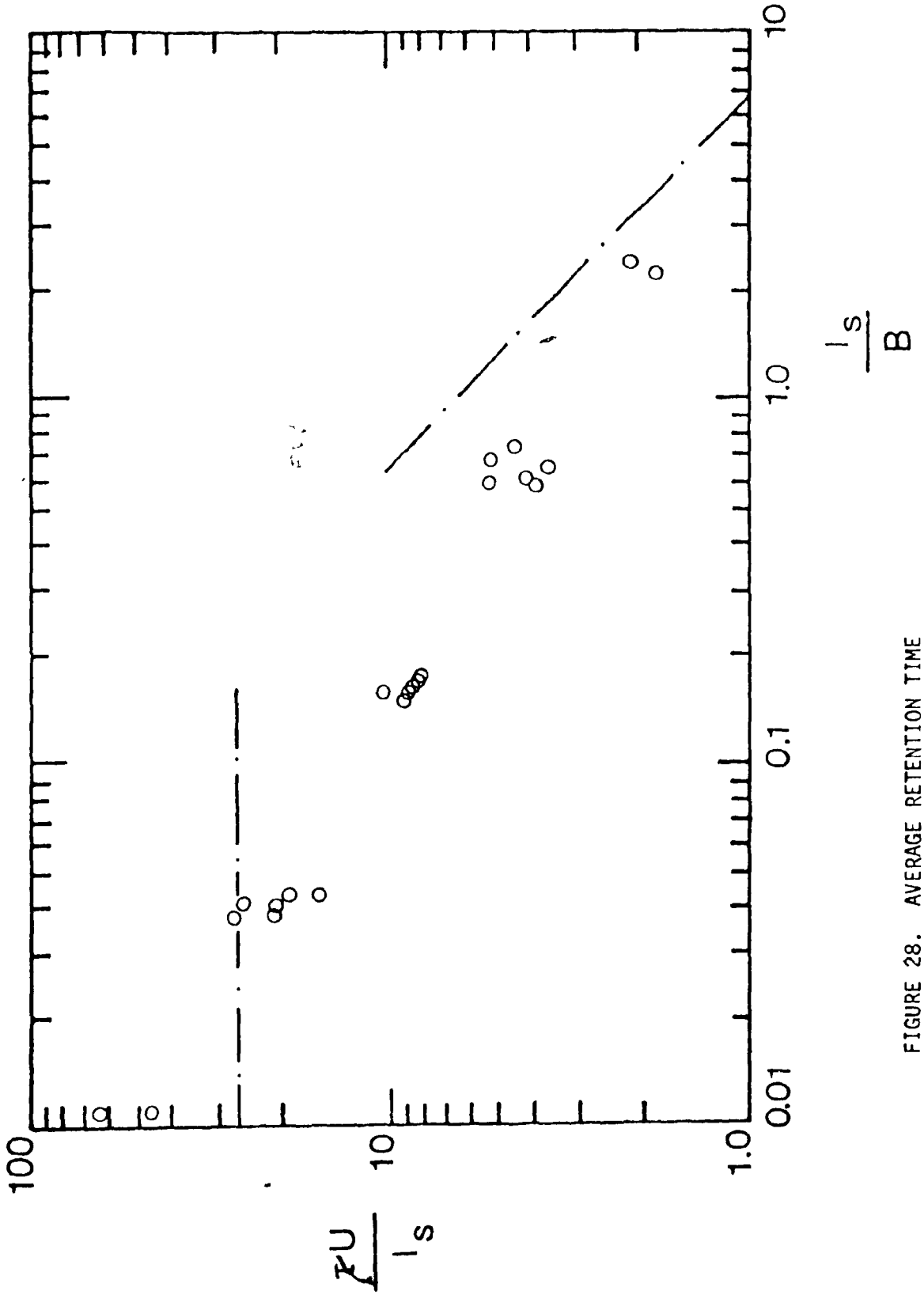

FIGURE 28. AVERAGE RETENTION TIME

$$\frac{c_s U l_s}{c_o Q_o} = 0.31, \qquad \frac{\tau U}{l_s} = 26 \tag{22a, b}$$

or equivalently,

$$\frac{c_s B U}{c_o b V} = 0.31, \qquad \frac{\tau U^3}{b V^2} = 26 \tag{22c, d}$$

On the other hand, for narrow crossflow, i.e., $\frac{l_s}{B} = \frac{V^2 b}{U^2 B} \to \infty$

$$\frac{c_s U l_s}{c_o Q_o} = 1.25 \frac{l_s}{B}, \qquad \frac{\tau U}{l_s} = 6.6 \frac{B}{l_s} \tag{23a, b}$$

or equivalently,

$$\frac{c_s B U}{c_o b V} = 1.25, \qquad \frac{\tau U}{B} = 6.6 \tag{23c, d}$$

There is some evidence that the entraining characteristic is dependent on the curvature of the curved jet. A suitable length scale for the curvature of the jet would be the height of the eddy, H_i. In Figs. 29 and 30, the experimental data is correlated with the height of the eddy, H_i, rather than with the jet exit conditions. It was found that the dimensionless variable $\tau U/H_i$ is nearly constant, that is:

$$\frac{\tau U}{H_i} = 11 \tag{24}$$

A similar relationship was obtained by Humphries and Vincent (1976) in their study of the entrapment process in the wake bubble behind a circu-

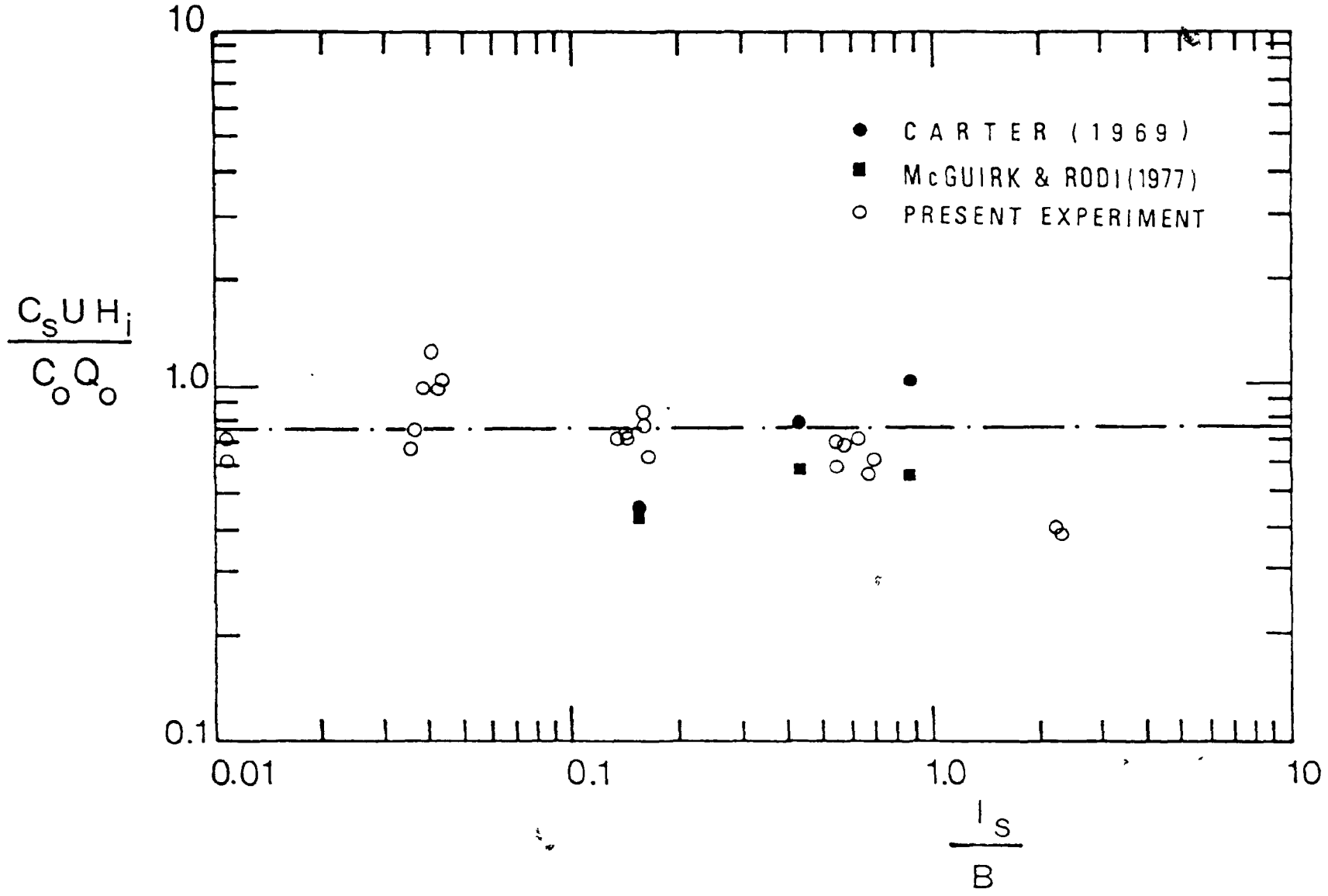

FIGURE 29. AVERAGE STEADY-STATE CONCENTRATION; NORMALIZATION BASED ON THE HEIGHT OF THE EDDY

lar disk.

For a circular disk of diameter D, in a mainstream velocity U, they obtained the following formula:

$$\frac{\tau U}{D} = 7.44 \pm 0.52 \qquad (25)$$

The height of the wake bubble, H, according to the experiments of Carmody (1964), is about 0.81D, this then leads to:

$$\frac{\tau U}{H} = 9.14 \pm 0.63 \qquad (26)$$

The close agreement between the two constants that appeared in Equation 26 for wake bubbles and in Equation 24 for eddies formed by jet reattachment is not coincidental. It suggests a certain universality in the entrapment process of recirculating flows.

Similar correlations of the eddy height H_i with steady-state concentration c_s is given in Figure 29. Following a similar argument, it is reasonable to propose the following constant:

$$\frac{c_s U H_i}{c_o Q_o} = 0.75 \qquad (27)$$

The two data points with the largest l_s/B in Figures 27 and 29 appear to be low as compared to the general trend of the other data. This can be attributed to the possible inaccuracy in measuring low con-

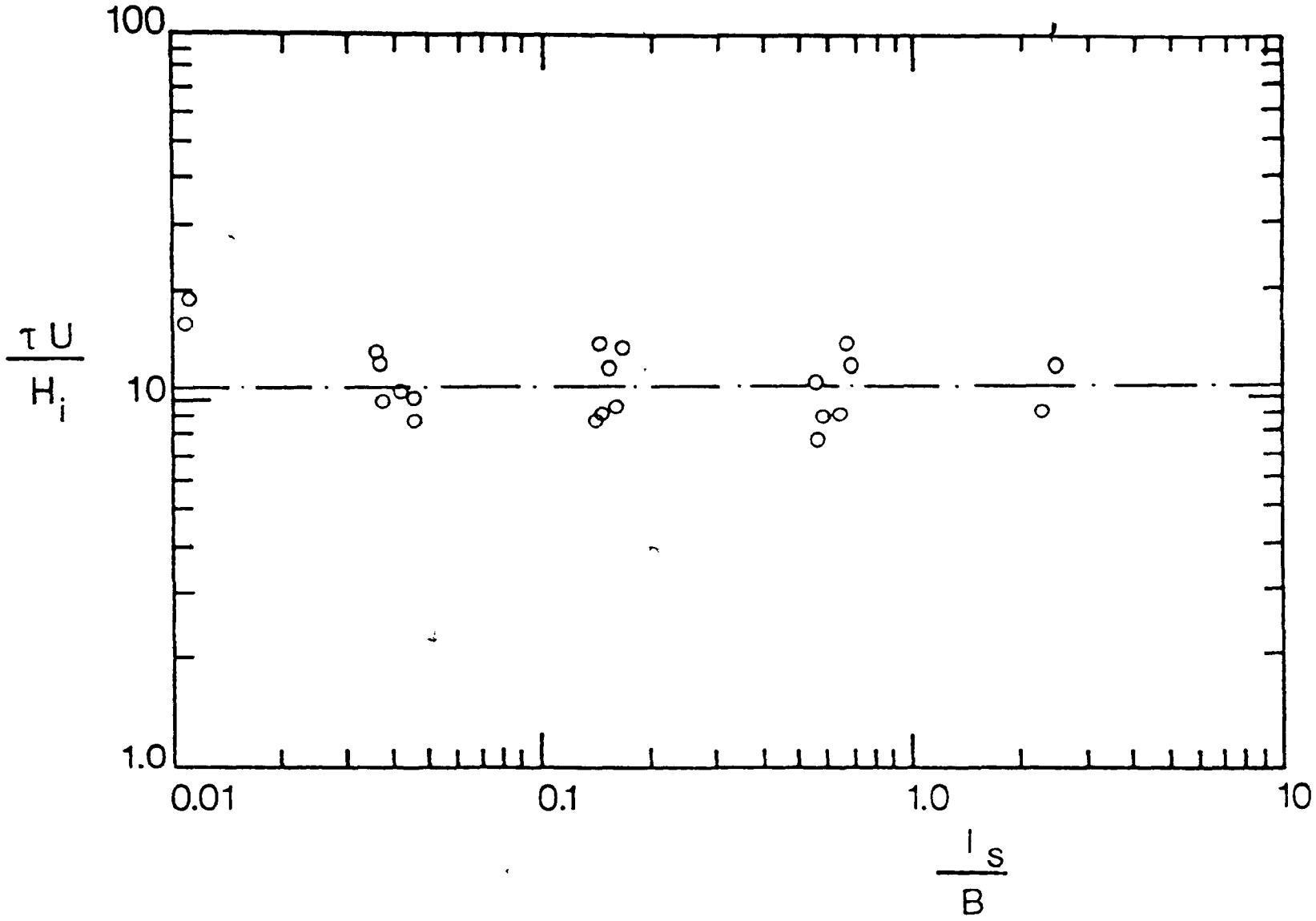

FIGURE 30. AVERAGE RETENTION TIME; NORMALIZATION BASED ON THE HEIGHT OF THE EDDY

centrations in these experiments (see Appendix II, Test Nos. 8-1-B and 8-1-T).

CHAPTER V

SUMMARY AND CONCLUSIONS

Experimental investigation was carried out to study the entrapment phenomenon in a recirculating eddy. It was found that it is possible to describe the transport process by two overall parameters, namely, the steady-state concentration, c_s, and retention time, τ.

The experimental results for eddy height H_i, length L, steady-state concentration c_s and retention time τ were successfully correlated by the following dimensionless variables as derived from a point source model:

$$\frac{H_i}{l_s} = \text{fn.}\ (\frac{l_s}{B})$$

$$\frac{L}{l_s} = \text{fn.}\ (\frac{l_s}{B}) \qquad (28)$$

$$\frac{c_s U l_s}{c_o Q_o} = \text{fn.}\ (\frac{l_s}{B})$$

and

$$\frac{\tau U}{l_s} = \text{fn.}\ (\frac{l_s}{B})$$

Asymptotic formulae for the two limiting cases with $l_s/B \to 0$ and $l_s/B \to \infty$ have been derived from the experiment, and they are summarized in Table 2.

TABLE 2. ASYMPTOTIC FORMULAE

For unbounded crossflow, i.e., $\frac{V^2 b}{U^2 B} \to 0$

$$\frac{H_i U^2}{bV^2} = 2.4$$

$$\frac{LU^2}{bV^2} = 18$$

$$\frac{c_s V}{c_o U} = 0.31$$

$$\frac{\tau U^3}{bV^2} = 26$$

For narrow crossflow, i.e., $\frac{V^2 b}{U^2 B} \to \infty$

$$\frac{H_i}{B} = 0.60$$

$$\frac{L}{B} = 4.4$$

$$\frac{c_s BU}{c_o bV} = 1.25$$

$$\frac{\tau U}{B} = 6.6$$

The transport process was found to have some properties that apparently are common to all recirculating eddies. Two universal constants were determined for the retention time τ and the steady-state concentration c_s; these are:

$$\frac{\tau U}{H_i} = 11 \tag{29}$$

and

$$\frac{c_s U H_i}{c_o Q_o} = 0.75 \tag{30}$$

Note that the dimensionless variables in Equations 29 and 30 are related to the scale of the eddies rather than to the jet discharging conditions.

However, it should be pointed out that a number of difficulties were encountered during the course of the experiments. Some of the eddies were small compared with the thickness of the boundary layer of the crossflow (eg., TESTS 1-1-B, 1-1-T). Concentration is difficult to determine accurately in some other tests with a large eddy size (eg., TEST 8-1-T). All these difficulties are believed to have contributed to the scatter of the data as presented in this thesis.

Some caution should be exercised in the application of the various formulae proposed in this thesis. Assumptions have been made in correlating the experimental data. The side channel discharge has been approximated as a point source; the friction in the channel bottom is ignored. These approximations may be inaccurate in some practical applications.

REFERENCES

1. Carter, H. H. (1969) " A preliminary report on the characteristics of a heater jet discharged horizontally into a transverse current. Part I - Constant Depth," Technical Report No. 61, Chesapeake Bay Institute, Johns Hopkins University.

2. Carmody, T. (1964) "Establishment of the wake behind a disk," Journal of Basic Engineering - Transactions ASME, pp. 869-882.

3. Chu, V. H. (1978) Private Communication.

4. Humphries, W., amd J. H. Vincent. (1976) "An experimental investigation of the detention of airborne smoke in the wake bubble behind a disk," Journal of Fluid Mechanics, Vol. 73, Part 3, pp. 453-464.

5. Humphries, W., and J. H. Vincent. (1976) "Near wake properties of axisymmetric bluff body flows," Paper of the 14th International Congress of Theoretical and Applied Mathematics, Aug. - Sept. 1976, Delft.

6. McGuirk, J. J., and W. Rodi. (1977) "A depth averaged mathematical model for the near field of side discharges into open channel flow," Journal of Fluid Mechanics, Vol. 86, pp. 761-781.

7. Mikhail, R., V. H. Chu, and S. B. Savage. (1975) "The reattachment of a two-dimensional turbulent jet in a confined crossflow," Proceedings of the 16th IAHR Congress, São Paulo, Brazil, pp. 414-419.

8. Rouse, H. (1957) "Diffusion in the lee of a two-dimensional jet," 9ième Congress International de Mechanique Appliquée, Vol I, pp. 307-312.

9. Strazisar, A., and J. Prahl. (1973) "The effects of bottom friction on river entrance flow with crossflow," Proceedings of the 16th Conference of Great Lakes Research, pp. 615-625.

APPENDIX I

EXPERIMENTAL RESULTS OF PRESENT AND PREVIOUS INVESTIGATIONS

TABLE 3a. RESULTS OF THE EXPERIMENT

TEST NO.	c_i (mℓ/ℓ * 10^3)	τ_i (secs)	H_o (cm)	H_1 (cm)	L (cm)	c_s (mℓ/ℓ * 10^3)	τ (secs)
1-1-B	375	3.80	6.35	1.62	11.0	375	3.80
1-1-T	319	4.00	6.35	1.62	11.0	319	4.00
2-1-B	c_1 381	τ_1 4.67	8.90	4.80	30.0	378	4.66
	c_2 375	τ_2 4.65					
2-2-B	c_1 371	τ_1 4.78	8.90	4.80	30.0	307	4.65
	c_2 243	τ_2 4.52					
2-1-T	c_1 285	τ_1 4.34	8.90	4.80	30.0	282	4.30
	c_2 279	τ_2 4.26					
2-2-T	c_1 277	τ_1 4.26	8.90	4.80	30.0	273	3.92
	c_2 268	τ_2 3.58					
3-1-B	c_1 936	τ_1 8.80	11.45	7.00	50.0	702	7.88
	c_2 633	τ_2 8.61					
	c_3 539	τ_3 7.46					

TABLE 3a (continued)

TEST NO.	c_i	τ_i	H_o	H_i	L	c_s	τ
3-2-B	c_1 821	τ_1 9.25	11.45	7.00	50.0	607	8.93
	c_2 508	τ_2 8.99					
	c_3 493	τ_3 8.55					
3-4-T	c_1 578	τ_1 10.48	11.45	7.00	50.0	434	8.74
	c_2 407	τ_2 9.84					
	c_3 319	τ_3 5.90					
3-2-T	c_1 367	τ_1 7.48	13.95	7.62	50.0	278	6.89
	c_2 355	τ_2 6.79					
	c_3 202	τ_3 6.39					
4-1-B	c_1 420	τ_1 19.55	19.05	14.60	85.0	372	19.27
	c_2 315	τ_2 19.48					
	c_3 340	τ_3 18.79					
4-2-B	c_1 380	τ_1 19.00	19.05	14.60	85.0	328	16.13
	c_2 379	τ_2 17.03					
	c_3 290	τ_3 12.40					

TABLE 3a (continued)

TEST NO.	c_f	τ_f	H_o	H_f	L	c_s	τ
4-1-T	c_1 428	τ_1 15.55	19.05	14.60	85.0	362	12.40
	c_2 379	τ_2 13.65					
	c_3 278	τ_3 10.82					
4-2-T	c_1 463	τ_1 19.15	19.05	14.60	85.0	407	17.12
	c_2 418	τ_2 17.64					
	c_3 340	τ_3 14.57					
5-1-B	c_4 292	τ_4 10.90	11.43	5.08	40.0	255	10.25
	c_5 218	τ_5 9.60					
5-1-T	c_4 239	τ_4 10.60	11.43	5.08	40.0	220	10.55
	c_5 202	τ_5 10.50					
6-1-B	c_1 570	τ_1 15.83	15.24	8.89	70.0	440	13.51
	c_2 410	τ_2 12.47					
	c_3 340	τ_3 12.23					

TABLE 3a (continued)

TEST NO.	c_f	τ_f	H_o	H_f	L	c_s	τ
6-1-T	c_1 418	τ_1 17.50	15.24	8.89	70.0	308	13.67
	c_2 274	τ_2 13.20					
	c_3 232	τ_3 10.30					
7-1-B	c_1 451	τ_1 26.50	35.56	16.51	100.0	348	21.20
	c_2 326	τ_2 24.60					
	c_3 259	τ_3 12.50					
7-1-T	c_1 449	τ_1 26.45	35.56	16.51	100.0	353	24.07
	c_2 342	τ_2 23.85					
	c_3 269	τ_3 21.90					
8-1-B	c_1 273	τ_1 52.97	31.75	24.13	120.0	254	37.66
	c_2 260	τ_2 35.13					
	c_3 230	τ_3 25.00					
8-1-T	c_1 158	τ_1 66.30	31.75	24.13	120.0	138	46.95
	c_2 135	τ_2 41.00					
	c_3 120	τ_3 31.55					

TABLE 3b. DIMENSIONLESS PARAMETERS

TEST NO.	$\frac{l_s}{B}$	$\frac{H_i}{B}$	$\frac{H_i}{L}$	$\frac{H_i}{l_s}$	$\frac{L}{B}$	$\frac{L}{l_s}$	$\frac{H_o - H_i}{L}$	$\frac{c_s U l_s}{c_o Q_o}$	$\frac{c_s U H_i}{c_o Q_o}$	$\frac{U}{l_s}$	$\frac{U}{H_i}$
1-1-B	0.011	0.041	0.125	3.87	0.33	30.96	0.430	0.289	0.725	45.49	15.32
1-1-T	0.011	0.041	0.125	3.87	0.33	30.96	0.430	0.244	0.612	65.39	18.54
2-1-B	0.043	0.079	0.160	1.85	0.49	11.55	0.137	0.548	1.013	18.92	10.23
2-2-B	0.041	0.079	0.160	1.94	0.49	12.12	0.137	0.645	1.251	20.29	10.46
2-1-T	0.038	0.079	0.160	2.06	0.49	12.85	0.137	0.491	1.001	20.46	9.95
2-2-T	0.043	0.079	0.160	1.86	0.49	11.61	0.137	0.529	0.982	16.01	8.62
3-1-B	0.164	0.115	0.140	0.70	0.82	5.00	0.089	1.18	0.826	8.29	11.84
3-2-B	0.167	0.115	0.140	0.69	0.82	4.91	0.089	0.934	0.642	9.22	13.41
3-1-T	0.153	0.115	0.140	0.76	0.82	5.36	0.089	0.962	0.722	10.22	13.62
3-2-T	0.165	0.125	0.140	0.70	0.82	4.97	0.127	1.048	0.795	9.32	9.69
4-1-B	0.654	0.240	0.172	0.37	1.39	2.13	0.052	1.486	0.544	5.15	14.06
4-2-B	0.559	0.240	0.172	0.43	1.39	2.49	0.052	1.399	0.599	5.12	11.01
4-1-T	0.622	0.240	0.172	0.39	1.39	2.24	0.052	1.854	0.714	3.57	9.28
4-2-T	0.668	0.240	0.172	0.36	1.39	2.09	0.052	1.703	0.611	4.28	12.26
5-1-B	0.037	0.083	0.127	2.25	0.66	17.73	0.159	0.338	0.761	26.85	11.92
5-1-T	0.036	0.083	0.127	2.31	0.66	18.22	0.159	0.284	0.657	28.84	12.46

TABLE 3b (continued)

TEST NO.	$\frac{l_s}{B}$	$\frac{H_i}{B}$	$\frac{H_i}{L}$	$\frac{H_i}{T_s}$	$\frac{L}{B}$	$\frac{L}{T_s}$	$\frac{H_o - H_i}{L}$	$\frac{c_s U l_s}{c_o Q_o}$	$\frac{c_s U H_i}{c_o Q_o}$	$\frac{U}{T_s}$	$\frac{U}{H_i}$
6-1-B	0.147	0.146	0.127	0.99	1.15	7.81	0.091	0.726	0.720	8.96	8.98
6-1-T	0.149	0.146	0.127	0.98	1.15	7.71	0.091	0.763	0.747	8.90	9.16
7-1-B	0.554	0.271	0.165	0.49	1.64	2.96	0.191	1.423	0.696	3.82	8.14
7-1-T	0.579	0.271	0.165	0.47	1.64	2.83	0.191	1.458	0.682	4.06	9.09
8-1-B	2.13	0.396	0.201	0.19	1.97	0.92	0.064	2.041	0.379	1.80	9.69
8-1-T	2.22	0.396	0.201	0.18	1.97	0.89	0.064	2.022	0.361	2.11	11.85

TABLE 4. RESULTS OF PREVIOUS INVESTIGATORS

Carter (1969) [B = 70.33 cm]

$\frac{l_s}{B}$	$\frac{c_s}{c_o}$	$\frac{c_s U l_s}{c_o Q_o}$	$\frac{c_s U H_i}{c_o Q_o}$	b (cm)	U (cm/sec)	V (cm/sec)
0.163	0.48	0.96	0.43	3.05	1.89	3.66
0.422	0.42	2.07	0.77	1.22	1.89	9.45
0.834	0.24	2.35	1.00	0.61	1.92	18.90

McGuirk & Rodi (1977) [B, b, U, and V the same as in Carter]

$\frac{l_s}{B}$	$\frac{c_s}{c_o}$	$\frac{c_s U l_s}{c_o Q_o}$	$\frac{c_s U H_i}{c_o Q_o}$
0.163	0.48	0.96	0.43
0.422	0.42	2.07	0.77
0.834	0.24	2.35	1.00

TABLE 4 (continued)

Strazisar and Prahl (1973)

$\frac{l_s}{B}$	$\frac{L}{B}$	$\frac{L}{T_s}$
0.04	0.53	13.25
0.05	0.68	13.60
0.066	0.82	12.42
0.086	0.80	9.30
0.095	1.2	12.63
0.12	1.0	8.33
0.16	1.2	7.50
0.18	1.7	10.62
0.22	1.7	7.73
0.33	2.1	6.36
0.35	1.0	2.86
0.46	1.3	2.83
0.60	1.6	2.66
0.85	1.95	2.29
1.40	2.8	2.00

TABLE 4 (continued)

Mikhail et al. (1975)

L (cm)	H_i (cm)	H_o (cm)	$\frac{T_s}{B}$	$\frac{L}{B}$	$\frac{L}{T_s}$	$\frac{H_i}{B}$	$\frac{H_i}{L}$	$\frac{H_i}{T_s}$	$\frac{H_o - H_i}{L}$
8.08	1.27	2.97	0.010	0.133	12.76	0.02	0.157	2.01	0.289
26.46	3.39	7.83	0.042	0.434	10.41	0.43	0.128	1.33	0.168
24.55	3.81	7.41	0.042	0.403	9.67	0.40	0.155	1.50	0.147
47.41	7.66	13.12	0.094	0.778	8.27	0.78	0.162	1.34	0.115
102.45	12.70	24.55	0.167	1.681	10.07	1.60	0.124	1.25	0.116
79.80	13.13	18.42	0.167	1.309	7.88	1.31	0.167	1.32	0.064
98.42	16.51	24.34	0.261	1.615	6.21	1.61	0.168	1.04	0.080
153.24	19.47	34.71	0.375	2.514	6.70	2.51	0.127	0.85	0.099
121.50	18.42	30.06	0.375	1.993	5.31	1.99	0.152	0.81	0.096
144.78	21.59	35.56	0.511	2.375	4.66	2.37	0.149	0.69	0.096
168.49	22.44	37.26	0.667	2.764	4.14	2.76	0.133	0.55	0.088
154.30	23.82	37.46	0.667	2.531	3.79	2.53	0.154	0.59	0.088
182.88	25.41	39.37	0.844	3.000	3.55	3.00	0.139	0.49	0.076

TABLE 4 (continued)

L (cm)	H_i (cm)	H_o (cm)	$\frac{l_s}{B}$	$\frac{L}{B}$	$\frac{L}{l_s}$	$\frac{H_i}{B}$	$\frac{H_i}{L}$	$\frac{H_i}{l_s}$	$\frac{H_o - H_i}{L}$
186.69	28.58	41.91	1.042	3.063	2.88	3.06	0.153	0.45	0.072
201.29	30.48	45.08	1.261	3.302	2.62	3.30	0.151	0.40	0.073
207.43	27.52	46.57	1.500	3.403	2.27	3.40	0.133	0.30	0.092
179.05	29.21	40.00	1.500	2.937	1.96	2.94	0.163	0.32	0.060
193.04	29.85	40.64	1.761	3.167	1.80	3.17	0.155	0.28	0.056
220.98	30.48	40.64	2.042	3.625	1.78	3.63	0.138	0.25	0.046
223.52	30.48	41.27	2.344	3.667	1.57	3.67	0.136	0.21	0.048
256.54	34.71	46.57	2.667	4.208	1.58	4.21	0.135	0.21	0.046
223.52	31.75	42.54	2.667	3.667	1.37	3.67	0.142	0.20	0.048
226.06	31.75	43.18	3.011	3.708	1.23	3.71	0.140	0.17	0.051
231.14	32.38	46.99	3.376	3.792	1.12	3.79	0.140	0.16	0.063
280.25	35.98	59.26	4.170	4.597	1.10	4.60	0.128	0.14	0.083
269.24	36.83	60.96	7.040	4.417	0.63	4.42	0.137	0.09	0.090

APPENDIX II

TEMPORAL CONCENTRATION VARIATION AT DIFFERENT LOCATIONS IN THE EDDY

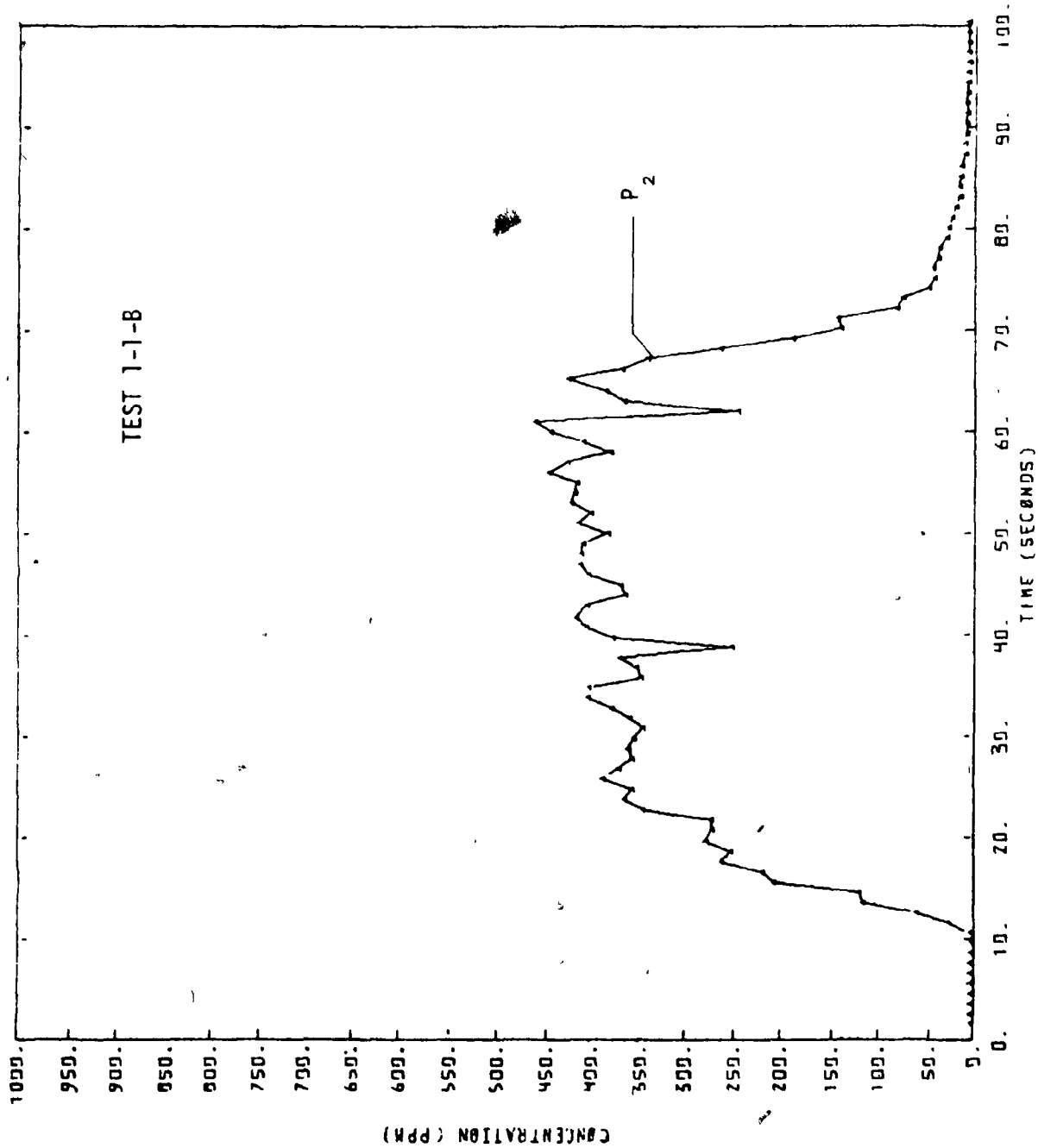
TEST 1-1-B
P_2
CONCENTRATION (PPM)
TIME (SECONDS)
0.
10.
20.
30.
40.
50.
60.
70.
80.
90.
100.
50.
100.
150.
200.
250.
300.
350.
400.
450.
500.
550.
600.
650.
700.
750.
800.
850.
900.
950.
1000.

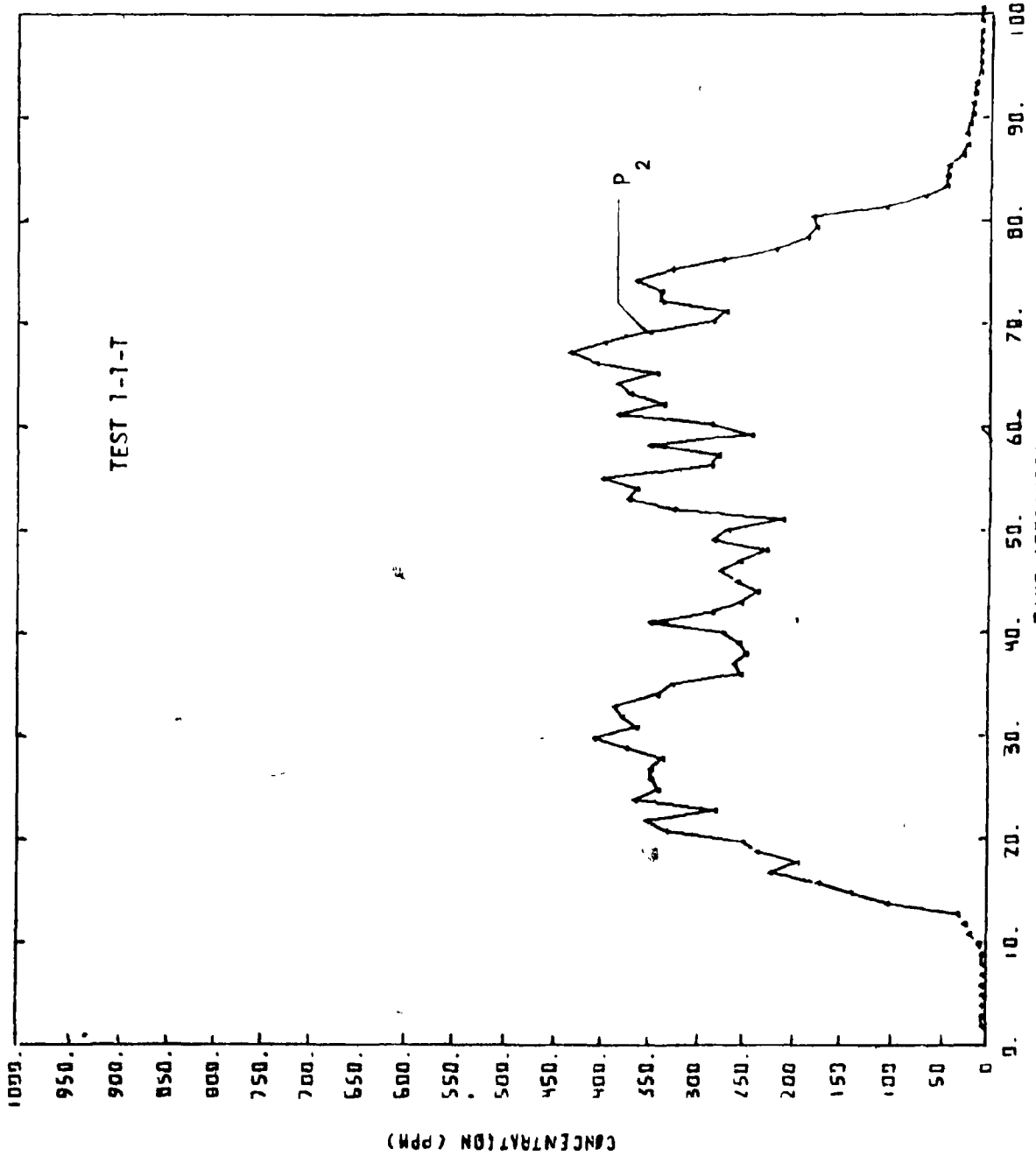
TEST 1-1-T
P2
CONCENTRATION (PPM)
TIME (SECONDS)
0.
10.
20.
30.
40.
50.
60.
70.
80.
90.
100
50
100
150
200
250
300
350
400
450
500
550
600
650
700
750
800
850
900
950
1000.

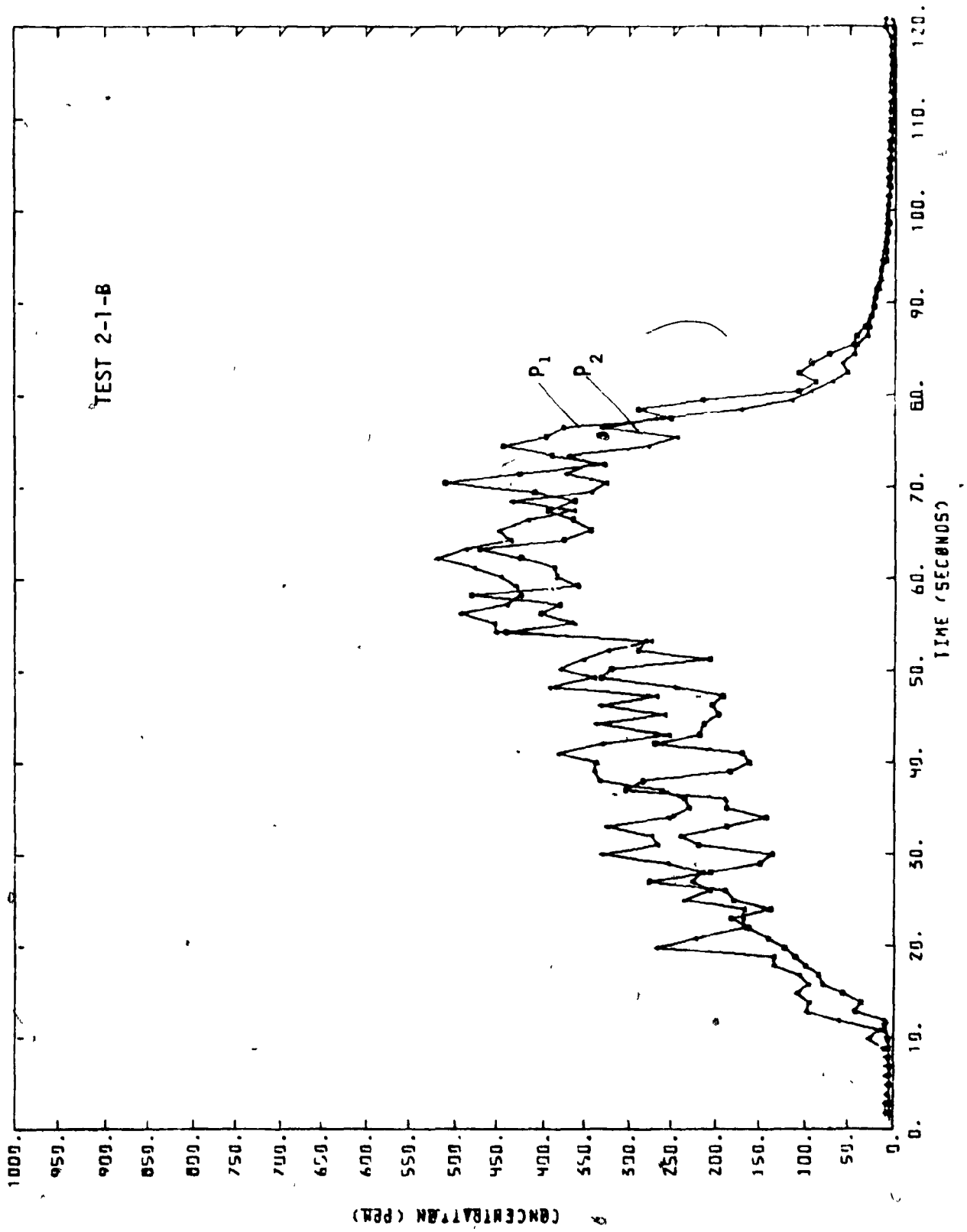
TEST 2-1-B
P_1
P_2
CONCENTRATION (PPM)
TIME (SECONDS)
0.
10.
20.
30.
40.
50.
60.
70.
80.
90.
100.
110.
120.
50.
100.
150.
200.
250.
300.
350.
400.
450.
500.
550.
600.
650.
700.
750.
800.
850.
900.
950.
1000.

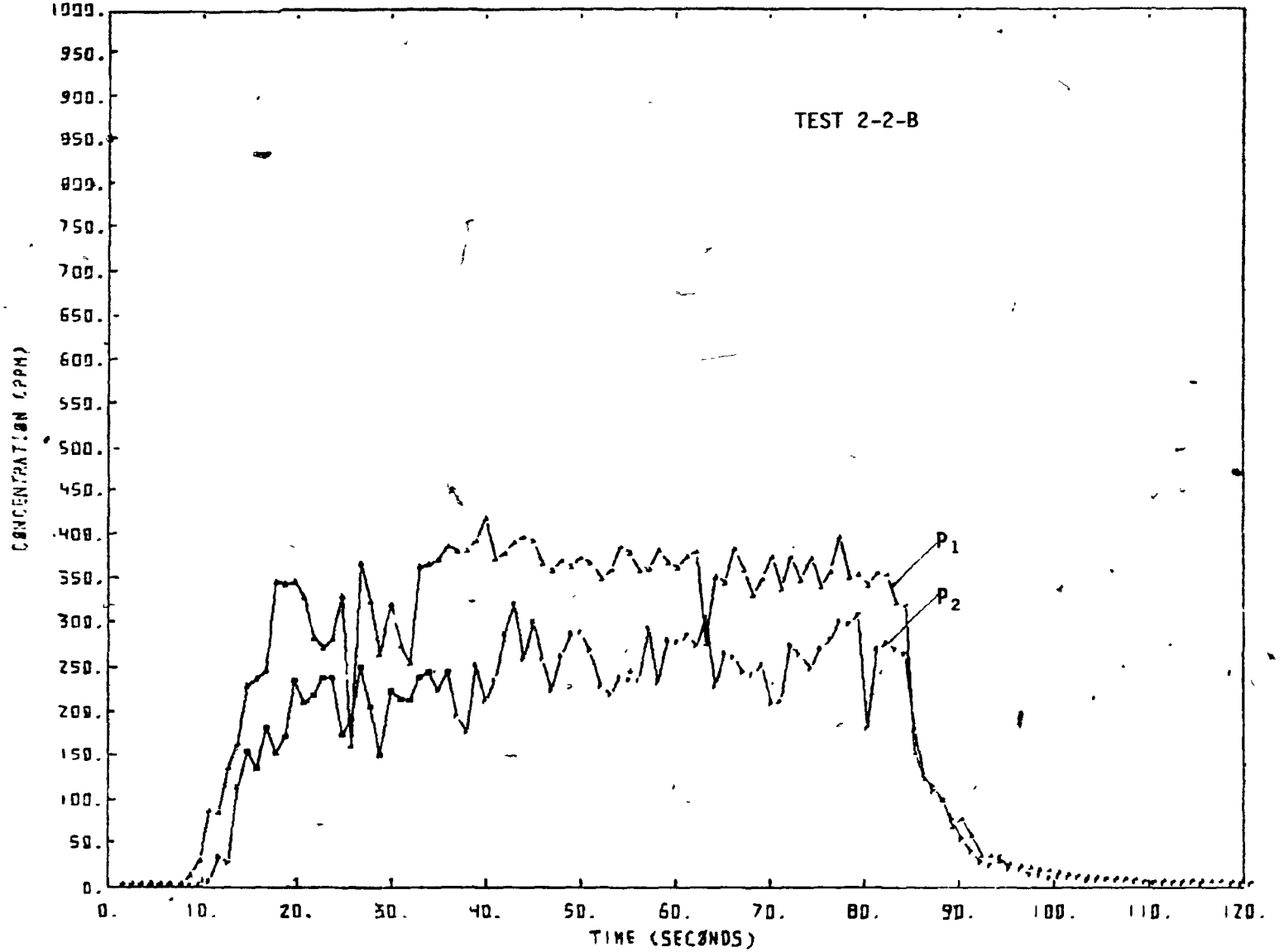
TEST 2-2-B
CONCENTRATION (PPM)
1000.
950.
900.
850.
800.
750.
700.
650.
600.
550.
500.
450.
400.
350.
300.
250.
200.
150.
100.
50.
0.
0.
10.
20.
30.
40.
50.
60.
70.
80.
90.
100.
110.
120.
TIME (SECONDS)
P1
P2

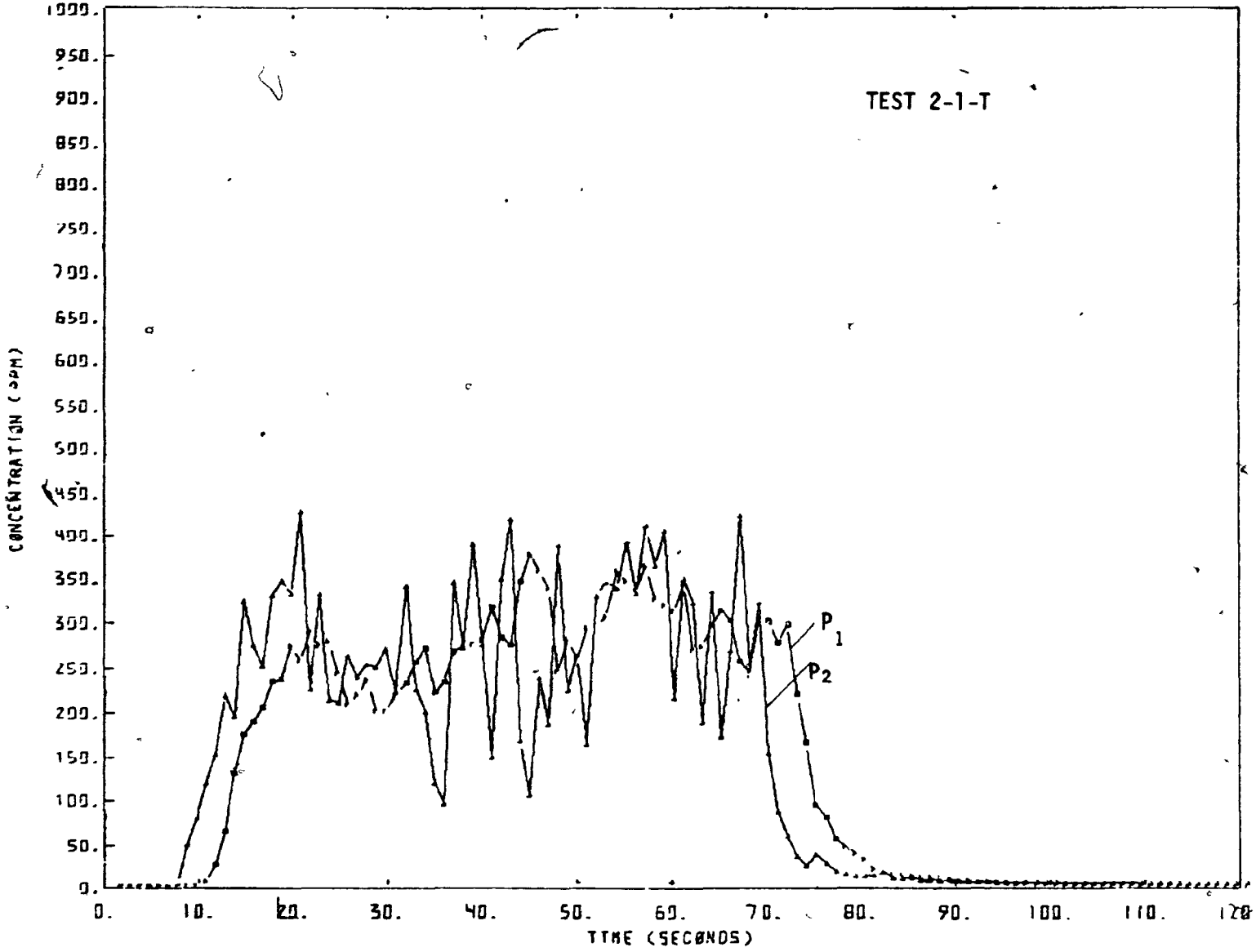
TEST 2-1-T
CONCENTRATION (PPM)
1000.
950.
900.
850.
800.
750.
700.
650.
600.
550.
500.
450.
400.
350.
300.
250.
200.
150.
100.
50.
0.
0.
10.
20.
30.
40.
50.
60.
70.
80.
90.
100.
110.
120
TIME (SECONDS)
P1
P2

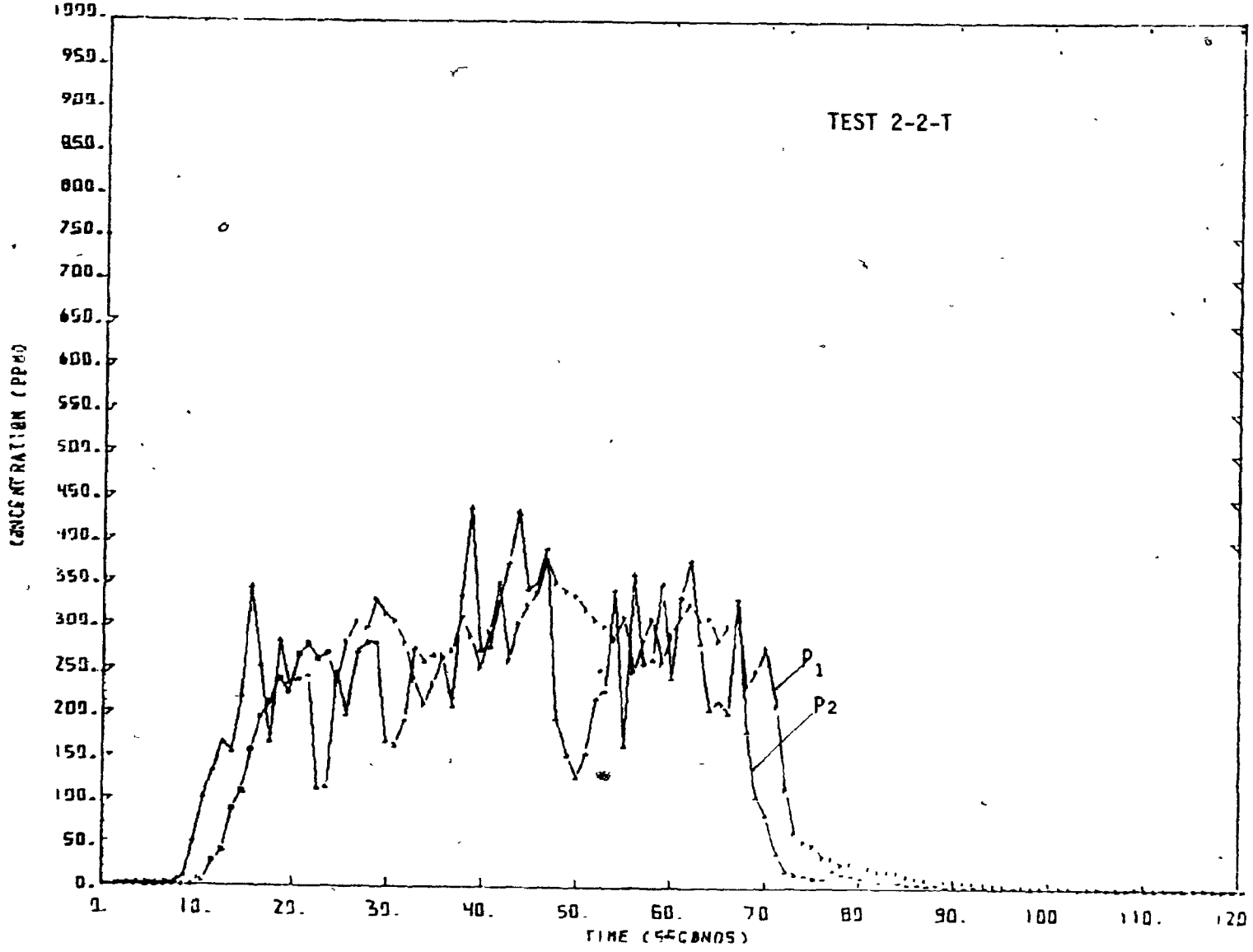
TEST 2-2-T
CONCENTRATION (PPM)
1000.
950.
900.
850.
800.
750.
700.
650.
600.
550.
500.
450.
400.
350.
300.
250.
200.
150.
100.
50.
0.
1.
10.
20.
30.
40.
50.
60.
70
80
90.
100
110.
120
TIME (SECONDS)
P1
P2

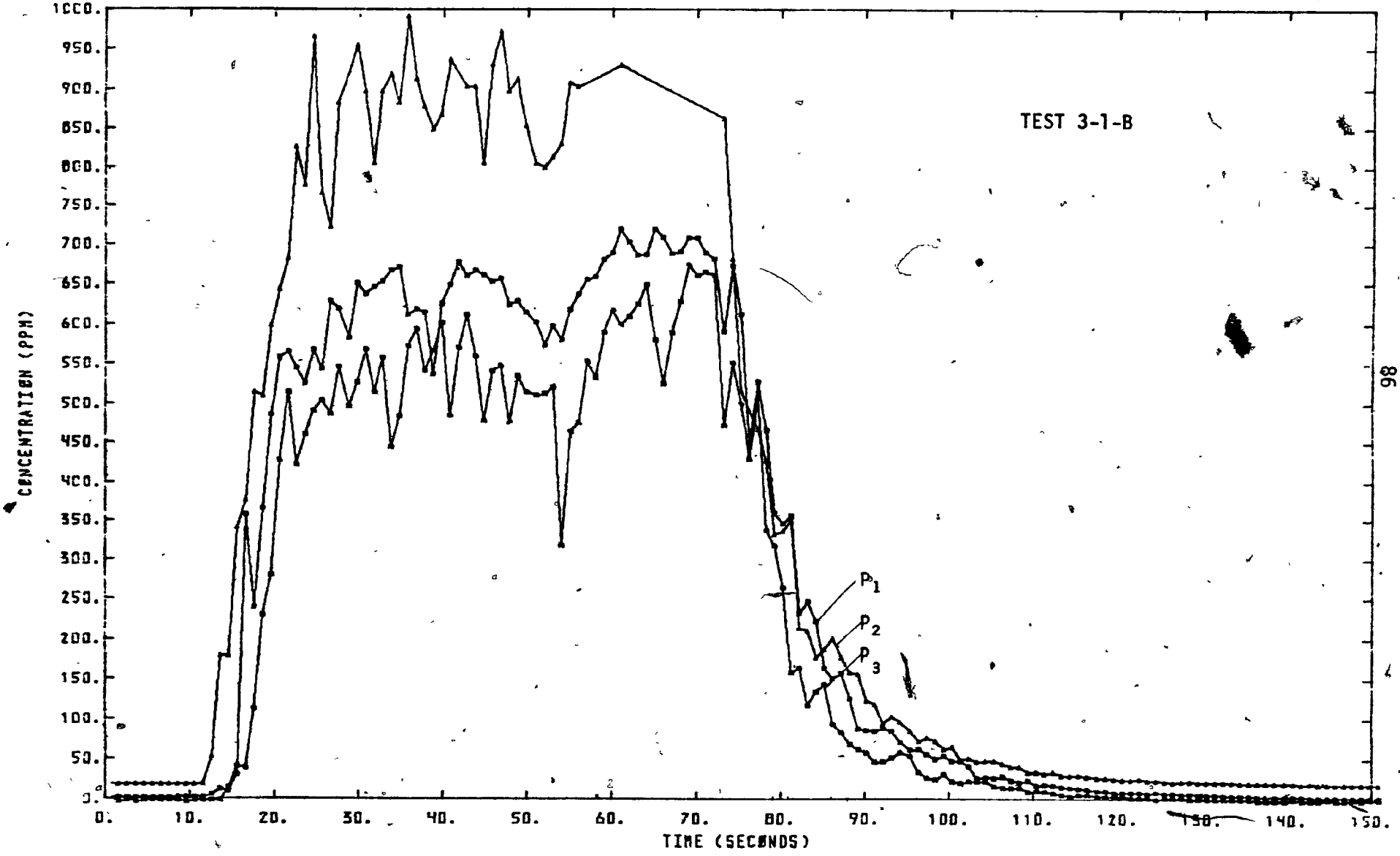
TEST 3-1-B
CONCENTRATION (PPM)
TIME (SECONDS)
P1
P2
P3
1000.
950.
900.
850.
800.
750.
700.
650.
600.
550.
500.
450.
400.
350.
300.
250.
200.
150.
100.
50.
0.
0.
10.
20.
30.
40.
50.
60.
70.
80.
90.
100.
110.
120.
130.
140.
150.

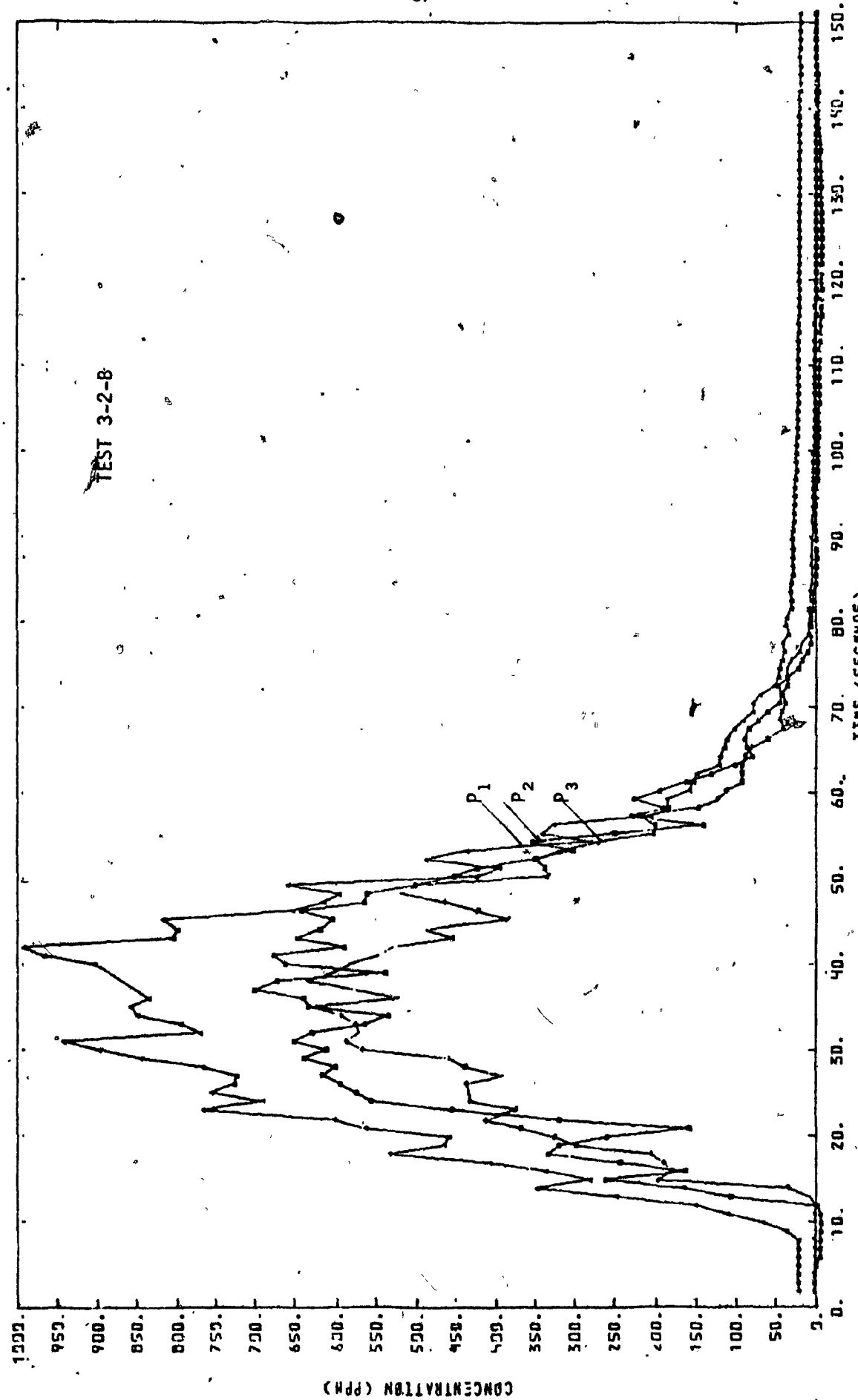
TEST 3-2-B
P1
P2
P3
CONCENTRATION (PPM)
TIME (SECONDS)
0.
50.
100.
150.
200.
250.
300.
350.
400.
450.
500.
550.
600.
650.
700.
750.
800.
850.
900.
950.
1000.
10.
20.
30.
40.
50.
60.
70.
80.
90.
100.
110.
120.
130.
140.
150.

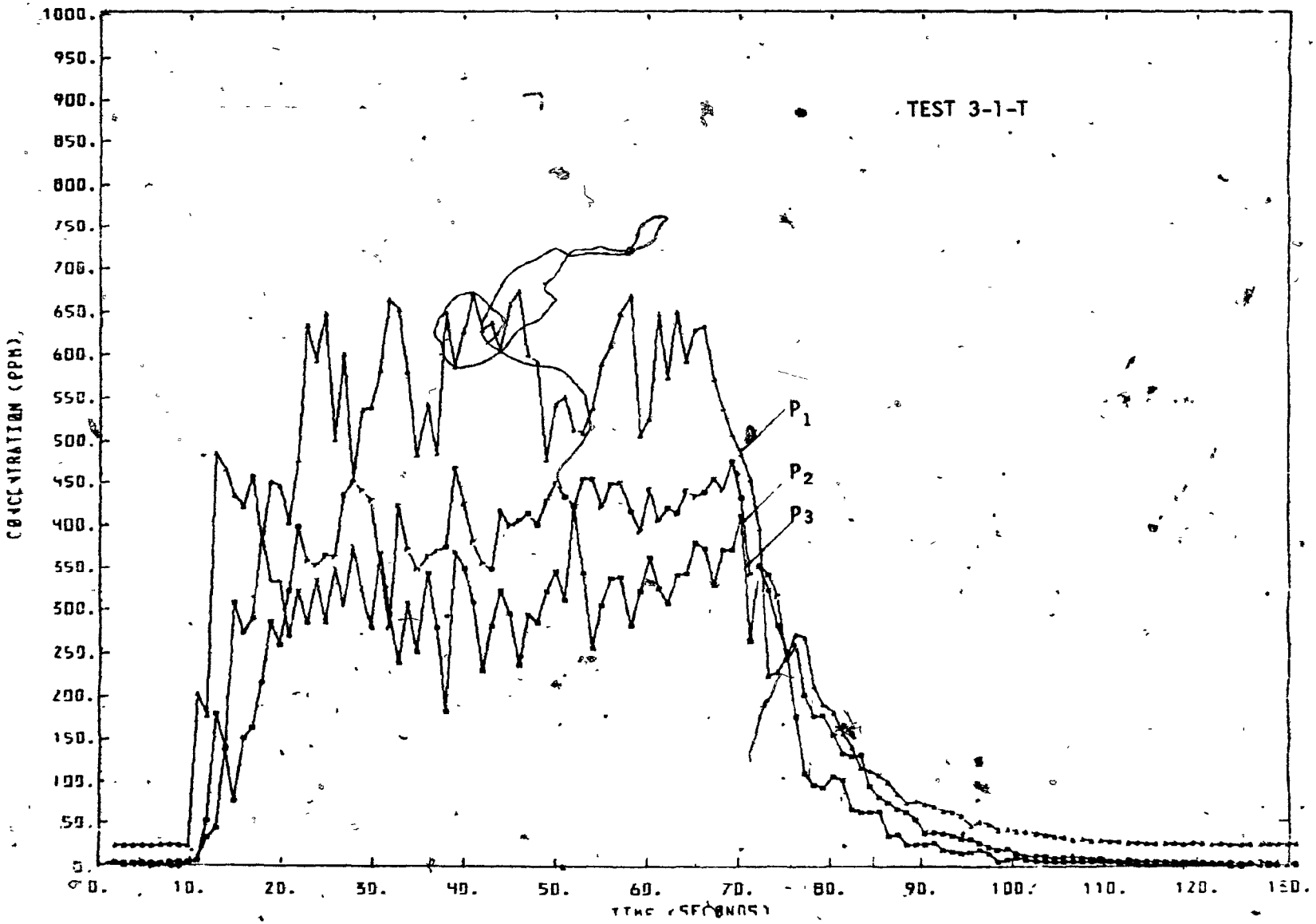
TEST 3-1-T
CONCENTRATION (PPM)
TIME (SECONDS)
P1
P2
P3
1000.
950.
900.
850.
800.
750.
700.
650.
600.
550.
500.
450.
400.
350.
300.
250.
200.
150.
100.
50.
0.
0.
10.
20.
30.
40.
50.
60.
70.
80.
90.
100.
110.
120.
130.

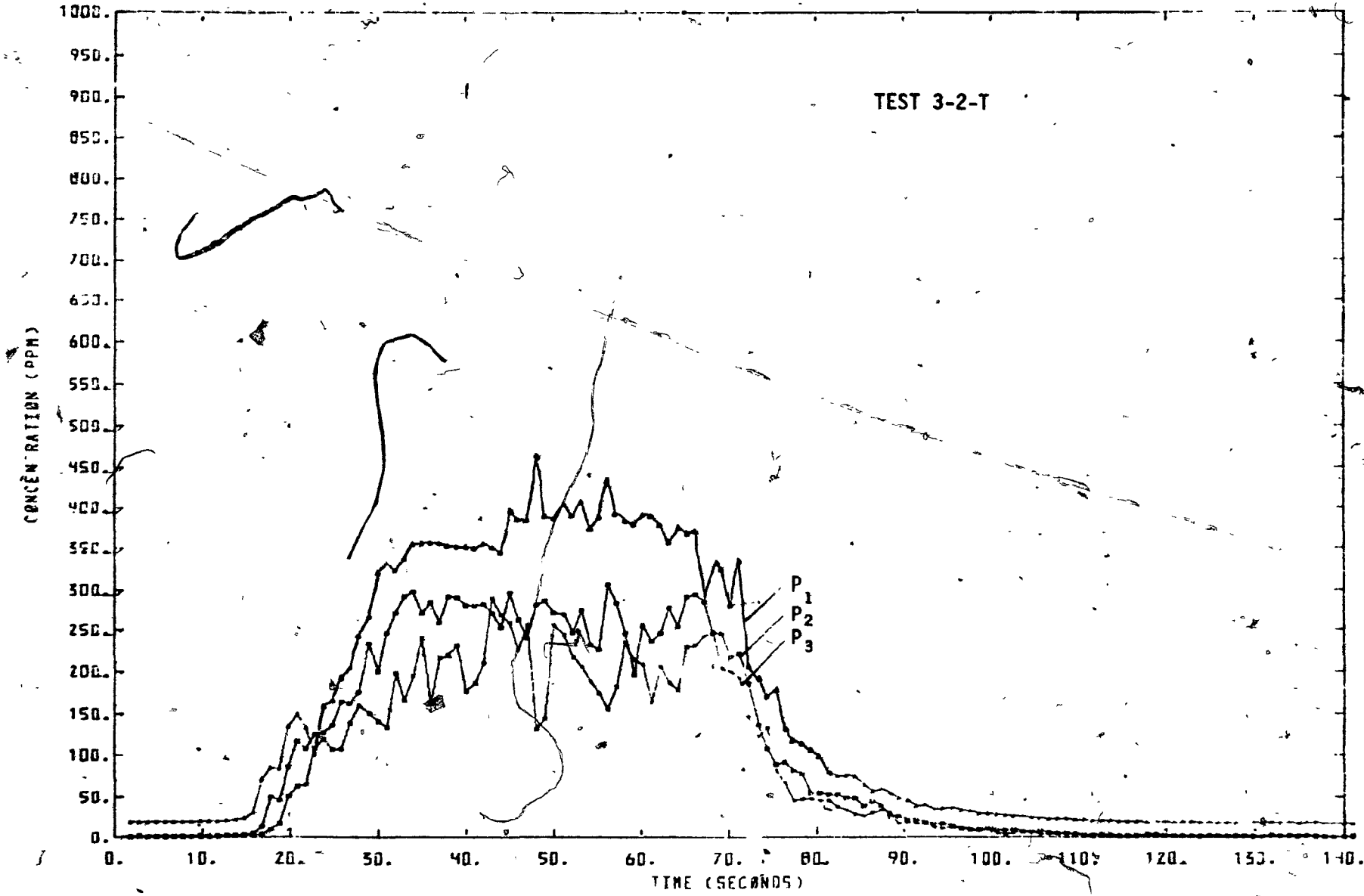
TEST 3-2-T
CONCENTRATION (PPM)
TIME (SECONDS)
P1
P2
P3
1000.
950.
900.
850.
800.
750.
700.
650.
600.
550.
500.
450.
400.
350.
300.
250.
200.
150.
100.
50.
0.
0.
10.
20.
30.
40.
50.
60.
70.
80.
90.
100.
110.
120.
130.
140.

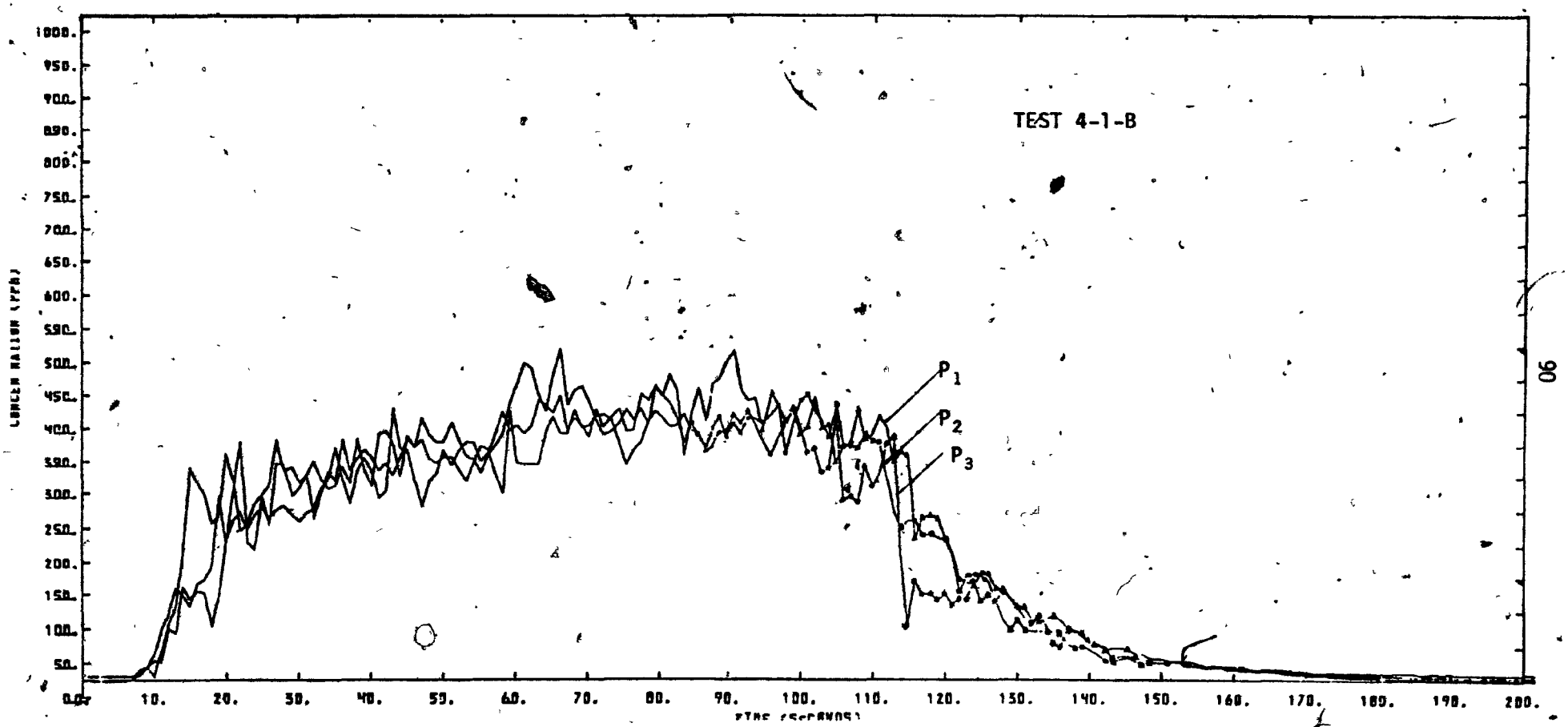
TEST 4-1-B
P1
P2
P3
1000.
950.
900.
850.
800.
750.
700.
650.
600.
550.
500.
450.
400.
350.
300.
250.
200.
150.
100.
50.
0.0
10.
20.
30.
40.
50.
60.
70.
80.
90.
100.
110.
120.
130.
140.
150.
160.
170.
180.
190.
200.

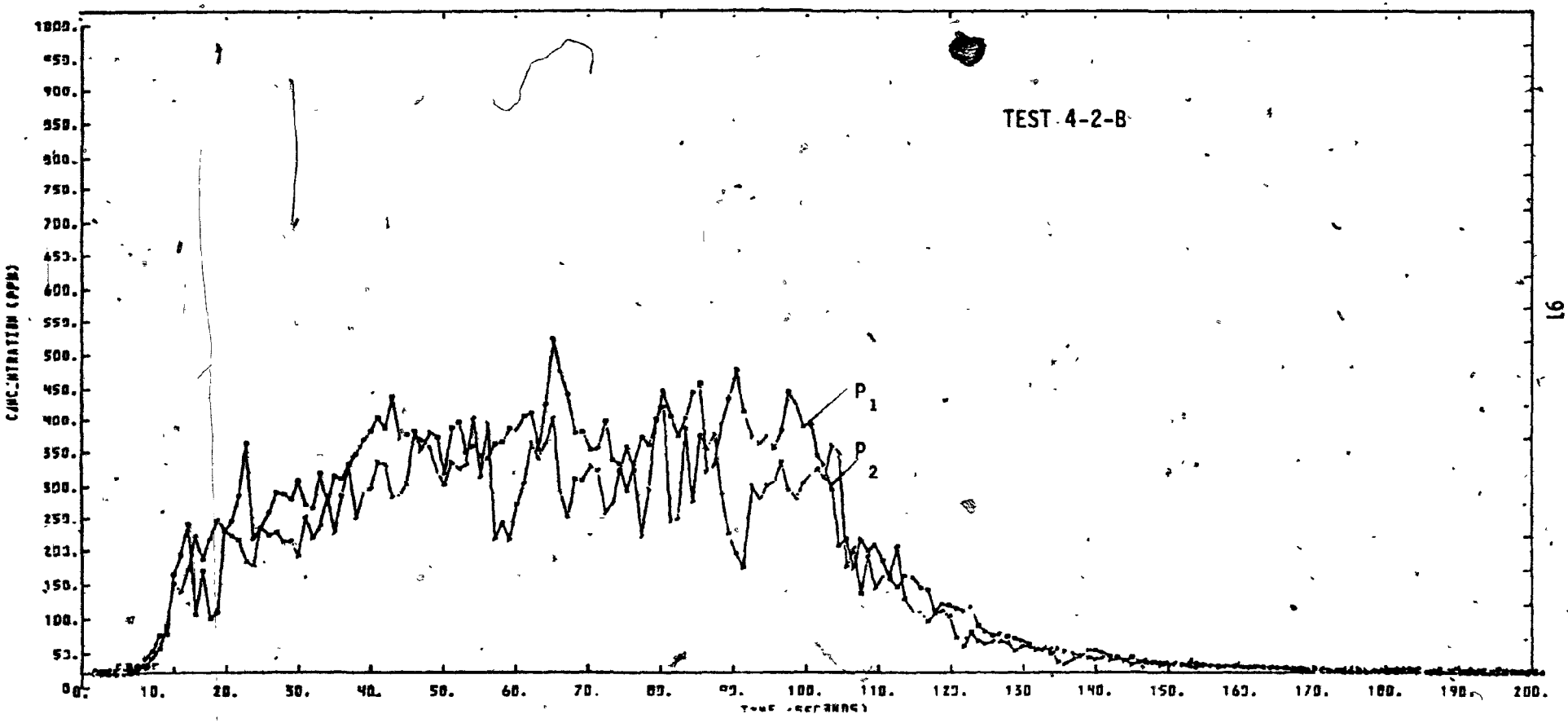
TEST 4-2-B
P1
P2
CONCENTRATION (PPB)
1000.
950.
900.
850.
800.
750.
700.
650.
600.
550.
500.
450.
400.
350.
300.
250.
200.
150.
100.
50.
0.
10.
20.
30.
40.
50.
60.
70.
80.
90.
100.
110.
120.
130
140.
150.
160.
170.
180.
190.
200.

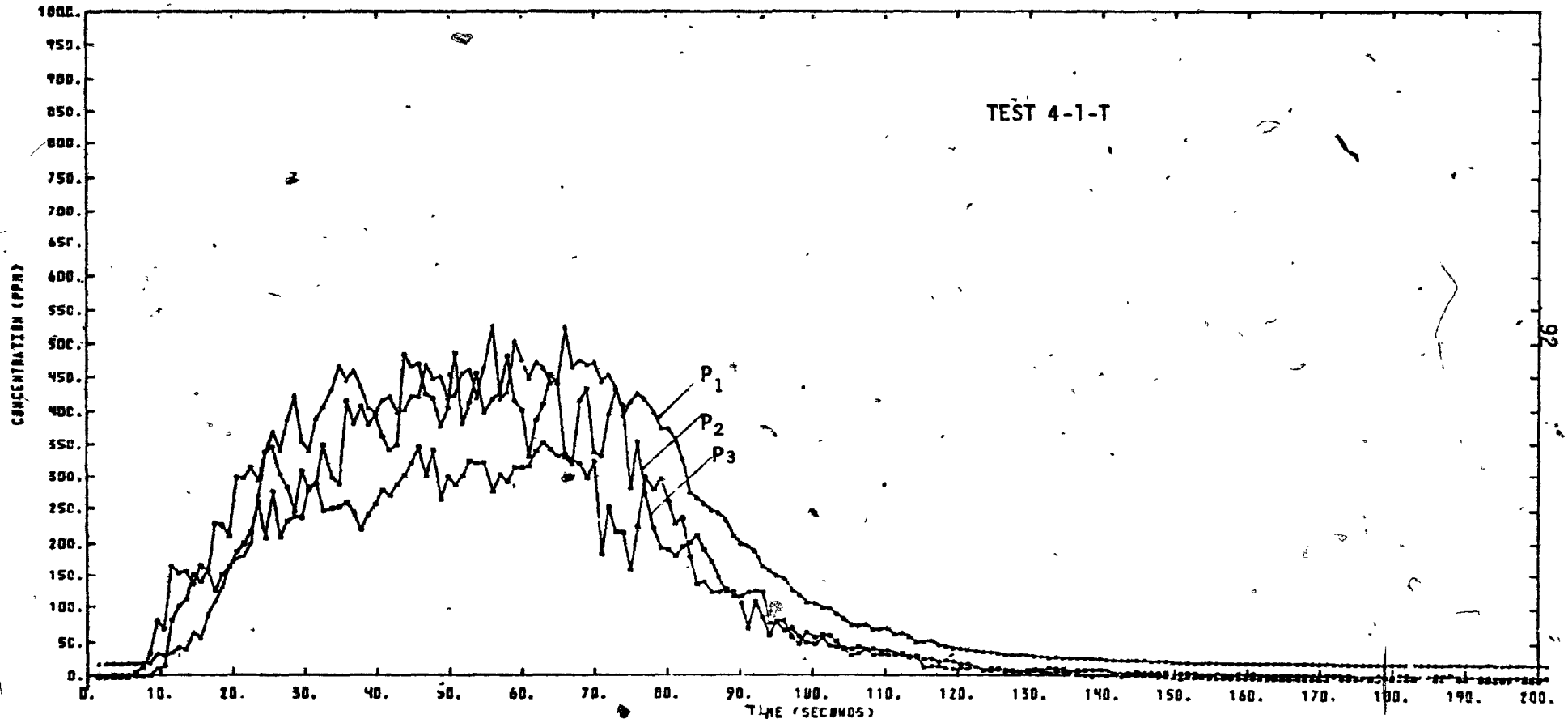
TEST 4-1-T
CONCENTRATION (PPM)
TIME (SECONDS)
P1
P2
P3
1000.
950.
900.
850.
800.
750.
700.
650.
600.
550.
500.
450.
400.
350.
300.
250.
200.
150.
100.
50.
0.
0.
10.
20.
30.
40.
50.
60.
70.
80.
90.
100.
110.
120.
130.
140.
150.
160.
170.
180.
190.
200.

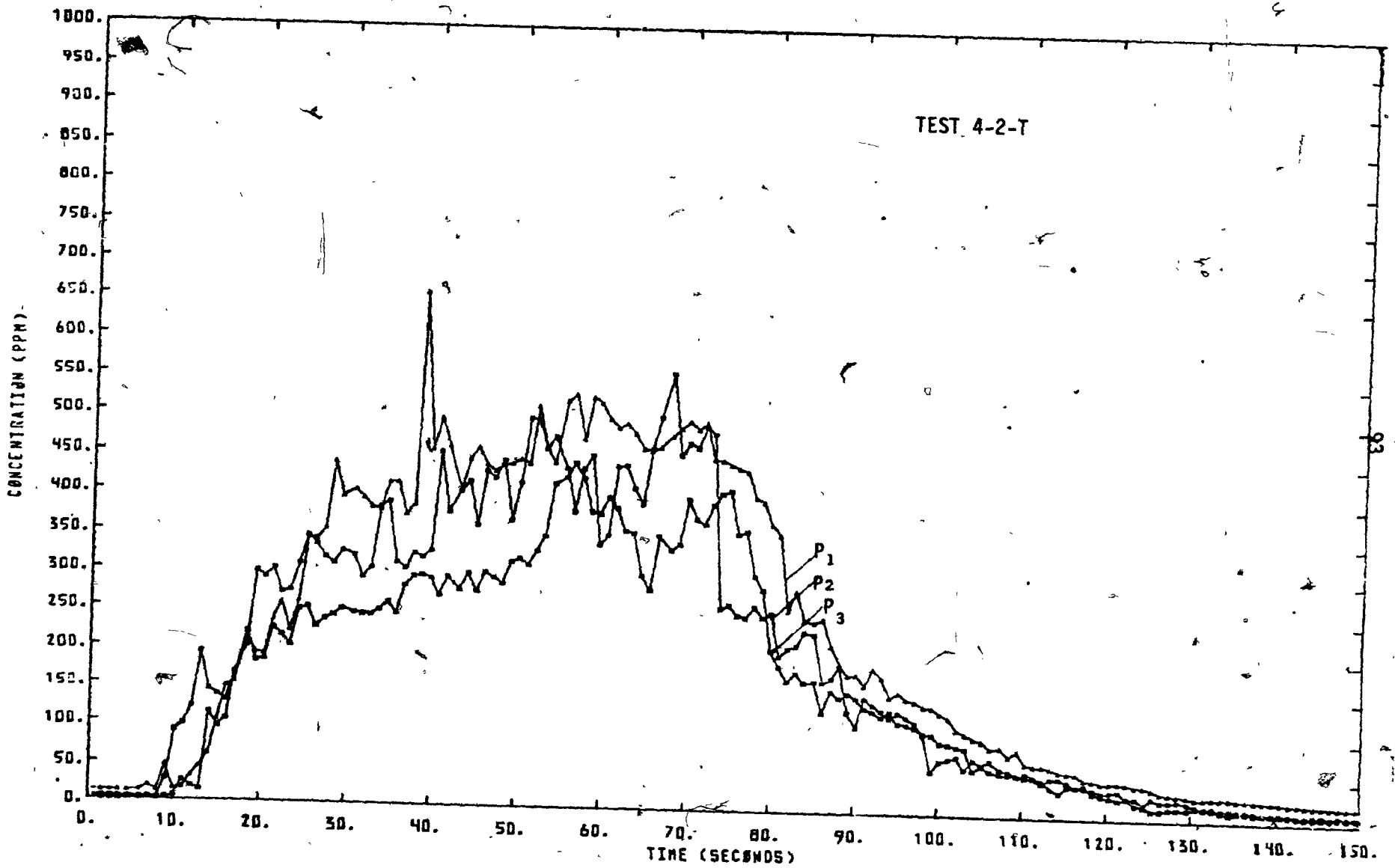
TEST 4-2-T
CONCENTRATION (PPM)
TIME (SECONDS)
P1
P2
P3
1000.
950.
900.
850.
800.
750.
700.
650.
600.
550.
500.
450.
400.
350.
300.
250.
200.
150.
100.
50.
0.
0.
10.
20.
30.
40.
50.
60.
70.
80.
90.
100.
110.
120.
130.
140.
150.

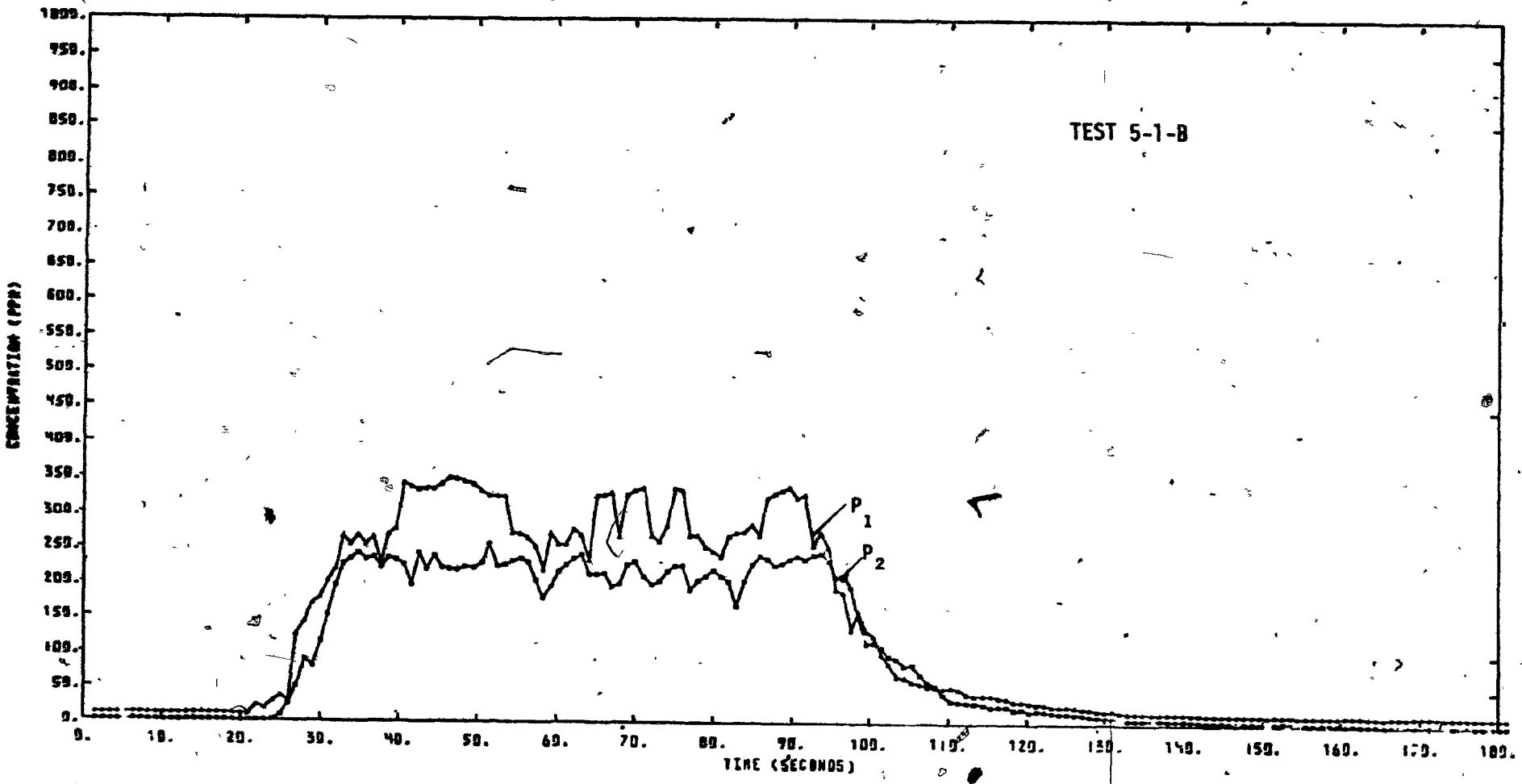
TEST 5-1-B
CONCENTRATION (PPB)
TIME (SECONDS)
P1
P2
0.
50.
100.
150.
200.
250.
300.
350.
400.
450.
500.
550.
600.
650.
700.
750.
800.
850.
900.
950.
1000.
0.
10.
20.
30.
40.
50.
60.
70.
80.
90.
100.
110.
120.
130.
140.
150.
160.
170.
180.

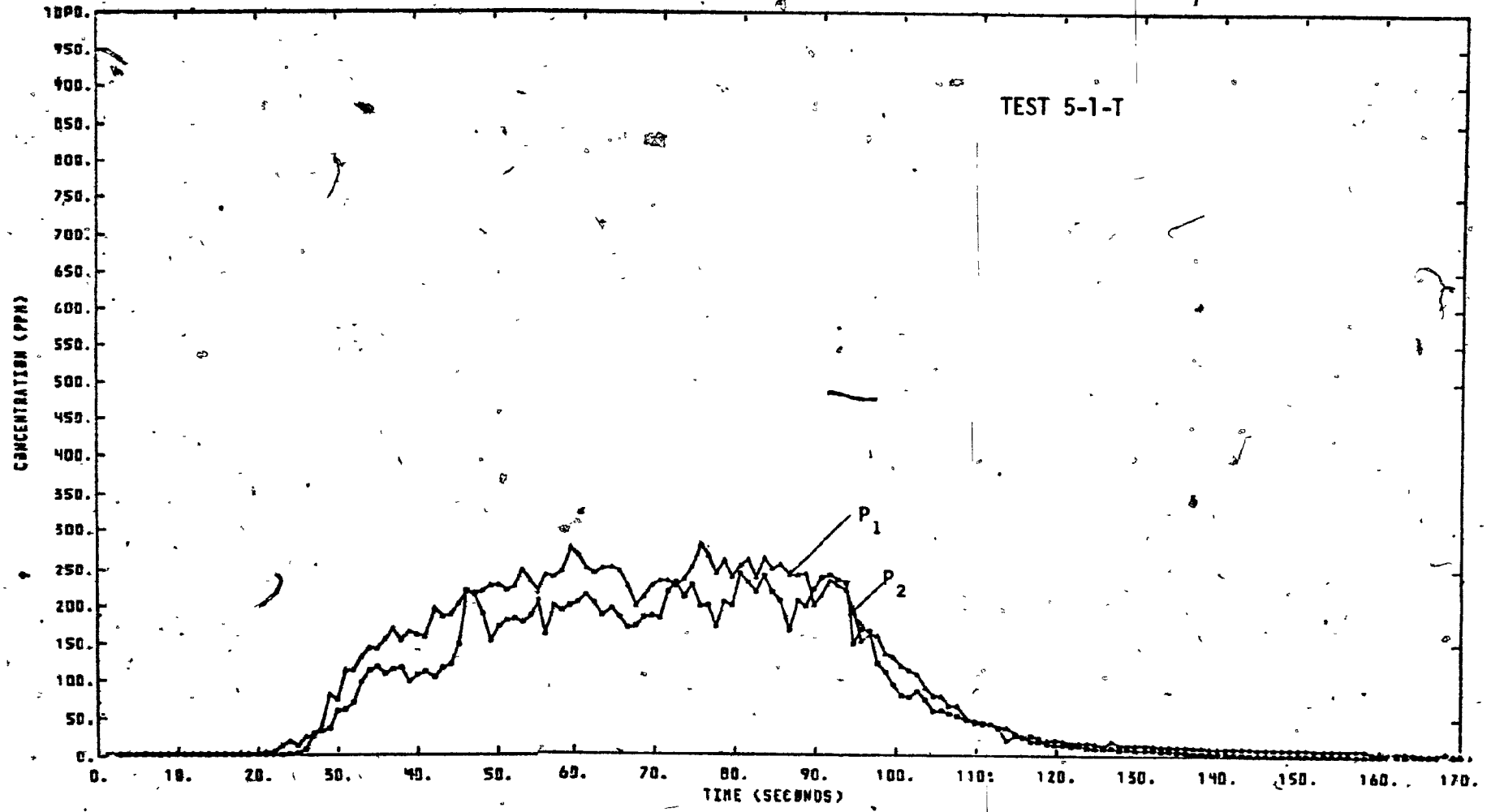
TEST 5-1-T
CONCENTRATION (PPM)
1000.
950.
900.
850.
800.
750.
700.
650.
600.
550.
500.
450.
400.
350.
300.
250.
200.
150.
100.
50.
0.
0.
10.
20.
30.
40.
50.
60.
70.
80.
90.
100.
110.
120.
130.
140.
150.
160.
170.
TIME (SECONDS)
P_1
P_2

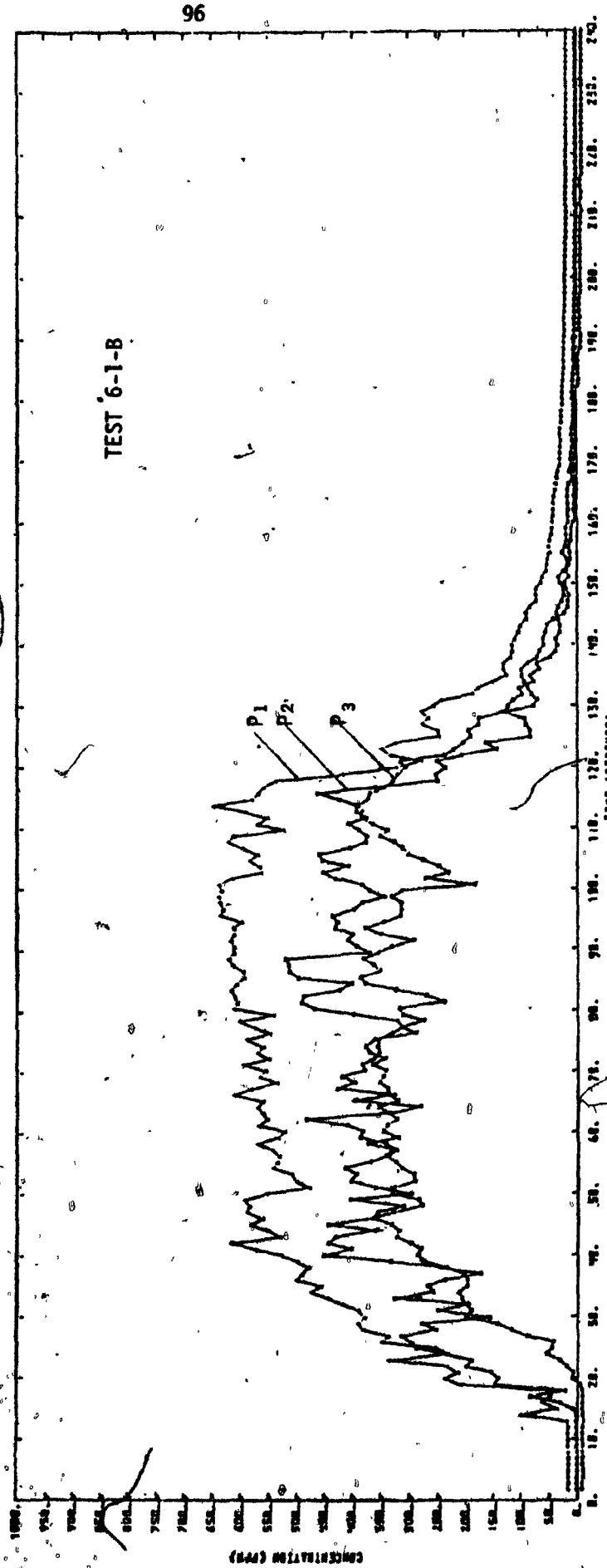
TEST 6-1-B
P1
P2
P3
TIME (SECONDS)
CONCENTRATION (PPM)

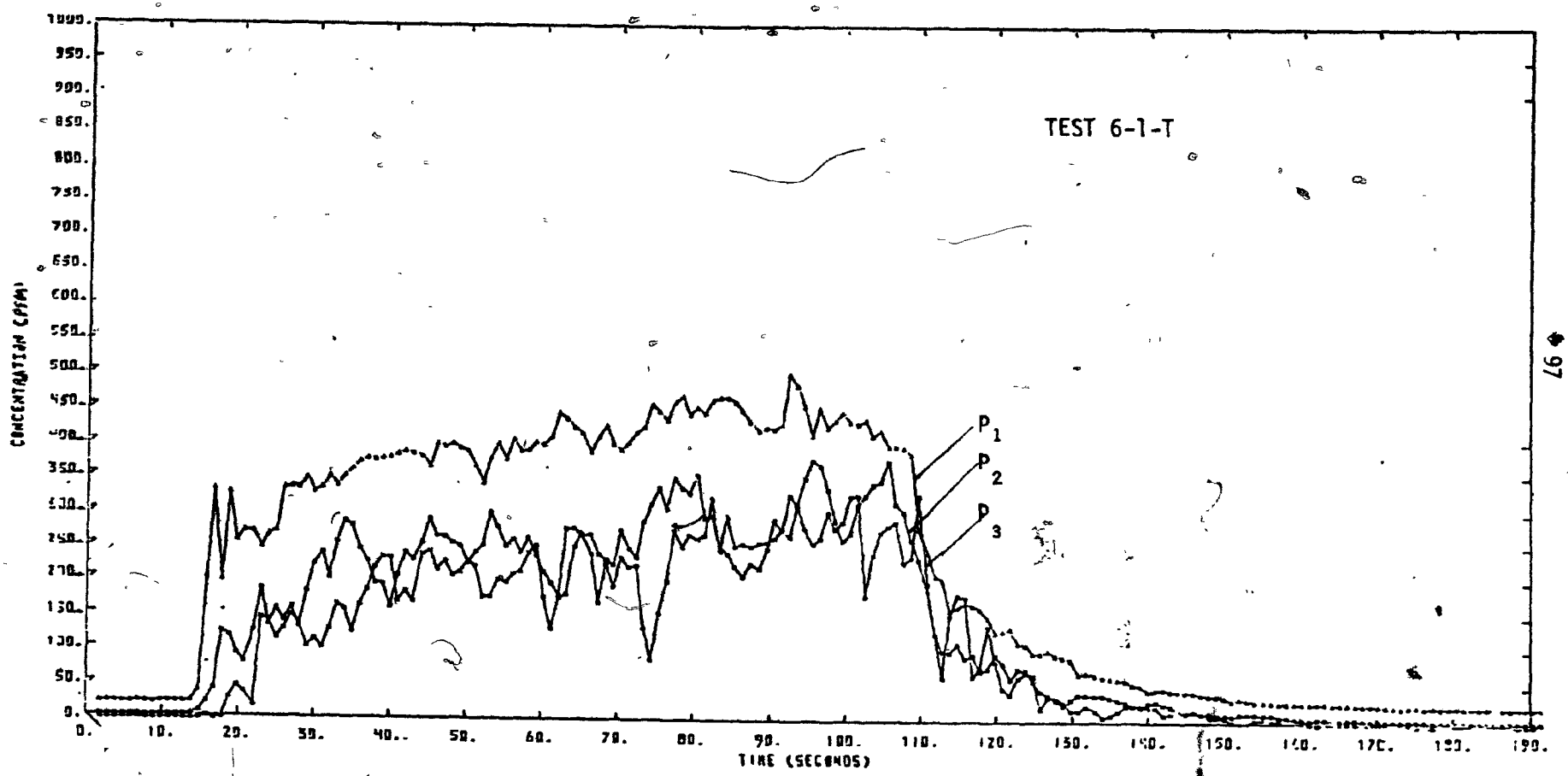
TEST 6-1-T
CONCENTRATION (PPM)
TIME (SECONDS)
P1
P2
P3
0.
50.
100.
150.
200.
250.
300.
350.
400.
450.
500.
550.
600.
650.
700.
750.
800.
850.
900.
950.
1000.
0.
10.
20.
30.
40.
50.
60.
70.
80.
90.
100.
110.
120.
130.
140.
150.
160.
170.
180.
190.

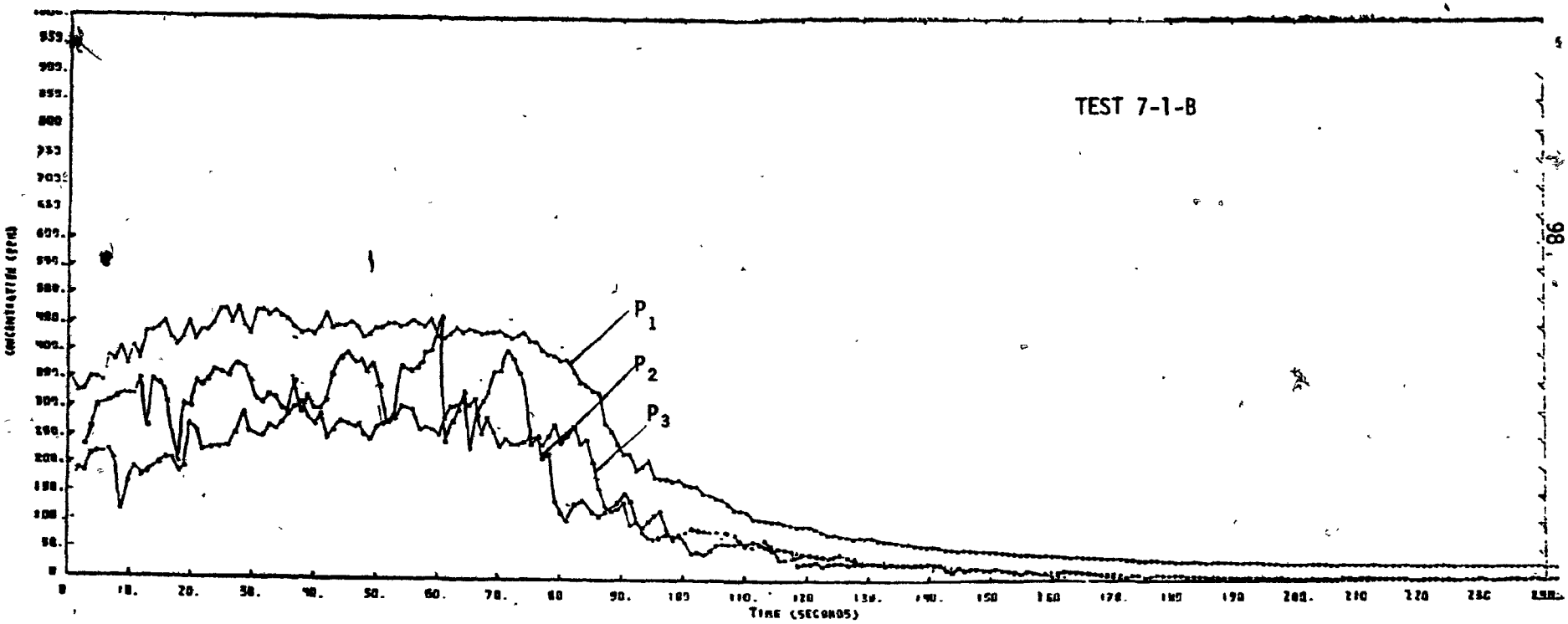
TEST 7-1-B
P1
P2
P3
TIME (SECONDS)

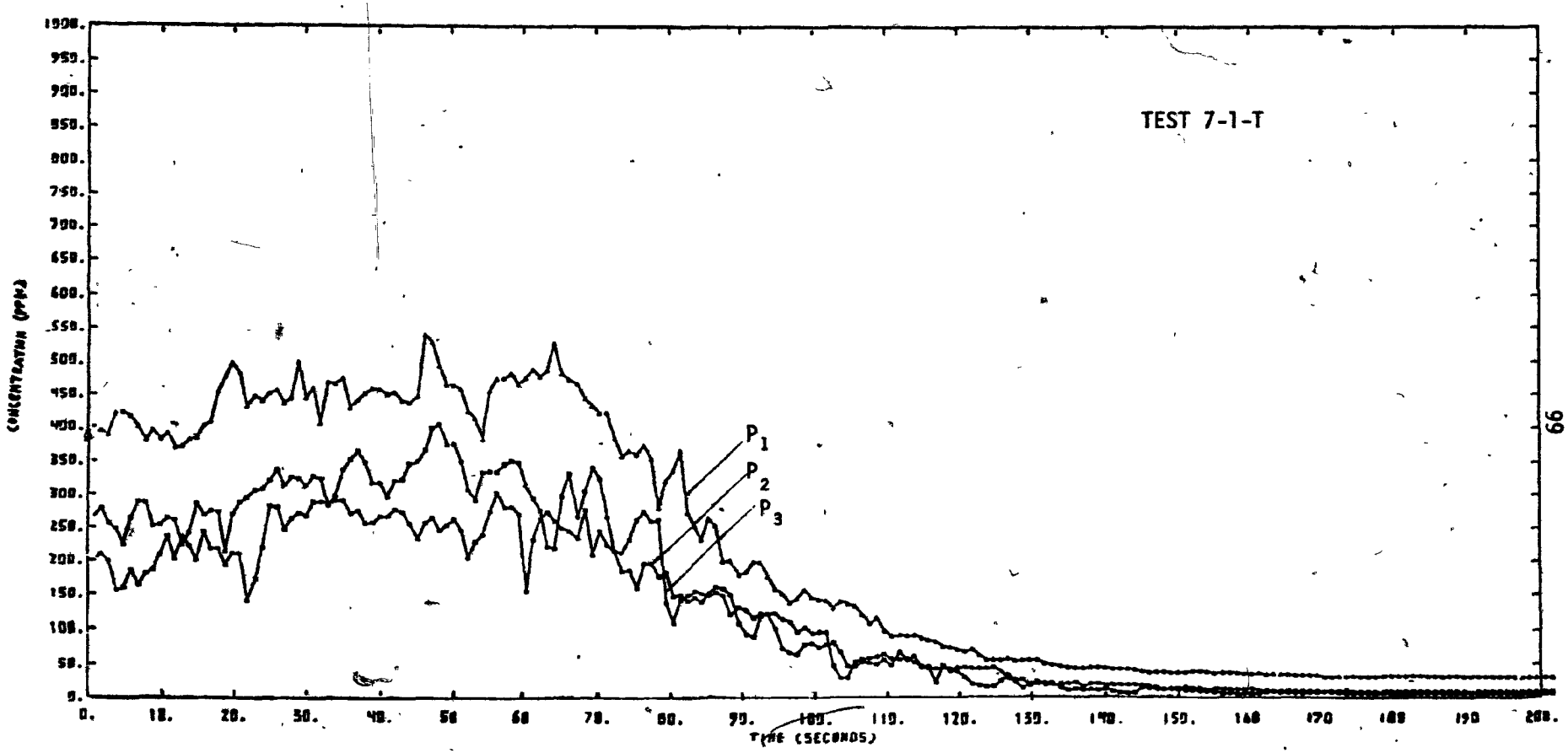
TEST 7-1-T
CONCENTRATION (PPM)
TIME (SECONDS)
P1
P2
P3
1000.
950.
900.
850.
800.
750.
700.
650.
600.
550.
500.
450.
400.
350.
300.
250.
200.
150.
100.
50.
0.
0.
10.
20.
30.
40.
50.
60.
70.
80.
90.
100.
110.
120.
130.
140.
150.
160.
170.
180.
190.
200.

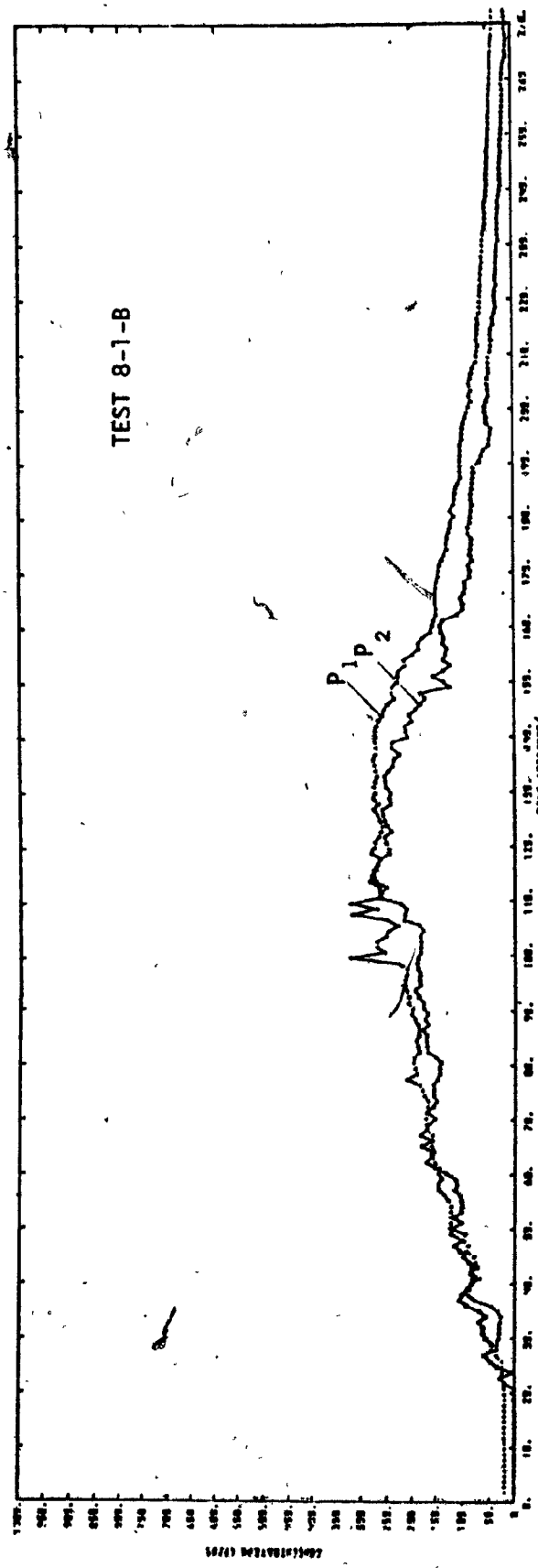
TEST 8-1-B
P1
P2

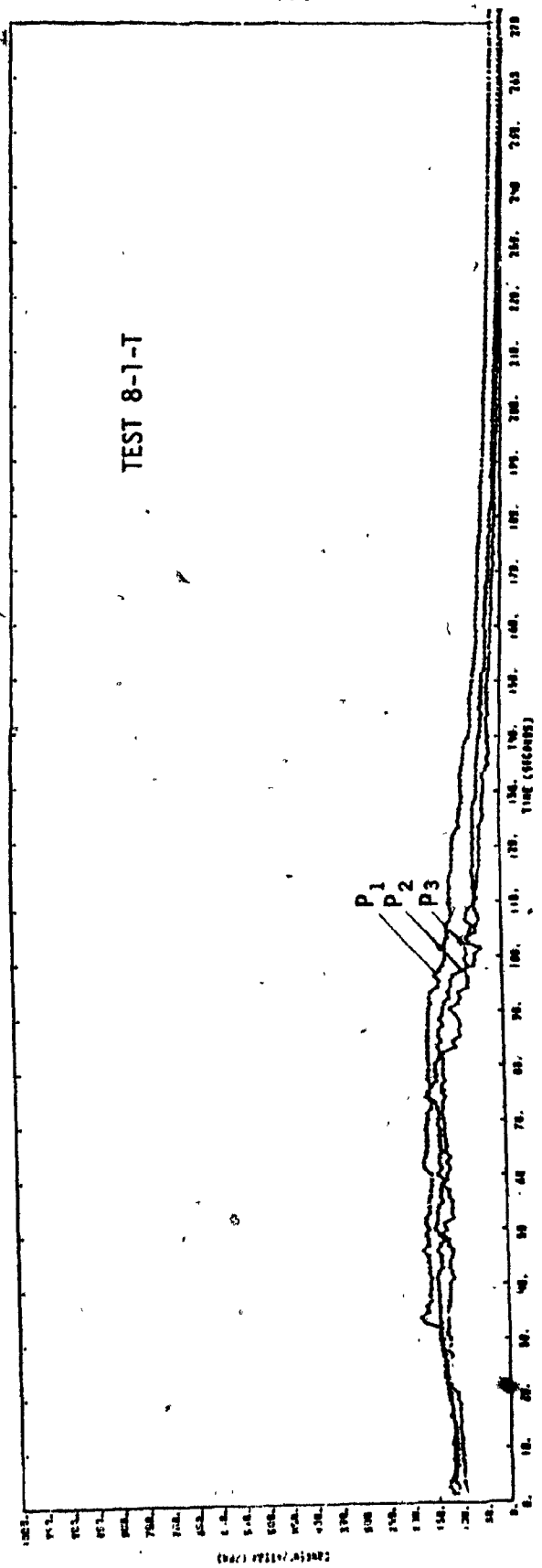
TEST 8-1-T
P1
P2
P3